PRECAST CONCRETE CONNECTIONS
WITH EMBEDDED STEEL MEMBERS

by

KOSTAS MARCAKIS

A thesis submitted to the Faculty of Graduate Studies and Research in partial fulfillment of the requirements for the degree of

Master of Engineering

Department of Civil Engineering
and Applied Mechanics
McGill University
Montreal, Quebec

March 1979

PRECAST CONNECTIONS WITH EMBEDDED STEEL MEMBERS

Kostas Marcakis

Department of Civil Engineering
and Applied Mechanics

M. Eng.
March 1979

ABSTRACT

This thesis presents the results of twenty one tests of precast concrete connections incorporating embedded structural steel members. The effects of axial load, concrete cover, presence of additional reinforcement, shape of embedded member and type of loading on the behaviour of the connection were studied. A rational analytical model was developed based on equilibrium and strain compatibility. Based on the analytical model which was developed and on the experimental results, a design method was formulated. This design method is compared with the design approach adopted in the second edition of the Prestressed Concrete Institute Design Handbook.

ASSEMBLAGES PRÉFABRIQUÉS DE BÉTON AVEC DES PROFILÉS D'ACIER ENCASTRÉS

Kostas Marcakis

Département de Génie Civil et de Mécanique Appliquée

Maîtrise en Génie Civil
mars 1979

RÉSUMÉ

Les résultats de vingt-et-un essais d'assemblages préfabriqués de béton avec des profilés d'acier de charpente sont présentés. Les effets de la charge axiale, du recouvrement de béton, de la présence d'armature supplémentaire, du profil du membre encastré et du type de charge sur le comportement de l'assemblage sont etudiés. Un modèle analytique rationnel, fut mis au point, basé sur les conditions d'équilibre statique et de compatibilité des déformations proportionnelles.

Une méthode de calcul basée sur ce modèle ainsi que sur les résultats expérimentaux fut développée. Cette méthode est comparée avec celle utilisée dans la seconde édition du manuel de calcul du Prestressed Concrete Institute.

ACKNOWLEDGEMENTS

The author wishes to express his appreciation to his research director, Professor D. Mitchell, for his unceasing guidance and encouragement throughout this entire endeavour.

Thanks are due to Mr. Nelu Wexler for his assistance in the experiments and to Mr. Pierre Desautels and Mr. Dohyung Ahn for their assistance in the experiments and in the preparation of this thesis.

Thanks are also due to Miss Joan Armour for her quick and excellent typing.

This study was sponsored by the National Research Council of Canada. The experiments reported in this thesis were carried out in the Jamieson Structures Laboratory of the Department of Civil Engineering and Applied Mechanics of McGill University.

TABLE OF CONTENTS

LIST OF FIGURES

LIST OF TABLES

CHAPTER 1 INTRODUCTION

1.1 The Advantages of Embedded Steel Members in Precast Connections

Embedded structural steel shapes have been popular for many years as connectors in precast concrete construction. The advantages of this type of connection over other precast connections has encouraged its use in precast panel connections and in beam to column connections as shown in Fig. 1.1.

Connections made by embedded structural steel members in concrete have the following advantages over other types of precast connections:

1] the connection strength does not depend on welding and is therefore more reliable than some other types of connections.

2] the connection is simple, requiring no special formwork or reinforcing cages

3] the simplicity of the connection makes it more economical than other types of connections.

4] the connection can be easily designed to attain the full strength of the embedded steel member which results in larger ductilities

and 5] the strength of these connections is not as sensitive to construction errors.

Due to the increasing popularity of this type of precast connection there is a need for a rational design method based on an understanding of the behaviour of these connections.

1.2 Background

Currently there is little information on the behaviour of precast connections incorporating embedded structural steel members. The strength of these connections depends on the width of the structural steel member, the embedment length of the steel member, the concrete strength and the eccentricity of the applied load.

Until recently the most widely used method of designing these connections was that presented in the Prestressed Concrete Institute's (PCI) Design Handbook[1]. This design method was extended by Raths[2] to include the effects of additional reinforcement welded to the steel member. The Second Edition of the PCI Design Handbook[3] includes equations for the design of these connections with and without additional welded reinforcement.

Although some precast concrete fabricators have performed tests on these types of connections the results are not generally available. In view of the absence of experimental evidence in the literature there is a need for an experimental investigation of the behaviour of these types of connections.

1.3 PCI Design Method

1.3.1 Embedded Connections Protruding from One Side

The PCI method is based on a number of simplifying assumptions which are meant to conservatively approximate the complex bearing conditions occuring at ultimate (see Fig. 1.2). The compressive stress block on the front face at ultimate is assumed to have a width, b, equal to the width of the embedded steel member and a depth equal to one third of the embedment length, ℓ_e. The stress block has a uniform stress of $0.85\ f'_c$ and the compressive strain at the front face is assumed to be 0.003.

The resultant compressive force, C_b, at the back of the embedded member is assumed to be located at 11/12 ℓ_e from the front face of the column.

The stress resultant, C_f, on the front face is given by:

$$C_f = 0.85\ f'_c\ b\ \ell_e/3 \tag{1.1}$$

where f'_c = compressive strength of concrete

b = width of structural steel member

ℓ_e = embedment length of structural steel member

Taking moments about C_b gives:

$$V_c\ (a + 11/12\ \ell_e) = C_f\ (3/4\ \ell_e) \tag{1.2}$$

where V_c = nominal capacity of the connection

a = eccentricity of the load from the face of the column

therefore: $$V_c = \frac{3C_f}{3.67 + 4\ a/\ell_e} \tag{1.3}$$

Substitution for C_f gives

$$V_c = \frac{0.85\ f'_c\ b\ \ell_e}{3.67 + 4\ a/\ell_e} \tag{1.4}$$

Equation 1.4 is the PCI ultimate capacity of the connection when failure takes place in the concrete.

1.3.2 Embedded Connections Protruding from Two Sides

For situations where beams frame into both sides of a column, a connection as shown in Fig. 1.3 may be used. The assumption of an equivalent rectangular stress block over a distance of $\ell_e/3$ from each face of the column leads to the following PCI design equation:

$$V_n = 0.85\ f'_c\ b\ \ell_e/3 \tag{1.5}$$

where V_n is the strength on each side of the steel member as governed by

the capacity of the concrete.

1.3.3 Embedded Connections with Additional Welded Reinforcement

Raths[2] has extended the PCI Design Method to include the effects of additional welded reinforcement on the strength of embedded connections which protrude from one side only. Figure 1.4 illustrates Raths assumptions of the strain distribution at failure in a connection containing additional welded reinforcement. Raths assumes a linear strain distribution with a maximum strain of 0.003 at the front face of the column and zero strain at a distance of $\ell_e/3$ from the front face. The additional reinforcement is welded to the structural steel member and is assumed to act at the locations of C_f and C_b.

Taking moments about C_b and assuming that the steel yields gives:

$$V_r\ (a + 11/12\ \ell_e) = A_s\ f_y\ (3/4\ \ell_e) \qquad (1.6)$$

where A_s = area of additional welded reinforcement at the front of the steel member

f_y = yield stress of reinforcement

V_r = additional capacity of the connection due to the reinforcement

Therefore:

$$V_r = \frac{3\ A_s\ f_y}{3.67 + 4\ a/\ell_e} \qquad (1.7)$$

which is the PCI design equation for the additional capacity of a connection due to the welded reinforcement.

Assuming the steel near the back of the column yields, equilibrium of vertical forces gives:

$$V_r = A_s\ f_y - A'_s\ f_y \qquad (1.8)$$

where A_s' is the area of the additional reinforcement at the rear of the connection.

Substituting Equation 1.7 for V_r in Equation 1.8 and rearranging terms results in

$$A_s' = \left[\frac{12\ a + 2\ \ell_e}{12\ a + 11\ \ell_e}\right] A_s \qquad (1.9)$$

Equation 1.9 gives the required area of reinforcing steel near the back of the steel member.

1.3.4 Comments on the PCI Design Method

There are a number of assumptions used in the PCI Design Method which appear to be inconsistent. The neutral axis depth of the assumed strain distribution coincides with the depth of the equivalent rectangular stress block. This is inconsistent with the well known flexural theory for reinforced concrete. The PCI Design Method assumes a constant depth of $\ell_e/3$ for both the strain distribution and the equivalent rectangular stress distribution. This depth should not be constant but should vary with the eccentricity of the applied load and with the area of additional reinforcement. Equilibrium conditions are violated since the strain distribution is not chosen to ensure that:

$$C_f - C_b = V_c \qquad (1.10)$$

1.4 Objectives of the Research Program

An experimental investigation of precast connections incorporating embedded steel members is needed in order to develop a rational understanding of the behaviour. The main objective of the experimental program is to develop a rational analytical model of the behaviour of these types of connections

on which a design procedure could be based. The experimental program enabled a study of the effects of the following variables:

1] the axial load on the column

2] the concrete cover of the column

3] additional welded reinforcement

4] the shape of the embedded steel member

5] the type of loading on the connection

a) pure moment

b) embedded member protruding from one side of column

c) embedded member protruding from opposite sides of column.

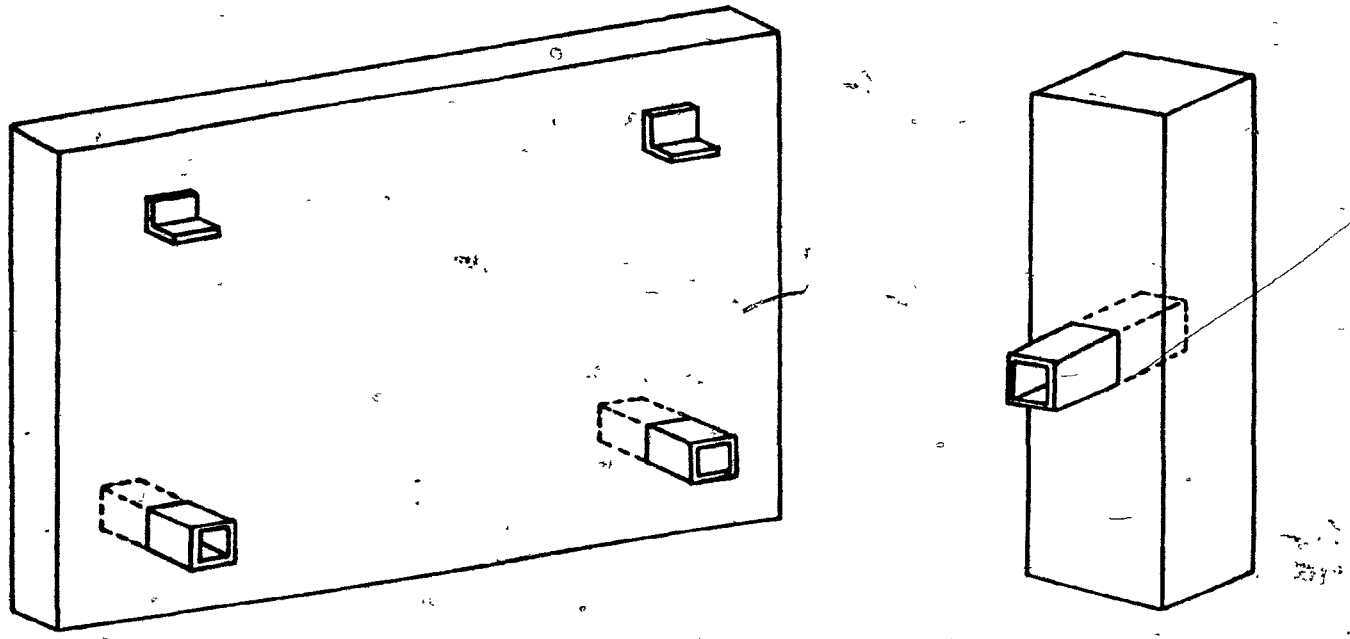

Figure 1.1 Typical wall panel and beam to column connections incorporating embedded structural steel members

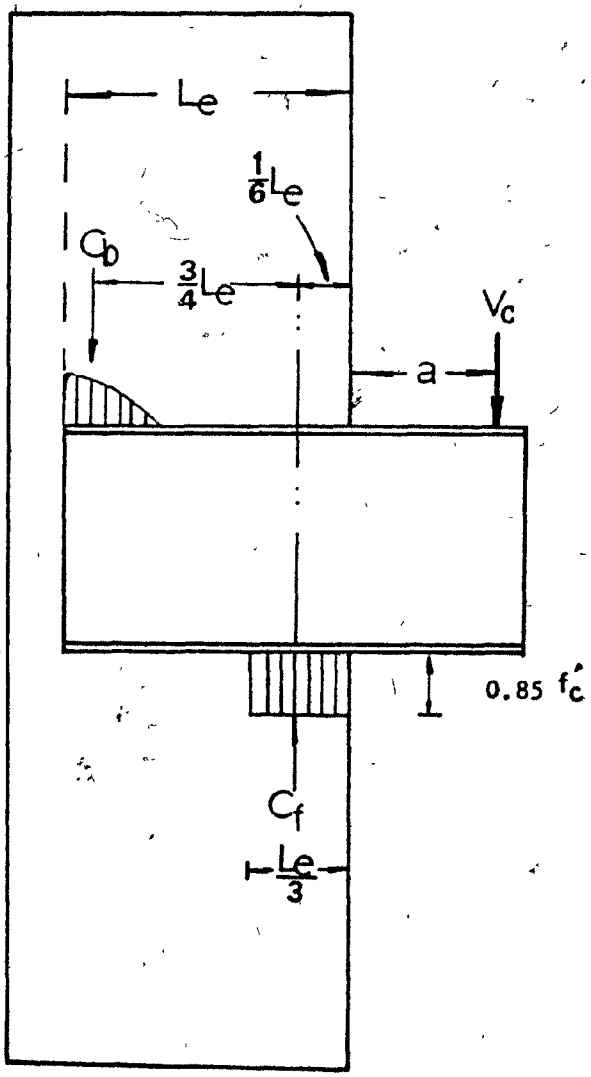

Figure 1.2 PCI stress distribution for steel members protruding from one side only

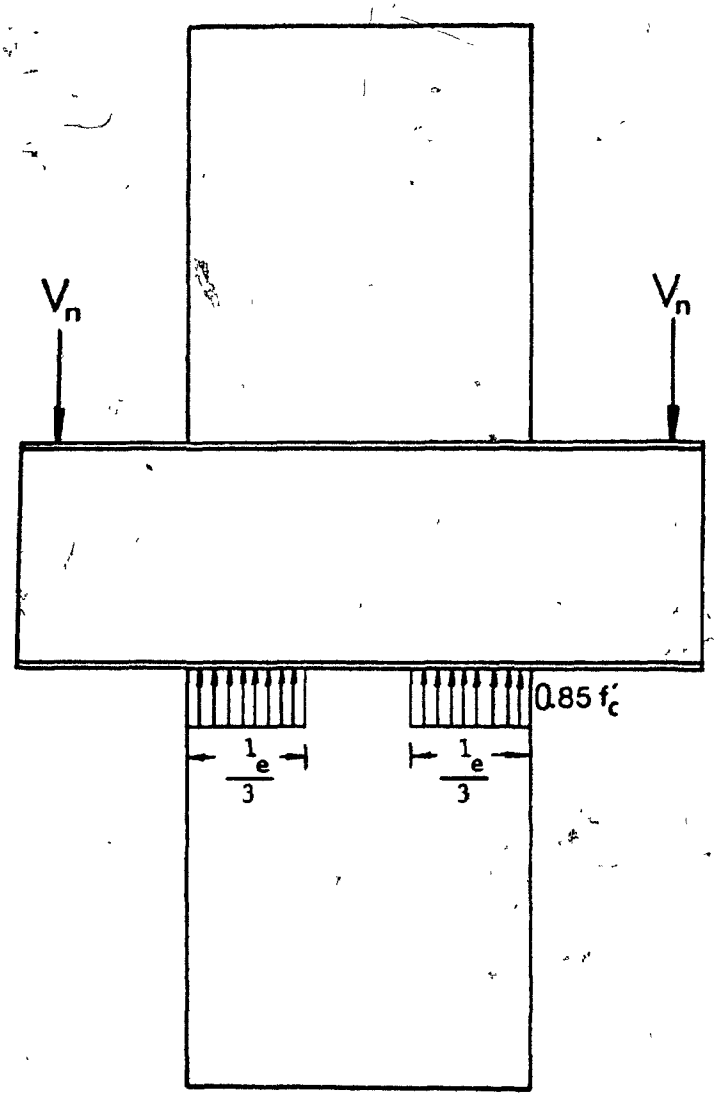

Figure 1.3 PCI stress distribution for steel members protruding from two sides

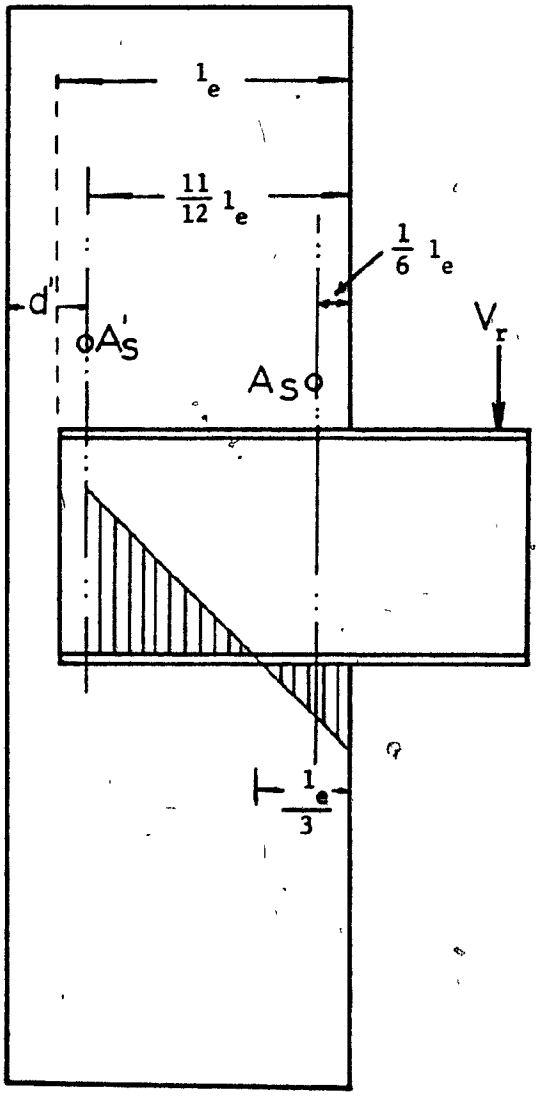

Figure 1.4 PCI strain distribution in a connection containing additional reinforcement

CHAPTER 2 EXPERIMENTAL PROGRAMME

Three different series comprising a total of twenty-one embedded member column connections were tested. The concrete strength, the embedment length of the steel member, the eccentricity of the applied load, the specimen dimensions, the type of embedded member and the failure loads are given in Table 2.1.

2.1 Series I

The four embedded member column connections, specimens C1 to C4, of the first series were used as pilot tests to identify the modes of failure of the connections and to refine the testing procedure. All four specimens incorporated 4 in. x 4 in. x 0.250 in. (102 mm x 102 mm x 6 mm) hollow structural members protruding from only one side of the column and had embedment lengths of 6 in. (152 mm). Each column was reinforced with four #4 bars and contained #3 ties at 3 inches (76 mm) center to center. The four specimens in this series are described in Fig. 2.1 and in Table 2.1.

Specimens C1, C2, C3 and C4 were tested under axial loads of 1 kip (4.45 kN), 30 kips (133.4 kN), 60 kips (266.9 kN) and 90 kips (400.3 kN) respectively.

The embedded hollow structural steel member for specimen C1 was blocked at its embedded end such that concrete did not enter the hollow tube. The test results of specimen C1 indicated excessive local bending of the thin walled hollow structural section due to concrete bearing. In order to alleviate this difficulty the embedded hollow structural steel members for specimens C2, C3 and C4 were filled with concrete along their embedment lengths.

2.2 Series II

A series of thirteen embedded member precast column connections were tested. Each column contained four #4 longitudinal bars and #3 column ties at 3 inches (76 mm) center to center.

2.2.1 Specimens Under Axial Load

Five specimens (SC1, SC2, SC3, SC4 and SC5) were tested with varying degrees of axial load. All specimens incorporated 4 in. x 6 in. x 0.375 in. (102 mm x 152 mm x 10 mm) hollow structural members protruding from one side of the column with an embedment length of 7 inches (178 mm) as shown in Fig. 2.2.

Specimen SC1 was tested under pure axial load. Specimens SC2, SC3, SC4 and SC5 were tested under axial loads of 240 kips(1068 kN), 160 kips(712 kN), 80 kips(356 kN) and zero axial load respectively. The purpose of these tests was to determine the interaction between the axial load on the column and the capacity of the connection.

2.2.2 Specimens with Embedded Members Having Different Cross-Section Shapes

Specimen SC6 incorporated a 6 in. x 6 in. (152 mm x 152 mm) wide flanged steel member with a weight of 25 lb/ft (37 kg/m) which was modified by cutting the flanges such that the flange width was reduced to 4 inches (102 mm). This specimen served as a companion to specimen SC5 and was chosen such that the widths of the embedded structural members were identical and their moments of inertia were comparable. The purpose of this test was to study the effect of shape of the embedded steel member on the response.

2.2.3 Specimens with Additional Welded Reinforcement

Two specimens, SC7 and SC8 were identical to SC5 except for the addition of eight #3 bars welded to the 6 in. x 4 in. x 0.375 in. (152 mm x 102 mm x 10 mm) hollow structural member as shown in Fig. 2.3. The purpose of these two tests was to study the effects of additional welded reinforcement on the response of the connections.

2.2.4 Specimens with Different Concrete Covers

Specimens SC5, SC9 and SC10 had the same column reinforcement and concrete strength but had different concrete covers as can be seen in Fig. 2.4. The details of the column reinforcement are shown in Fig. 2.2.

Specimens SC5 and SC10 had clear concrete covers of 1/2 in (13 mm) and 1 1/2 in (38 mm) respectively. Specimen SC9 had zero concrete cover. The embedded steel member was placed in the same position relative to the reinforcing cage for each specimen. The purpose of these tests was to study the effect of concrete cover on the response of the connections.

2.2.5 Specimens with Embedded Members Protruding from Two Sides

Three specimens were tested with embedded steel members passing through the column and protruding from each side. Specimen SC11 contained a 6 in. x 4 in. x 0.375 in (152 mm x 102 mm x 10 mm) hollow structural steel member and was tested with a 4 in. (102 mm) eccentricity from each column face. Specimen SC12 incorporated a wide flanged steel member which had the same properties as the one used in specimen SC6. Specimen SC13 was identical to specimen SC11. The purpose of these tests was to study the behaviour of precast connections with embedded steel members protruding from two sides of the column.

2.3 Series III

The third series comprised a total of four specimens, TC1, TC2, TC3 and TC4. The first three specimens incorporated 4 in. x 4 in. (102 mm x 102 mm) solid steel members while specimen TC4 used a 6 in. x 4 in. x 0.375 in. (152 mm x 102 mm x 10 mm) hollow structural steel member with the same properties as the members in Series II.

Specimen TC1 was 16 in. (406 mm) wide and 8 in. (203 mm) deep as shown in Fig. 2.5. The column contained four #8 longitudinal reinforcing bars in order to prevent flexural failure in the column and also contained #3 ties at 3 in. (76 mm) center to center. The column was built twice as wide as the columns of Series II in order to isolate the embedded steel member from the longitudinal reinforcement. In addition, the wide column and large column flexural capacity together with a rigid embedded steel member provided conditions that were favourable to spreading of the compressive load in the concrete. The purpose of this test was to study the extent of load spreading under very favourable conditions.

In each of specimens TC2 and TC3 two styrofoam blocks 8 in. x 8 in. x 2 in. (203 mm x 203 mm x 51 mm) were cast in the column adjacent to the embedded steel member. This resulted in a reduced 4 in (102 mm) width of concrete above and below the embedded steel member as can be seen in Fig. 2.6. The purpose of these two specimens was to prevent load spreading by limiting the effective width of the concrete in bearing. The known effective width together with uniform bearing provided by the rigid embedded member produced idealized conditions suitable for the development of an analytical model.

Both of these specimens had four #5 longitudinal reinforcing bars and #3 column ties at 3 in. (76 mm) center to center. Specimen TC2 had an embedment length of 7.25 in. (184 mm) with the embedded member protruding from one side only.

The solid steel member in specimen TC3 passed through the column and protruded from both sides giving an embedment length of 8 in. (203 mm). This specimen was tested under pure moment as shown in Fig. 2.7. The purpose of this test was to study the behaviour of the connection under the simpler loading conditions of pure moment in which the strain distributions and the effective width are both known.

Specimen TC4 contained a 6 in. x 4 in. x 0.375 in(152 mm x 102 mm x 10 mm) hollow structural steel member protruding from both sides of the column and was therefore similar to specimens SC11 and SC13 of Series II. The specimen was tested under pure moment in order to study the effect of spreading under this simpler loading condition. The column reinforcement for this specimen was identical to the reinforcement used in specimens TC2 and TC3.

2.4 Material Properties

2.4.1 Concrete Properties

The concrete compressive strength for each specimen is given in Table 2.1. In all three series the concrete compressive strength was determined at the time of testing of the connections.

2.4.1.1 Series I

Since each of the specimens was cast separately and since the concrete mix proportions were modified between castings a large variation in concrete properties was observed for this pilot test series. Four 6 in. x 12 in. (152 mm x 305 mm) test cylinders were used for each test specimen and the average concrete compressive strength of specimens C1, C2, C3 and C4 was 4800 psi (33.1 MPa), 3900 psi (26.9 MPa), 5200 psi (35.8 MPa) and 5800 psi (40.0 MPa) respectively. The age of the specimens at the time of testing varied from 15 days to 33 days.

SPECIMEN	f'_c psi	f'_c MPa	e_o in	e_o mm	a in	a mm	column width in	column width mm	column depth in	column depth mm	concrete cover in	concrete cover mm	Axial Load kips	Axial Load kN	Ultimate Shear kips	Ultimate Shear kN	TYPE OF EMBEDDED MEMBER	COMMENTS
SERIES I																		
C1	4800	33.1	6	152	3	76	7	178	7	178	½	12.5	-	-	27.8	125	HSS 4 in x 4 in x .250 in (102 mm x 102 mm x 6 mm)	HSS not filled
C2	3900	26.9	6	152	3	76	7	178	7	178	½	12.5	30	133	41.4	184	HSS 4 in x 4 in x .0250 in (102 mm x 102 mm x 6 mm)	
C3	5200	35.8	6	152	3	76	7	178	7	178	½	12.5	60	267	45.0	202	HSS 4 in x 4 in x .250 in (102 mm x 102 mm x 6 mm)	
C4	5800	40.0	6	152	3	76	7	178	7	178	½	12.5	90	400	53.5	240	HSS 4 in x 4 in x .250 in (102 mm x 102 mm x 6 mm)	
SERIES II																		
SC1	4500	31.0	7	178	-	-	8	203	8	203	½	12.5	326	1450	-	-	HSS 6 in x 4 in x .375 in (152 mm x 102 mm x 10 mm)	
SC2	4500	31.0	7	178	3	76	8	203	8	203	½	12.5	240	1068	55.8	250	HSS 6 in x 4 in x .375 in (152 mm x 102 mm x 10 mm)	
SC3	4500	31.0	7	178	4	102	8	203	8	203	½	12.5	160	712	70.7	317	HSS 6 in x 4 in x .375 in (152 mm x 102 mm x 10 mm)	
SC4	4500	31.0	7	178	4	102	8	203	8	203	½	12.5	80	356	66.8	299	HSS 6 in x 4 in x .375 in (152 mm x 102 mm x 10 mm)	
SC5	4500	31.0	7	178	4	102	8	203	8	203	½	12.5	-	-	55.0	246	HSS 6 in x 4 in x .375 in (152 mm x 102 mm x 10 mm)	zero axial load
SC6	4500	31.0	7	178	4	102	8	203	8	203	½	12.5	-	-	60.9	273	W 6 in x 25 lb/ft (152 mm x 37 kg/m)	flanges cut to 4 in (102 mm)
SC7	4500	31.0	7	178	4	102	8	203	8	203	½	12.5	-	-	80.5	361	HSS 6 in x 4 in x .375 in (152 mm x 102 mm x 10 mm)	reinforced with 8 #3 bars; d' = 1.5 in (38 mm)
SC8	4500	31.0	7	178	4	102	8	203	8	203	½	12.5	-	-	83.5	374	HSS 6 in x 4 in x .375 in (152 mm x 102 mm x 10 mm)	zero concrete cover
SC9	4500	31.0	7	178	4 3/8	111	7½	184	7½	184	1/8	3.2	-	-	49.1	220	HSS 6 in x 4 in x .375 in (152 mm x 102 mm x 10 mm)	1 1/2 in (38 mm) cover
SC10	4500	31.0	7 5/8	194	3	76	10	254	10	254	1½	12.5	-	-	62.8	281	HSS 6 in x 4 in x .375 in (152 mm x 102 mm x 10 mm)	protruding from two sides
SC11	4500	31.0	8	203	4	102	8	203	8	203	½	12.5	-	-	220.0	986	HSS 6 in x 4 in x .375 in (152 mm x 102 mm x 10 mm)	protruding from two sides
SC12	4500	31.0	8	203	4	102	8	203	8	203	½	12.5	-	-	212.0	950	W 6 in x 25 lb/ft (152 mm x 37 kg/m)	protruding from two sides
SC13	4500	31.0	8	203	4	102	8	203	8	203	½	12.5	-	-	210.0	941	HSS 6 in x 4 in x .375 in (152 mm x 102 mm x 10 mm)	
SERIES III																		
TC1	3400	23.4	7 1/4	184	4	102	8	203	16	406	½	12.5	-	-	58.9	264	4 in (102 mm) square steel bar	very wide column
TC2	3400	23.4	7 1/4	184	4	102	8	203	8	203	½	12.5	-	-	32.3	145	4 in (102 mm) square steel bar	reduced width at connection
TC3	3400	23.4	8	203	4	102	8	203	8	203	½	12.5	-	-	17.5	78	4 in (102 mm) square steel bar	reduced width; pure moment
TC4	3400	23.4	8	203	4	102	8	203	8	203	½	12.5	-	-	26.0	116	HSS 6 in x 4 in x .375 in (152 mm x 102 mm x 10 mm)	pure moment

TABLE 2.1 DETAILS OF TEST SPECIMENS

2.4.1.2 Series II

All thirteen specimens were cast together in order to minimize the variation in concrete properties. In all, fourteen 6 in. x 12 in. (152 mm x 305 mm) concrete cylinders were tested. The average concrete compressive strength was 4520 psi (31.3 MPa). A concrete compressive strength of 4500 psi (31.0 MPa) will be used in all strength calculations for this series. The age of the test specimens varied from 16 days to 20 days.

2.4.1.3 Series III

All four specimens were cast together in order to minimize the variation in concrete properties. In all four, 6 in. x 12 in. (152 mm x 305 mm) concrete cylinders were tested. The average concrete compressive strength at the time of testing was 3400 psi (23.4 MPa) for this series. The age of the specimens at the time of testing was 30 days to 32 days.

2.4.2 Reinforcing Steel

The properties of the reinforcing bars used in these experiments are shown in Table 2.2.

2.4.3 Embedded Structural Steel Members

The minimum specified yield strengths for the hollow structural sections, the square solid steel sections and the wide flange sections were 50 ksi (345 MPa), 47 ksi (324 MPa) and 44 ksi (303 MPa) respectively.

TABLE 2.2

PROPERTIES OF REINFORCING BARS

BAR SIZE DESIGNATION	DIAMETER		AREA		YIELD STRENGTH	
	in.	mm	in^2	mm^2	ksi	MPa
#3	0.375	9.5	0.11	71	73.0	503
#4	0.500	12.7	0.20	127	48.9	337
#6	0.625	15.9	0.31	198	60.3	416
#8	1.000	25.4	0.79	507	59.5	410

2.5 Test Set-Up

2.5.1 Series I

The test set-up for the specimens of Series I is shown in Fig. 2.8. The axial load was applied using a 100 ton (890 kN) capacity hydraulic loading ram. The shear in the connection was applied by a 30 ton (267 kN) capacity loading ram acting through a 100 kip (445 kN) capacity load cell. The ends of the columns were braced against lateral movement with two pairs of 3/4 in . (19 mm) diameter tie rods and freedom of rotation of the ends was obtained through the use of two ball joints.

2.5.2 Series II and Series III

2.5.2.1 Embedded Members Protruding from One Side

The test set-up for specimens with embedded members protruding from one side only is shown in Fig. 2.8. The axial load was applied through the head of a 400 kip (1780 kN) capacity Baldwin Universal Testing Machine. The shear in the connection was applied using a 100 ton (890 kN) capacity hydraulic loading ram acting through a 100 kip (445 kN) capacity load cell. The ends of each column were braced against lateral movement by two pairs of 3/4 in. (19 mm) diameter tie rods and ball joints were placed at the top and bottom of the column to allow rotation of the ends.

2.5.2.2 Embedded Members Protruding from Two Sides

The test set-up for specimens with embedded members protruding from opposite sides of a column is shown in Fig. 2.9. The load was applied to the column through a ball joint by the Baldwin Universal Testing Machine and the load was reacted through two rollers placed under the embedded structural steel member.

2.5.2.3 Pure Moment Tests

Specimens TC3 and TC4 were tested under pure moment as shown in Fig. 2.7. Equal and opposite forces were applied to the two arms of the embedded steel member by two 30 ton (267 kN) capacity hydraulic loading rams at eccentricities of 4 in. (102 mm) from the column face. The column was braced against lateral motion at the ends by two pairs of 3/4 in. (19 mm) diameter tie rods.

2.6 Instrumentation

The axial load in the columns of Series I was monitored by a pressure gauge in the hydraulic system. The axial load in the columns of Series II and Series III was monitored by the load cell in the Baldwin Universal Testing Machine. The load in the connection was monitored by a load cell and also by a pressure gauge in the hydraulic system. The deflection of the embedded steel member relative to the column at the point of application of the load was measured by a dial gauge to the nearest 0.001 inches (0.025 mm). Concrete strain measurements were taken in the region of bearing of the embedded steel member in order to determine the maximum strain on the surface and the strain distribution across the width of the connection. Reinforcing bar strain measurements were taken to determine the maximum steel strain at failure. The concrete strains were measured with 20 mm gauge length electrical resistance strain gauges. The strains in the reinforcing bars were measured using 10 mm gauge length electrical resistance strain gauges. The positions of the strain gauges for specimen C1 are shown in Fig. 2.10. The positions of the strain gauges for specimens C2, C3, C4, TC4 and all the specimens of Series II are shown in Fig. 2.11. The positions of the strain gauges in specimen TC3 are shown in Fig. 2.12. Specimen TC2 had the same strain gauge

instrumentation as TC3. The additional strain gauges in specimens TC2 and TC3 through the depth of the connection above and below the embedded steel member were used to determine the strain variation in the concrete along the length of the embedded member. Specimen TC1 had only one strain gauge positioned on the surface of the concrete at 1.0 inches (25.4 mm) above the center of the steel member.

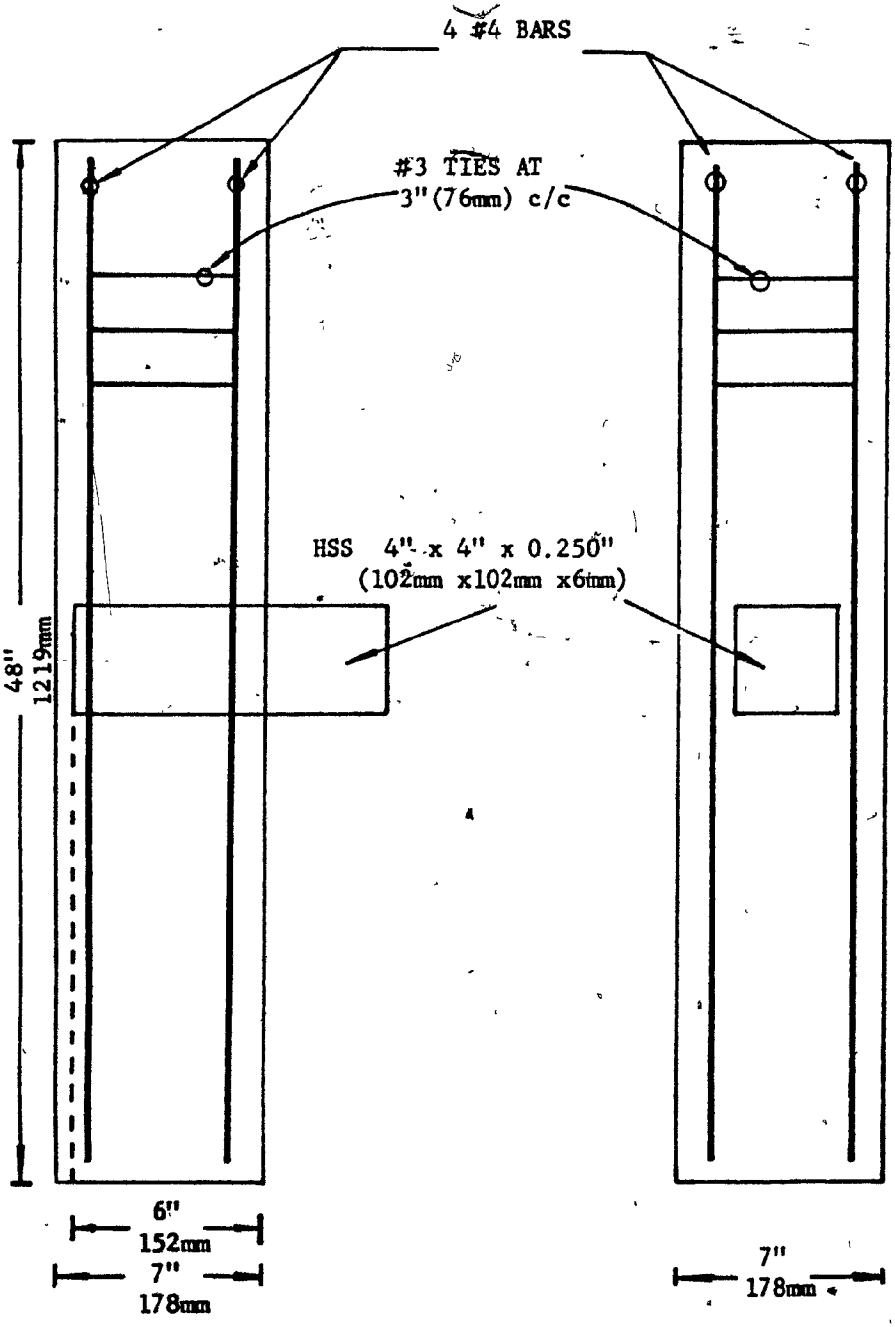

Figure 2.1 Typical test specimen used in Series I

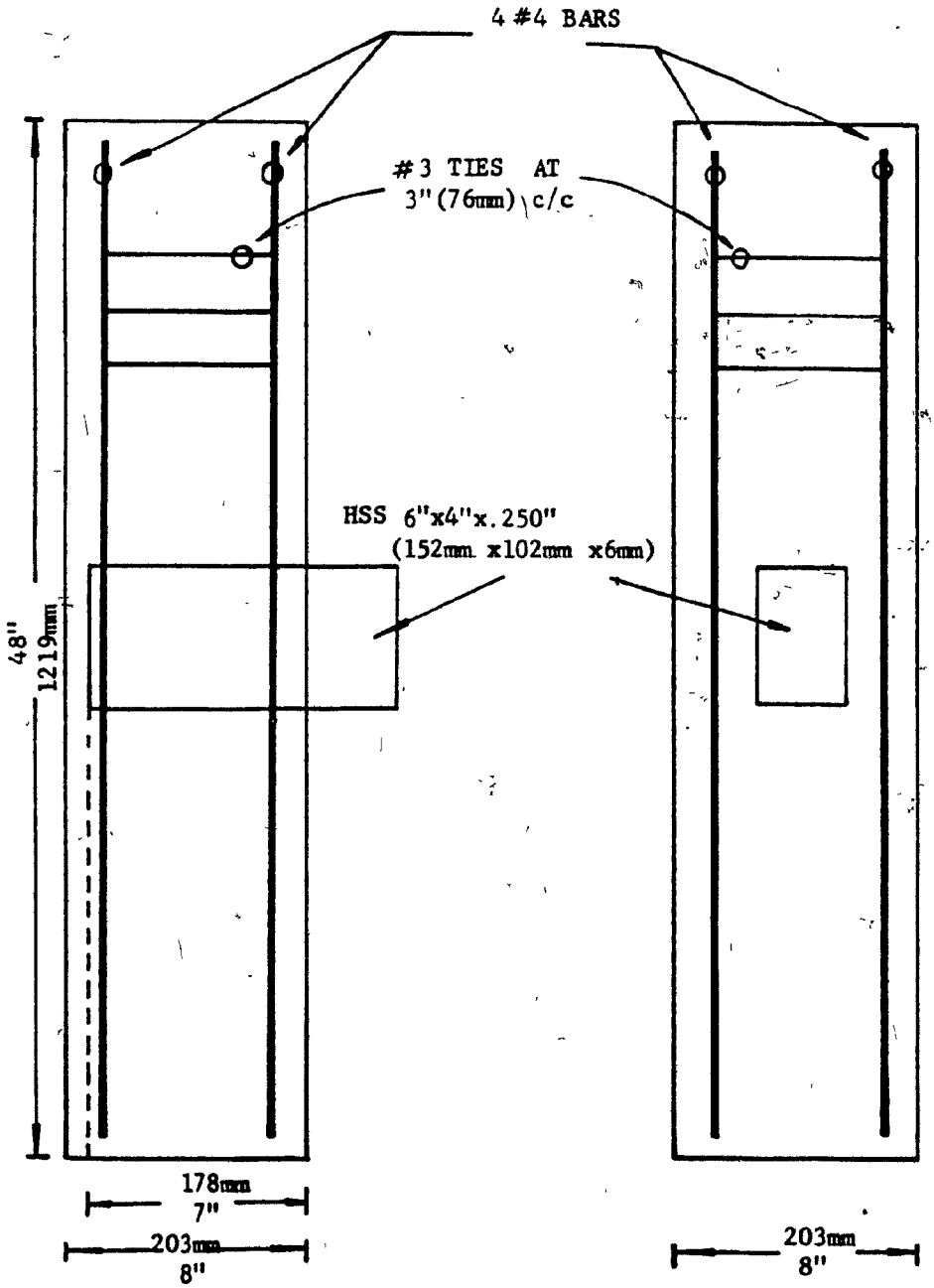

Figure 2.2 Typical test specimen used in Series II

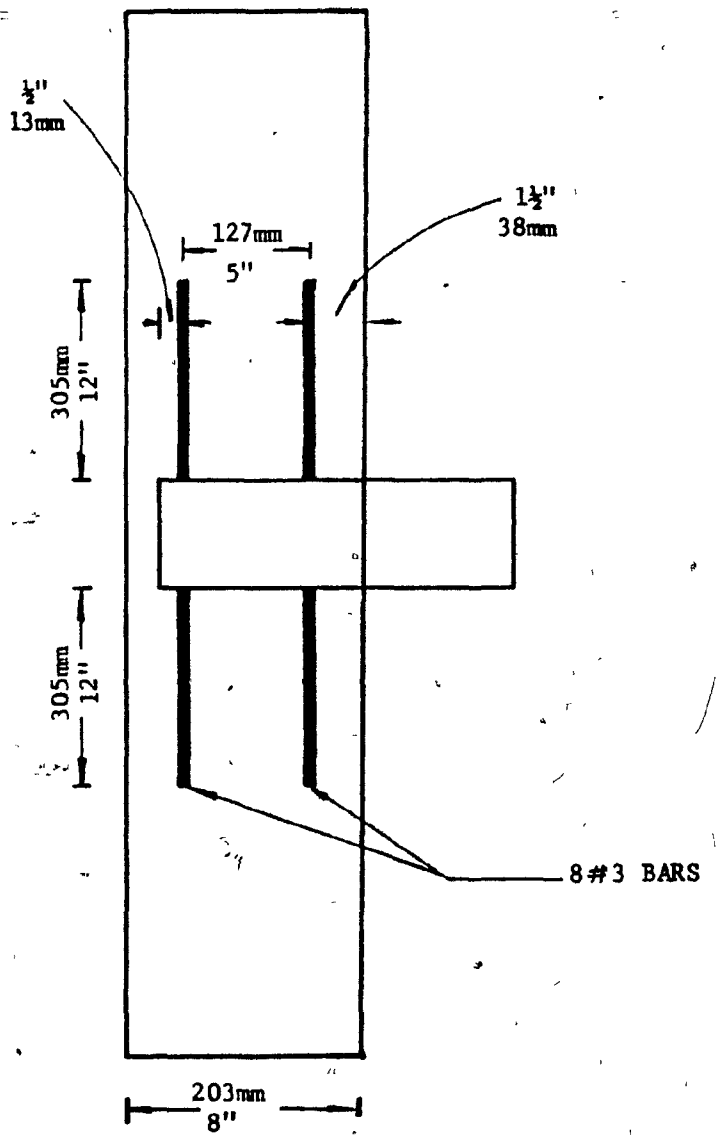

Figure 2.3 Test specimen with additional welded reinforcement

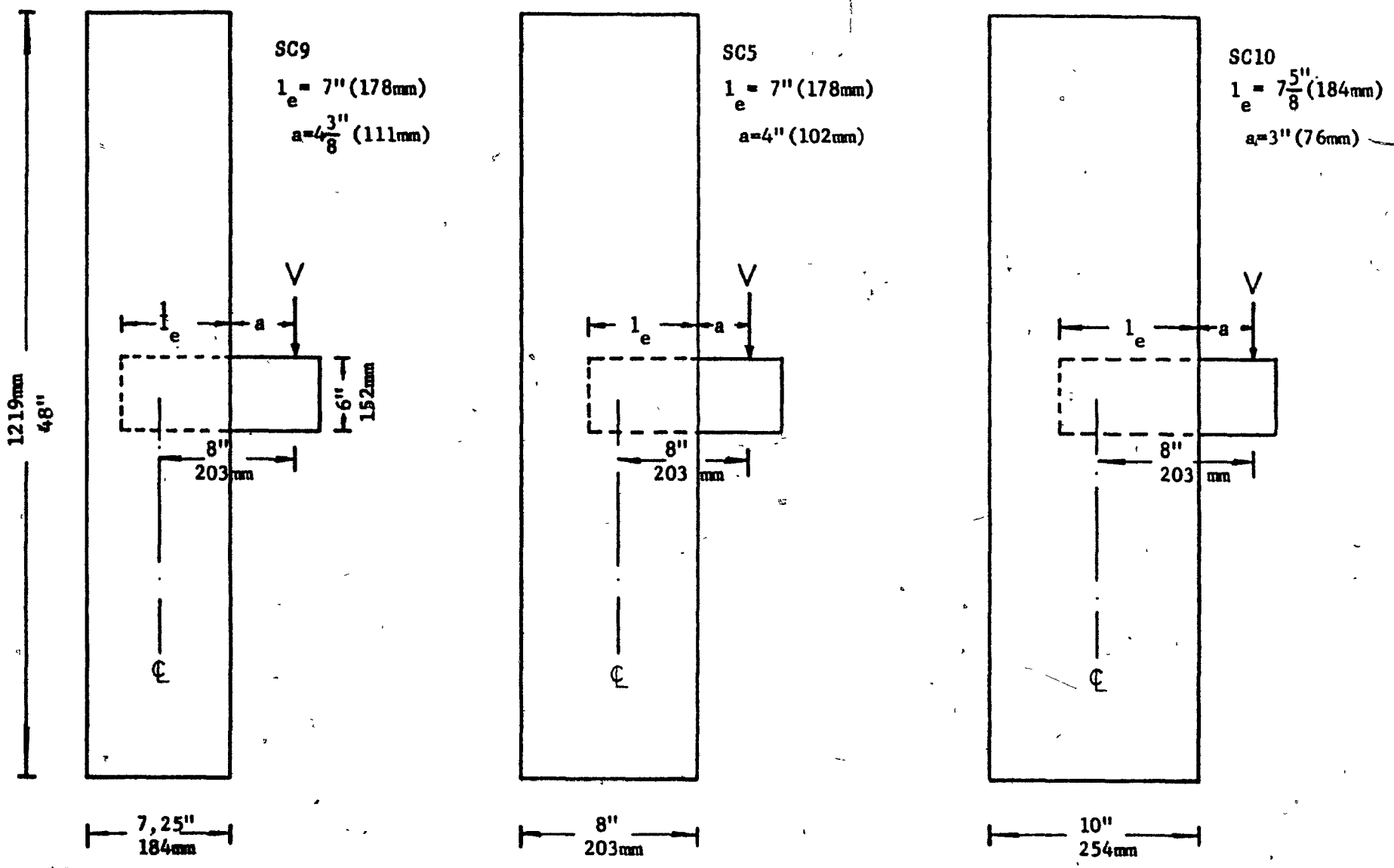

Figure 2.4 Specimens SC9, SC5 and SC10 - specimens with different concrete covers

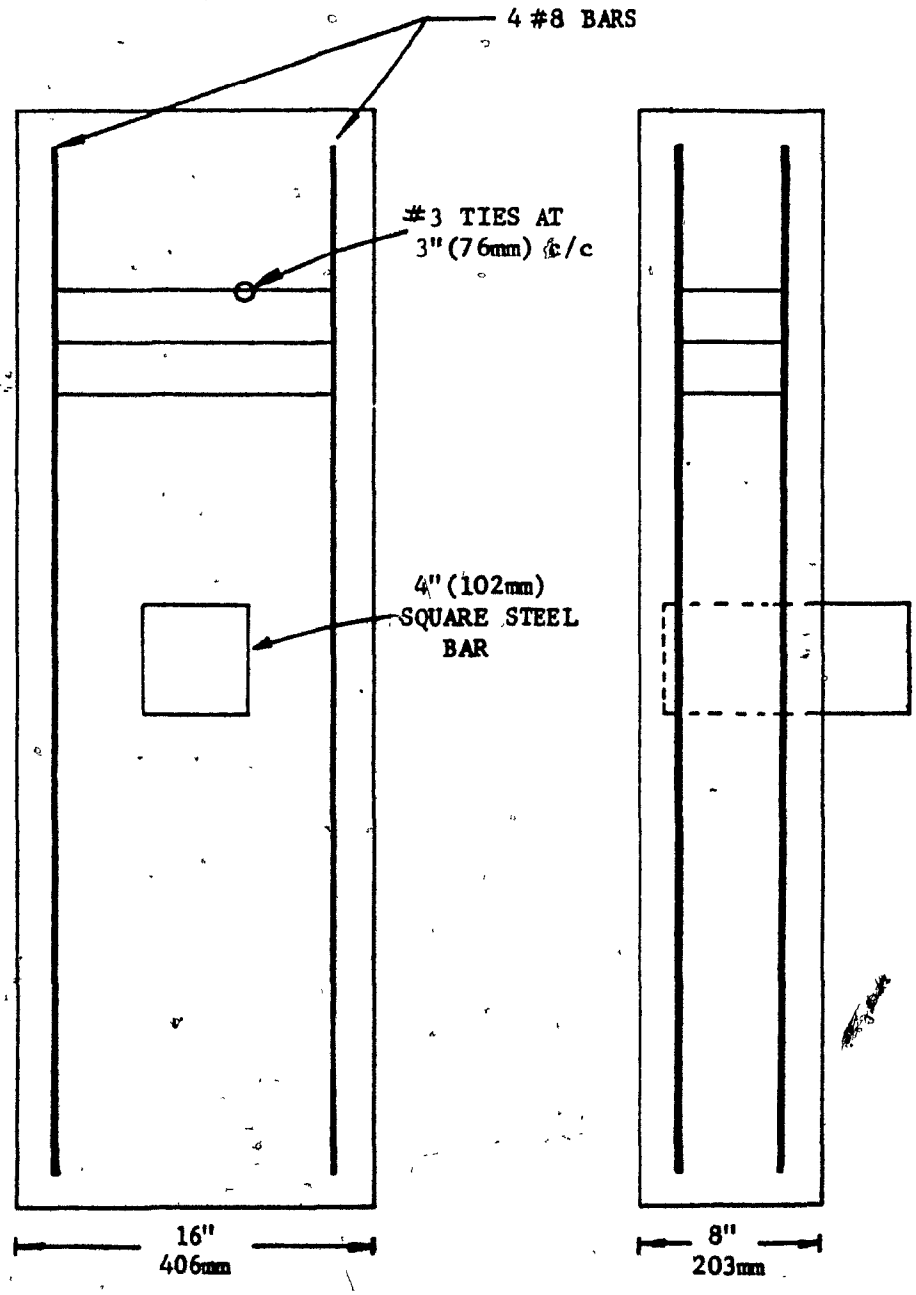

Figure 2.5 Specimen TC1 - very wide column

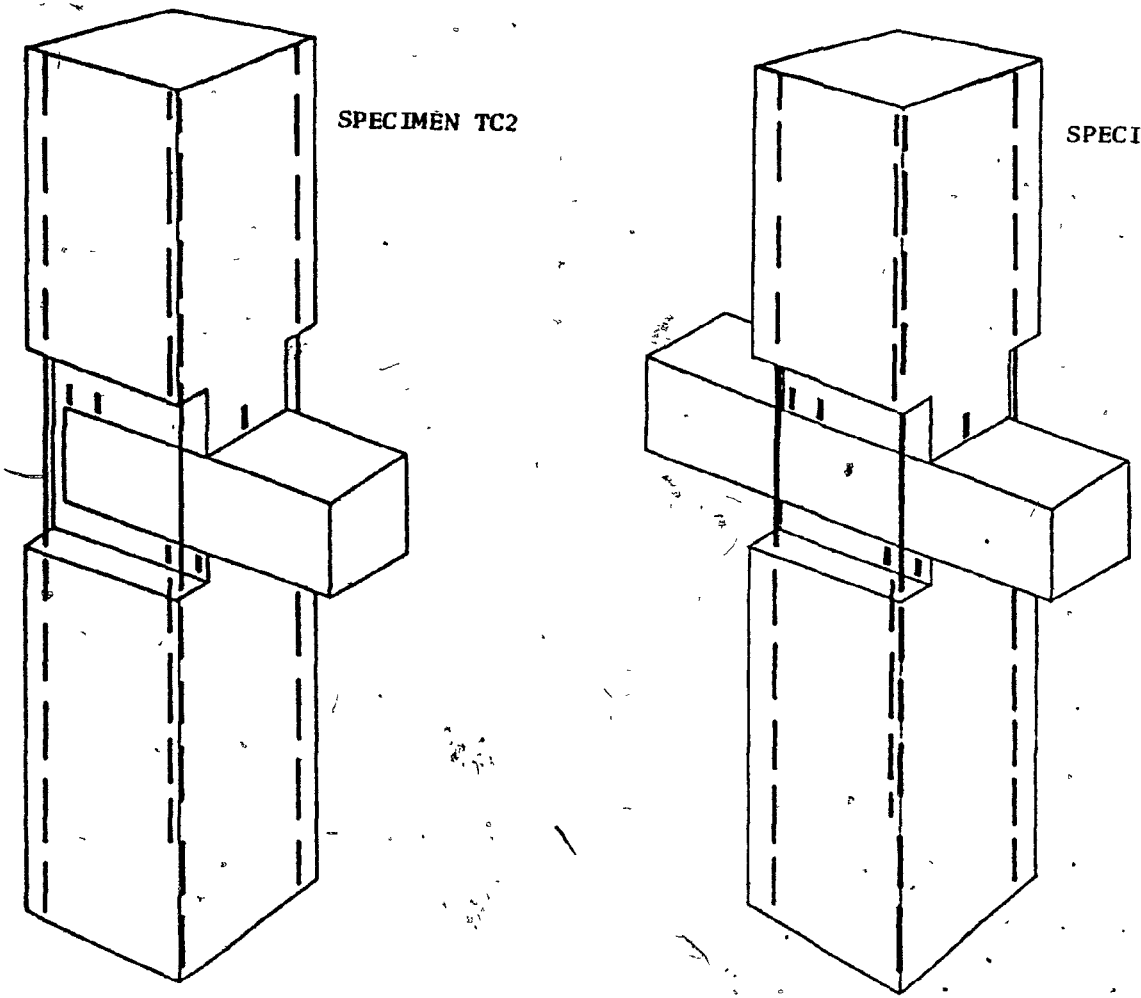

Figure 2.6 Specimens TC2 and TC3

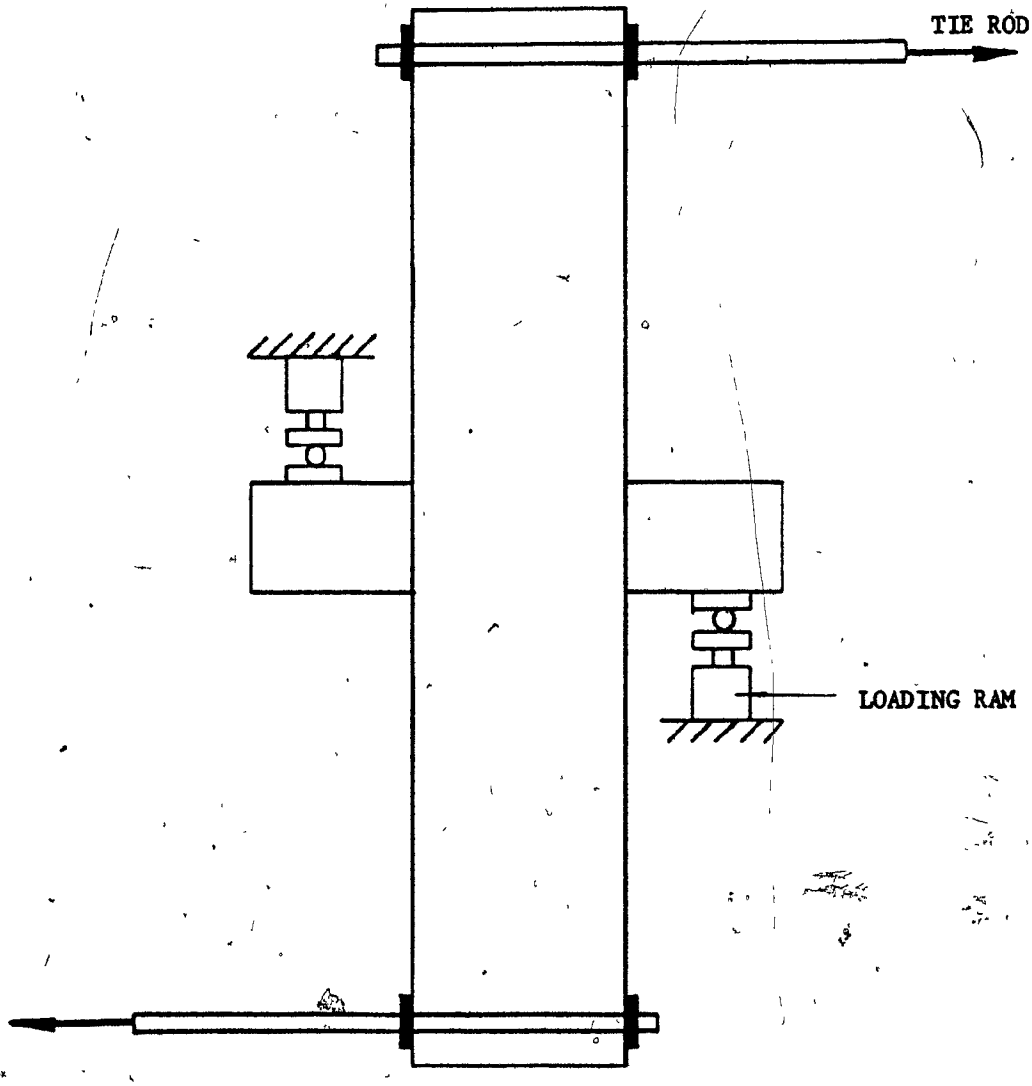

Figure 2.7 Set-up for pure moment tests

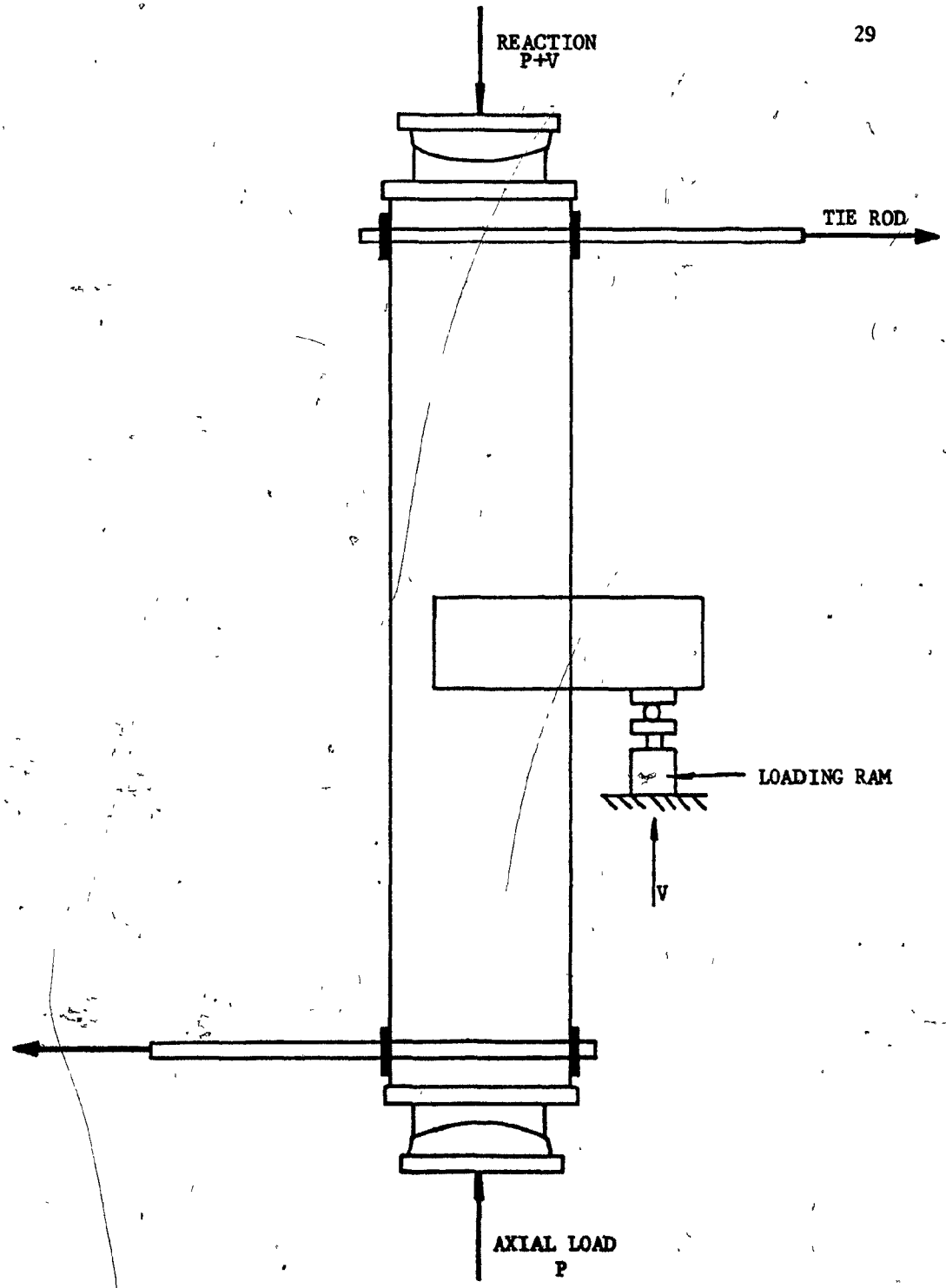

Figure 2.8 Set-up for connections with steel members protruding from one side only

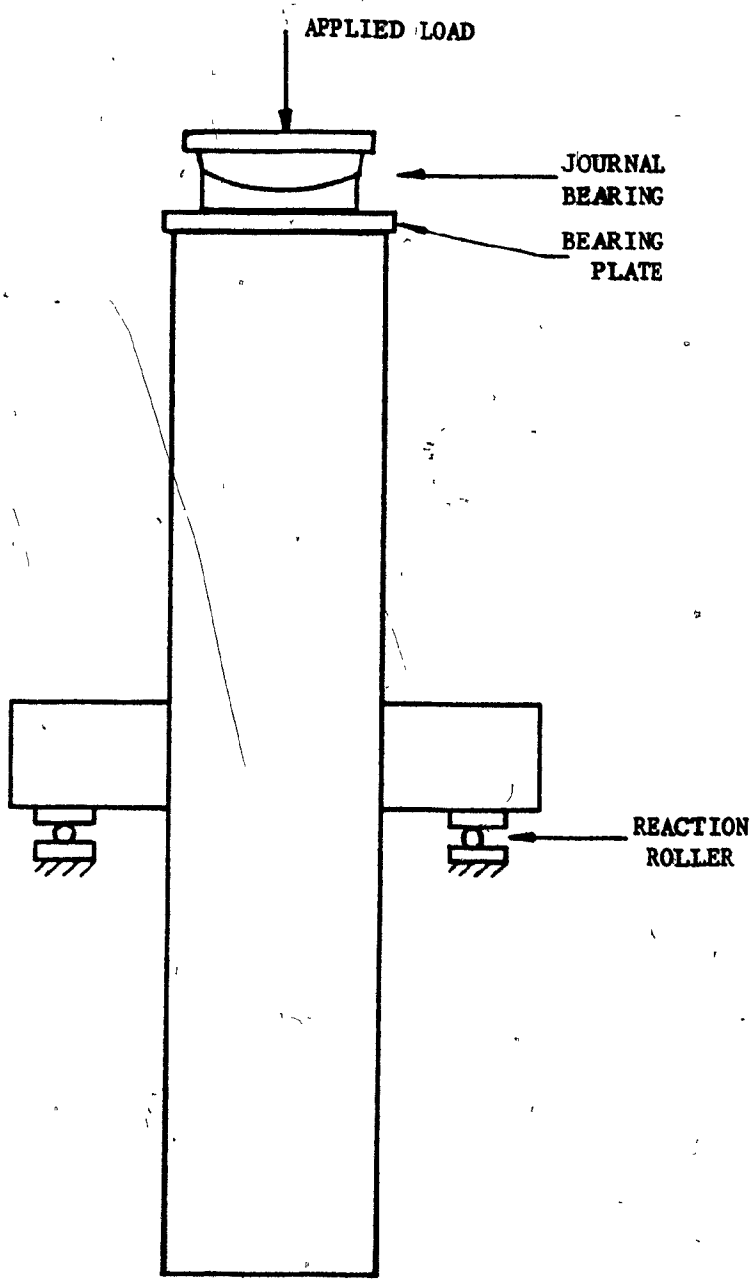

Figure 2.9 Set-up for connections with steel members protruding from two sides

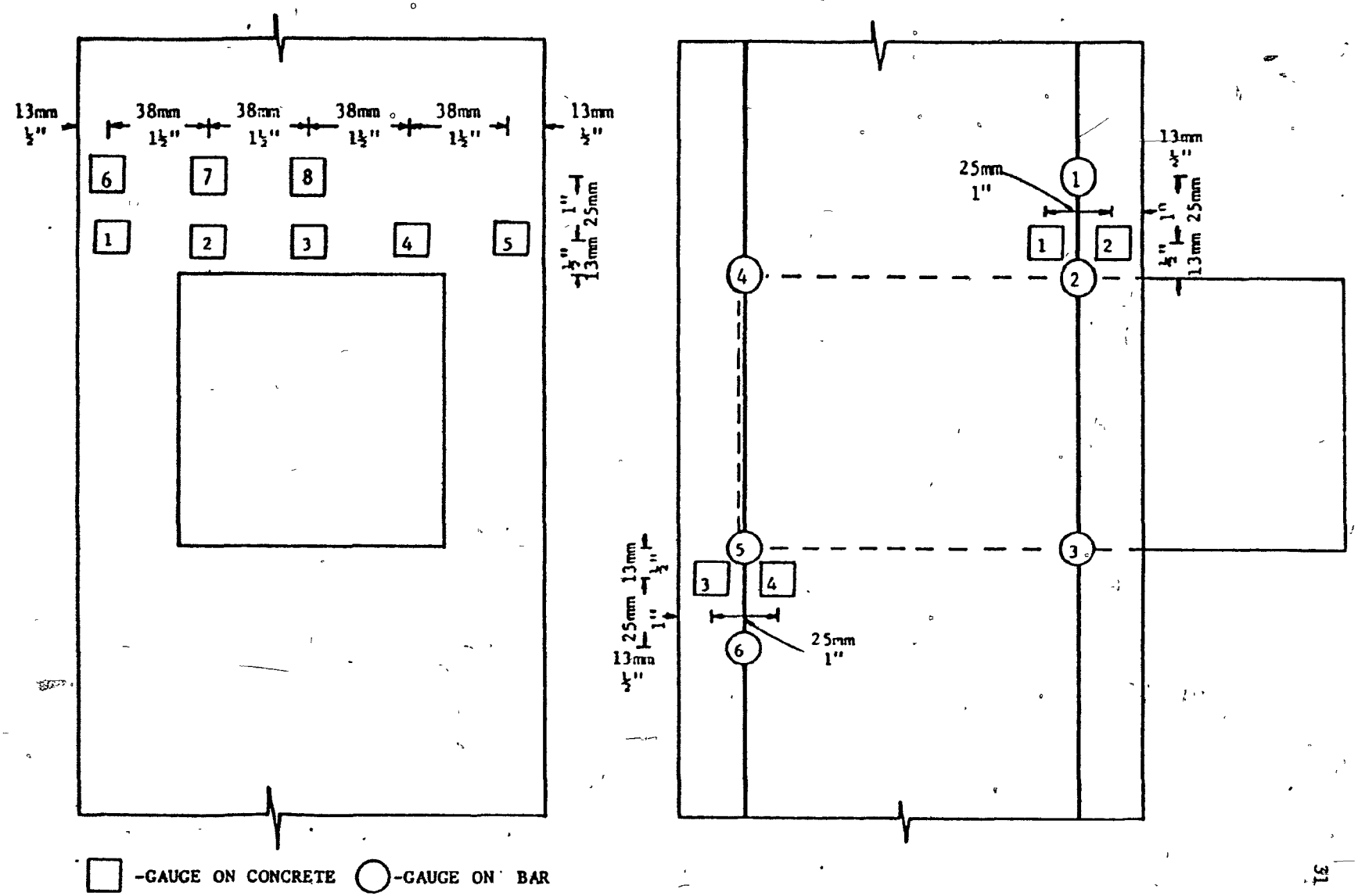

Figure 2.10 Strain gauge locations for specimen C1

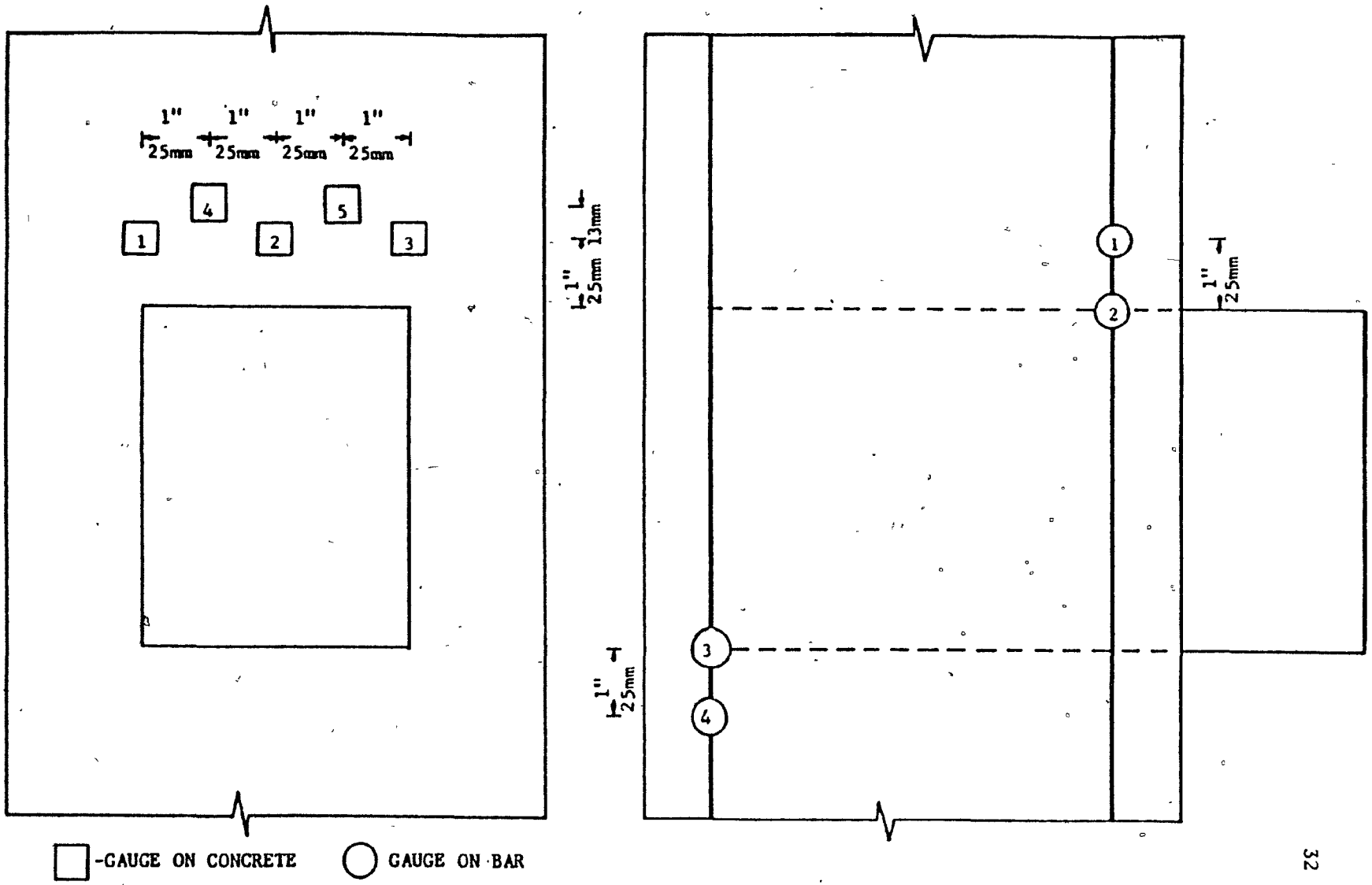

Figure 2.11 Strain gauge locations for specimens C2, C3, C4, TC4 and all the specimens of Series II

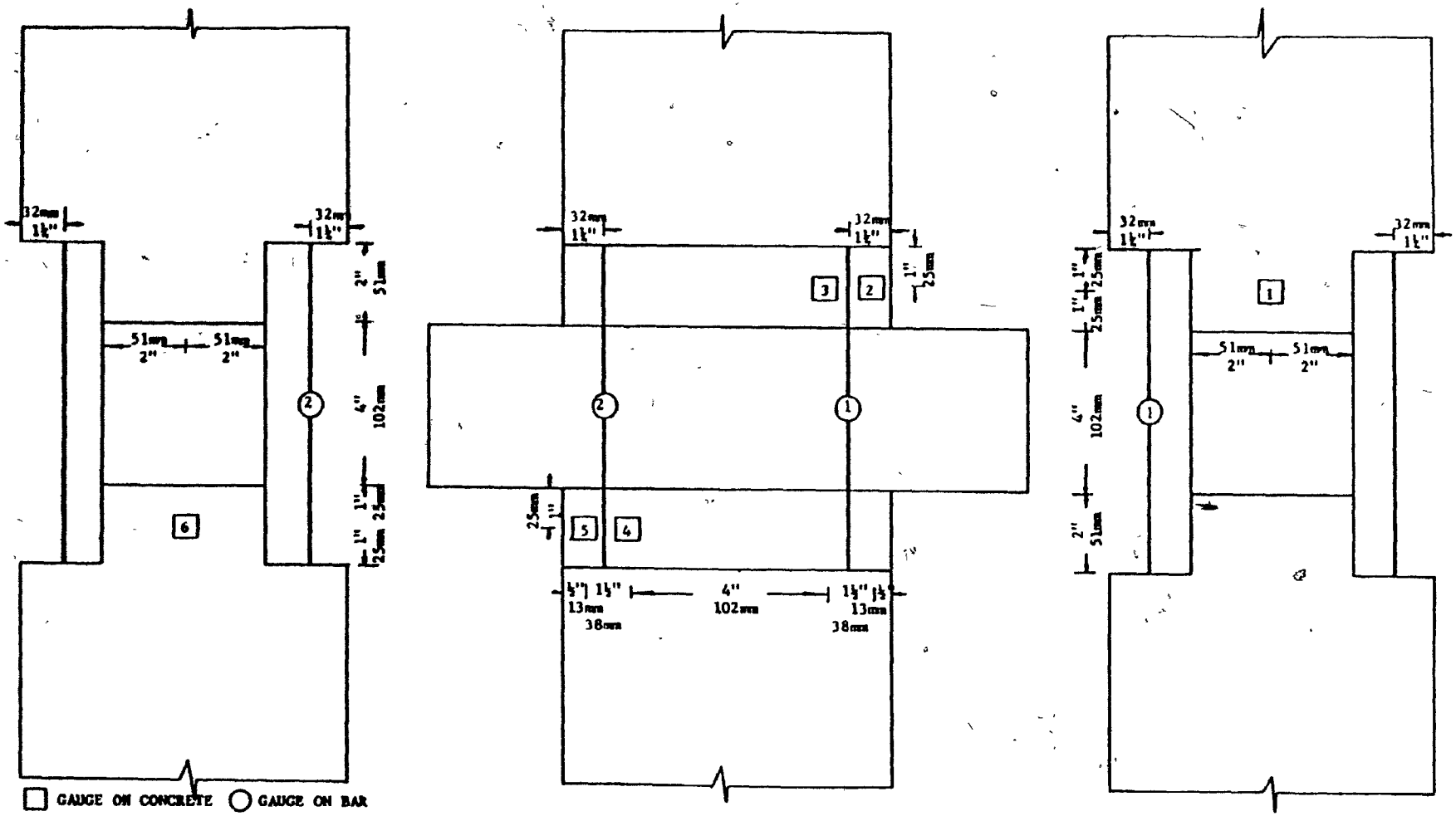

Figure 2.12 Strain gauge locations for specimens TC2 and TC3

CHAPTER 3 BEHAVIOUR OF TEST SPECIMENS

The experimental results of all the specimens are given in the tables of Appendix A. A summary of the significant behavioural observations in the response of each specimen is given in Table 3.1. The shear, V, and the deflection, Δ, are listed in Table 3.1 for each specimen for the following stages:

a] separation of the bottom of the embedded steel member from the concrete

b] first appearance of the inclined vertical cracking on the front face of the column at the upper edges of the steel member.

c] first appearance of diagonal cracking on the sides of the columns.

d] first yielding of the reinforcing bars of the column.

e] observed spalling of the concrete at the front face of the column directly above the embedded steel member.

f] the ultimate capacity of the connection.

3.1 Series I

The four specimens of Series I (C1, C2, C3 and C4) contained 4 in. x 4 in. x 0.250 in. (102 mm x 102 mm x 6 mm) hollow structural steel members and were tested under axial loads of zero, 30 kips(133.4 kN), 60 kips(266.9 kN) and 90 kips(400.3 kN) respectively.

	SEPARATION				INCLINED VERTICAL CRACKING				CRACKING IN SIDES				YIELDING IN BARS				SPALLING OF COVER				ULTIMATE CAPACITY			
	V		Δ		V		Δ		V		Δ		V		Δ		V		Δ		V		Δ	
SPECIMEN	kips	kN	in.	mm	kips	kN	in.	mm	kips	kN	in.	mm	kips	kN	in	mm	kips	kN	in.	mm	kips	kN	in.	mm
SERIES I																								
C1	6.5	29	.002	0.15	9.0	40	.006	.15	10.4	47	.009	.23	-	-	-	-	15.6	70	.023	.58	27.8	125	.032	.81
C2	7.0	31	.002	0.15	27.0	121	.022	.56	29.0	130	.029	.74	-	-	-	-	33.0	148	.049	1.24	41.4	184	.230	5.84
C3	10.0	45	.002	0.15	30.0	134	.023	.58	30.0	134	.023	.58	-	-	-	-	37.0	166	.139	3.53	45.0	202	.400	10.16
C4	10.0	45	.010	0.25	48.0	215	.104	2.64	46.8	210	.078	1.98	-	-	-	-	53.5	240	.200	5.08	53.5	240	.200	5.08
SERIES II																								
SC2	20.8	93	.011	0.28	48.0	215	.030	.76	48.0	215	.030	.76	-	-	-	-	51.9	233	.034	.86	55.8	250	.072	1.83
SC3	55.0	246	.027	0.69	62.8	281	.035	.89	62.8	281	.035	.89	-	-	-	-	66.8	299	.039	.99	70.7	317	.089	2.26
SC4	47.1	211	.019	0.48	55.0	246	.036	.91	64.8	290	.083	2.11	66.8	299	.111	2.82	62.8	281	.073	1.85	66.8	299	.111	2.82
SC5	11.8	53	.005	0.13	17.7	79	.012	.30	19.6	88	.015	.38	51.0	228	.025	.64	41.2	185	.047	1.19	55.0	246	.152	3.86
SC6	19.6	88	.011	0.28	51.0	228	.066	1.68	35.3	158	.029	.74	59.3	266	.110	2.79	58.9	264	.095	2.41	60.9	273	.131	3.33
SC7	23.6	106	.013	0.33	39.3	176	.028	.71	47.1	211	.040	1.02	78.6	352	.100	2.54	64.8	290	.067	1.70	80.5	361	.135	3.43
SC8	17.7	79	.008	0.20	39.3	176	.024	.61	35.3	158	.020	.51	83.5	374	.199	5.05	66.8	299	.057	1.45	83.5	374	.199	5.05
SC9	7.9	35	.004	0.10	31.4	141	.035	.89	11.8	53	.006	.15	43.2	194	.157	3.99	43.2	194	.080	2.03	49.1	220	.157	3.99
SC10	19.6	88	.006	0.15	31.4	141	.014	.36	31.4	141	.014	.36	-	-	-	-	51.1	229	.038	.97	62.8	281	.089	2.26
SC11	28.0	125	.001	0.03	130.0	582	.051	1.30	125.0	560	.046	1.17	-	-	-	-	150.0	672	.065	1.65	220.0	986	.230	5.84
SC12	40.0	179	.035	0.89	140.0	627	.113	2.87	130.0	582	.072	1.83	-	-	-	-	160.0	717	.165	4.19	212.0	950	1.150	29.21
SC13	40.0	179	.018	0.46	110.0	493	.042	1.07	130.0	582	.056	1.42	-	-	-	-	180.0	806	.117	2.97	210.0	941	.250	6.35
SERIES III																								
TC1	17.7	79	.012	0.30	29.4	131	.026	.66	41.2	183	.050	1.27	-	-	-	-	47.1	211	.066	1.68	58.9	264	.193	4.90
TC2	6.5	29	.027	0.69	-	-	-	-	13.0	58	.012	.30	-	-	-	-	31.2	140	.120	3.05	32.3	145	.141	3.58
TC3	5.2	23	.027	0.69	-	-	-	-	-	-	-	-	-	-	-	-	16.9	76	.185	4.70	17.5	78	.230	5.84
TC4	5.2	23	.013	0.33	20.8	92	.111	2.82	10.4	46	.041	1.04	16.0	72	.079	2.01	26.0	116	.198	5.03	26.0	116	.198	5.03

TABLE 5.1 SIGNIFICANT BEHAVIOURAL OBSERVATIONS

3.1.1 Specimen C1 - zero axial load test

The load deflection response and a photograph of specimen C1 after failure are shown in Fig. 3.1. The load deflection curve remained linear up to a load of 6.5 kips (28.9 kN) on the connection. At this point the bottom of the embedded steel member separated from the concrete below it. At a load of 9.0 kips(40.0 kN) and a deflection of 0.006 inches (0.15 mm) inclined vertical cracks appeared at the two top corners of the embedded hollow steel member. As the load increased these cracks widened and extended towards the edges of the column. Diagonal cracks appeared in the sides of the column in the region of the connection when a load of 10.4 kips(46.3 kN) was reached. At a load of 19.5 kips(86.7 kN) inclined vertical cracks appeared at the back of the column just below the connection. The concrete cover on the front face of the column just above the embedded steel member began spalling at a load of 15.6 kips(69.4 kN) and a deflection of 0.023 in. (0.58 mm). This was confirmed by the sudden drop in concrete strain after reaching a maximum measured strain of 0.0029 on the front face of the connection. At this load bending of the top wall of the hollow structural member was observed. This localized bending was due to the bearing of the concrete against the thin wall of the steel member. At a load of 22.75 kips(101.2 kN) crushing of the concrete above the corners of the embedded steel member was apparent. From that point on, the load deflection curve is relatively flat with the maximum load of 27.8 kips(123.6 kN) being attained at a deflection of 0.32 in (8.13 mm).

Concrete strain measurements on gauges 1 to 5 indicate that after the onset of inclined vertical cracking the largest strains occur above the vertical walls of the steel member with smaller strains towards the center of the thin walled hollow section and very small strains at the edges of the column. In subsequent tests it was decided to fill the steel member with

concrete in order to provide a more uniform bearing surface. There was no yielding of the reinforcing bars of the column.

3.1.2 Specimen C2 - constant axial load of 30 kips (133 kN)

The load deflection curve and a photograph of specimen C2 at failure are shown in Fig. 3.2. The first sign of distress in this specimen was the appearance of a separation crack between the concrete and the bottom of the embedded steel member at a load of 7 kips(31.1 kN) and a deflection of 0.002 in (0.05 mm). The load deflection curve indicates a decrease in stiffness of the connection at this point. The load deflection curve remained essentially linear up to a load of 27.0 kips(120.1 kN) and a deflection of 0.022 in. (0.56 mm) at which point inclined vertical cracks appeared in the concrete face at the two upper corners of the embedded hollow steel member.. From this point on the stiffness of the connection gradually decreased.

Diagonal cracks on the sides of the column appeared at a load of 29.0 kips(129.0 kN). At a load of 33.0 kips(146.8 kN) and a concrete strain of 0.0032 the concrete cover at the front face began to spall. The ultimate load was 41.4 kips(184 kN) at a deflection of 0.230 inches (5.83 mm). There was no measured yielding of the reinforcing bars of the column.

3.1.3 Specimen C3 - constant axial load of 60 kips (267 kN)

The load deflection curve and a photograph of specimen C3 at failure are shown in Fig. 3.3. Separation of the bottom of the embedded hollow steel member from the concrete occured at a load of 10.0 kips(44.5 kN) and a deflection of 0.002 in. (0.05 mm). The inclined vertical cracks at the top corners of the embedded steel member appeared at a load of 30.0 kips(133.4 kN) and a deflection of 0.023 in. (0.58 mm). The diagonal cracks on the sides

of the column also appeared at this load.

The concrete cover on the face of the column above the embedded steel member began to spall off at a load of 37.0 kips(164.6 kN) and a concrete strain 0.0029. At a load of 44.1 kips(196.2 kN) crushing of the concrete on the back of the column just below the embedded steel member was observed. At this point the sides of the hollow steel member showed signs of local buckling due to the large shear force. The ultimate load of 45.0 kips(200.2 kN) occurred at a deflection of 0.400 in. (10.16 mm). There was no yielding of the reinforcing steel in the column.

3.1.4 Specimen C4 - constant axial load of 90 kips (400 kN)

The load-deflection curve and a photograph of specimen C4 at failure are shown in Fig. 3.4. Separation of the bottom of the embedded steel member from the concrete occurred at a load of 10.0 kips(44.5 kN) and a deflection of 0.010 in. (0.25 mm). Diagonal cracks appeared on the sides of the column at a load of 46.8 kips(208.2 kN). The inclined vertical cracks at the corners of the embedded steel member appeared at a load of 48.0 kips(213.5 kN) and a deflection of 0.104 in. (2.64 mm).

The stiffness of the connection deteriorated very quickly beyond this load stage. There were no signs of spalling or crushing until the ultimate load of 53.5 kips(238.0 kN) was reached. At this point extensive crushing appeared on both the front and back faces of the column. The deflection at the point of ultimate load was 0.20 inches (5.08 mm). There was no yielding of the reinforcing bars of the column.

3.2 Series II

All the test specimens except SC6 and SC12 incorporated 6 in. x 4 in. x

0.375 in. (152 mm x 102 mm x 10 mm) hollow structural steel members. Specimens SC6 and SC12 incorporated wide flanged members with the same width and a comparable stiffness to that of the hollow structural steel members. Specimen SC1 was tested under pure axial load. Specimens SC2, SC3, and SC4 were tested under axial loads of 240 kips(106.7 kN), 160 kips(711.7 kN) and 80 kips(355.8 kN) respectively. The other specimens were tested under zero axial load. Specimens SC7 and SC8 were reinforced with four #3 bars welded to the embedded steel member. Specimens SC9 and SC10 had concrete covers of zero and 1 1/2 in. (38 mm) whereas the other specimens had 1/2 in. (13 mm) covers. Specimens SC11, SC12, and SC13 had embedded steel members which protruded from both sides of the column.

3.2.1 Specimen SC1 - Pure Axial Load Test

The load deflection response for this axially loaded member and a photograph of speciment SC1 at failure are shown in Fig. 3.5. The shortening of the column was measured over a gauge length of 6 inches (152 mm). Failure occurred in the bottom third of the column at a load of 326.0 kip (1450 kN) and a deflection of 0.017 in.(0.43 mm). The column reinforcing steel in the region of the connection did not yield.

3.2.2 Specimen SC2 - Constant Axial Load of 240 kips (1068 kN)

The load deflection response and a photograph of specimen SC2 at failure are shown in Fig. 3.6. Separation of the bottom of the embedded steel member from the concrete occurred at a load of 20.8 kips(92.5 kN) and a deflection of 0.011 in.(0.28 mm). The inclined vertical cracks in the concrete at the top corners of the embedded steel member and the diagonal cracks on the sides of the column appeared at a load of 48.0 kips(213.5 kN).

Spalling of the concrete cover began at a load of 51.9 kips(230.8 kN). The maximum recorded strain on the front face of the column was 0.004.

The ultimate load of 55.8 kips(248.2 kN) was reached at a deflection of 0.072 inches (1.83 mm). There as no measured yielding of the reinforcing steel of the column.

3.2.3 Specimen SC3 - Constant Axial Load of 160 kips(712 kN)

The load deflection response and a photograph of specimen SC3 at failure are shown in Fig. 3.7. Separation of the bottom of the embedded steel member from the concrete did not occur until a load of 55.0 kips(244.6 kN). At a load of 62.3 kips(279.3 kN) inclined vertical cracks formed in the concrete at the top corners of the steel member and diagonal cracks formed in the sides of the column. Spalling of the concrete cover began at a load of 66.8 kips(297.1 kN) with the ultimate load of 70.7 kips(314.5 kN) being reached at a deflection of 0.089 inches (2.26 mm). The maximum strain on the front face of the column was 0.0039. The column reinforcement did not yield.

3.2.4 Specimen SC4 - Constant Axial Load of 80 kips(356 kN)

The load deflection response and a photograph of specimen SC4 at failure are shown in Fig. 3.8. Separation of the bottom of the steel member from the concrete occurred at a load of 47.1 kips(209.5 kN). At a load of 55.0 kips(244.6 kN) inclined vertical cracks appeared in the concrete at the top corners of the embedded steel member. The stiffness of the connection quickly decreased after this load stage. The concrete cover above the steel member began to spall at a load of 62.8 kips(279.3 kN) and as strain of 0.0030. When the load reached 64.8 kips(288.2 kN) diagonal cracks formed

in the sides of the column in the region of the embedded steel member. Yielding of the reinforcing steel in the column occurred at the ultimate load on the connection of 66.8 kips(297.1 kN). The deflection at the ultimate load was 0.111 inches (2.82 mm).

3.2.5 Specimen SC5 - Zero Axial Load Test

The load deflection response and a photograph of specimen SC5 at failure are given in Fig. 3.9. Separation of the bottom of the steel member from the concrete occurred at a load of 11.8 kips(52.5 kN) and a deflection of 0.005 inches (0.13 mm). Inclined vertical cracks formed in the concrete at the top corners of the steel member at a load 17.7 kips (78.7 kN). Diagonal cracks appeared on the side of the column at a load of 19.6 kips(87.2 kN). The reinforcing steel in the column began yielding at a load of 51.0 kips(226.8 kN). The concrete cover spalled at a load of 41.2 kips(183.2 kN) and the ultimate load of 55.0 kips(244.6 kN) occurred at a deflection of 0.152 inches (3.86 mm). The maximum recorded concrete strain on the column face was 0.0032.

3.2.6 Specimen SC6 - Wide Flange Embedded Member

The load deflection curve and a photograph of specimen SC6 at failure are shown in Fig. 3.10. Separation of the bottom of the embedded wide flange steel member from the concrete occurred at a load of 19.6 kips (87.2 kN). Inclined vertical cracks formed in the concrete at the tip of the bottom flange of the steel member and diagonal cracks appeared in the side of the column at a load of 35.0 kips(155.7 kN). When the load reached 51.0 kips(226.8 kN) inclined vertical cracks appeared in the concrete at the tips of the top flange of the steel member. The longitudinal steel in the column yielded at a load of 59.3 kips(263.8 kN) on the connection.

The concrete cover began to spall at a load of 58.9 kips(262.0 kN) and as maximum strain of 0.0068. The ultimate load of 60.9 kips(270.9 kN) occurred at a deflection of 0.131 inches (3.33 mm).

3.2.7 Specimen SC7 - Member with Additional Welded Reinforcement

The load deflection curve and a photograph of specimen SC7 at failure are shown in Fig. 3.11. Separation of the bottom of the steel member from the concrete occurred at a load of 23.6 kips(105.0 kN). The inclined vertical cracks on the face of the column at the top corners of the steel member occurred at a load of 39.3 kips(174.8 kN) while the diagonal cracks on the sides of the column appeared at a load of 47.1 kips(209.5 kN). The concrete cover spalled at a load of 64.8 kips(285.2 kN) and a strain of 0.0035. The ultimate load of 80.5 kips(358.1 kN) occurred at a deflection of 0.135 inches (3.43 mm). The longitudinal reinforcing steel in the column yielded at a load of 78.6 kips (349.6 kN). This specimen contained additional reinforcement welded to the top and bottom of the embedded steel member. The weld between one of the bars of additional reinforcement and the steel member failed at ultimate.

3.2.8 Specimen SC8 - Member with Additional Welded Reinforcement

The weld failure in specimen SC7 made it necessary to repeat the test with this identical specimen in order to confirm the test results.

The load deflection curve and a photograph of specimen SC8 at failure are shown in Fig. 3.12. Separation of the bottom of the embedded steel member from the concrete occurred at a load of 17.7 kips(78.7 kN). Inclined vertical cracks in the column face at the top corners of the steel member appeared at a load of 39.3 kips(174.8 kN) and diagonal cracks in the sides of the column formed at a load of 35.3 kips(157.0 kN). The concrete cover spalled

at a load of 66.8 kips(297.1 kN) and a strain of 0.0032. The ultimate load of 83.5 kips(371.4 kN) occurred at a deflection of 0.199 inches (5.05 mm). The longitudinal steel in the column yielded at ultimate. Specimen SC8 failed at a load which was 4% higher than that of specimen SC7 and exhibited a deflection at ultimate which was 47% larger.

3.2.9 Specimen SC9 - Column with Zero Concrete Cover

The load deflection curve and a photograph of specimen SC9 at failure are shown in Fig. 3.13. Separation of the bottom of the embedded steel member from the concrete occurred at a load of 7.9 kips(35.1 kN). The diagonal cracks on the sides of the column appeared at a load of 11.8 kips(52.5 kN) however, the inclined vertical cracks on the column face at the top corners of the steel member did not form until a load of 31.4 kips(139.7 kN). The concrete cover on the face of the column spalled and the longitudinal steel in the column yielded at a load of 43.2 kips(192.2 kN). The ultimate load of 49.1 kips(218.4 kN) occurred at a deflection of 0.157 inches (3.99 mm). The maximum recorded strain on the front face of the column was 0.0064.

3.2.10 Specimen SC10 - Column with 1 1/2 in. (38 mm) Concrete Cover

The load deflection curve and a photograph of specimen SC10 at failure are shown in Fig. 3.14. Separation of the bottom of the embedded steel member from the concrete occurred at a load of 19.6 kips(87.2 kN). The inclined vertical cracks in the column face at the corners of the steel member and the diagonal cracks on the sides of the column both appeared at a load of 31.4 kips(139.7 kN). The concrete cover on the column face spalled at a load of 51.1 kips(227.9 kN) and a strain of 0.0027. The ultimate load of 62.8 kips(279.3 kN) occurred at a deflection of 0.089 in. (2.26 mm). The

longitudinal steel in the column did not reach the yield point.

3.2.11 Specimen SC11 - Hollow Structural Section Protruding from Two Sides

The load deflection curve and a photograph of specimen SC11 at failure are shown in Fig. 3.15. Separation of the bottom of the embedded steel member from the concrete occurred at a load of 28.0 kips(125.4 kN) on the column. A horizontal crack formed in the column at the centerline of the connection at a load of 125.0 kips(556.0 kN). Inclined vertical cracks appeared on both faces of the column at the top corners of the embedded steel member at a load of 130.0 kips(578.2 kN). The concrete cover on both faces spalled at a load of 150 kips(667.2 kN) and a strain of 0.0048. The ultimate load of 220 kips(978.6 kN) occurred at a deflection of 0.230 inches (5.84 mm). There was no yielding of the column reinforcing steel.

3.2.12 Specimen SC12 - Wide Flange Section Protruding from Two Sides

The load deflection curve and a photograph of specimen SC12 at failure are shown in Fig. 3.16. Separation of the bottom of the wide flange steel member from the concrete occurred at a load of 40.0 kips(178 kN). At a load of 130 kips (578. kN) a horizontal crack formed in the side of the column at the centerline of the embedded steel member. The load deflection response was linear up to a load of 140 kips (623 kN) at which point the embedded steel member started yielding due to the high shear load.

Inclined vertical cracks appeared at the tips of the top flange. At a load of 160 kips(712 kN) the concrete cover above the steel member began to spall. Failure occurred in the column at an ultimate load of 212 kips (943 kN) and a deflection of 1.150 inches (29.2 mm). There was no yielding of the longitudinal steel of the column. The maximum measured strain on the column face was 0.0013.

Although the wide flange member yielded in shear at a load of 140 kips (623 kN) it was able to carry additional loading causing eventual failure of the connection in the concrete at a load of 212 kips(943 kN) on the column and a corresponding deflection of 1.15 inches (29.2 mm).

3.2.13 Specimen SC13 - Hollow Structural Section Protruding from Two Sides

The load deflection response and a photograph of specimen SC13 at failure are shown in Fig. 3.17. Separation of the bottom of the embedded steel member from the concrete occurred at a load of 40.0 kips(177.9 kN) on the column. Inclined vertical cracks appeared in both faces of the column at the top corners of the steel member at a load of 110.0 kips(489.3 kN). A horizontal crack formed in the side of the column at the centerline of the connection at a load of 130.0 kips(578.2 kN). The concrete cover spalled at a load of 180.0 kips(800.6 kN) and a strain of 0.0019. The ultimate load of 210.0 kips(934.1 kN) was reached at a deflection of 0.250 inches (6.35 mm). There was no yielding of the longitudinal column reinforcement.

3.3 Series III

Specimens TC1, TC2 and TC3 incorporated 4 in. x 4 in. (102 mm x 102 mm) solid steel embedded members. Specimen TC4 used a 6 in. x 4 in. x 0.375 (152 mm x 102 mm x 10 mm) hollow structural steel member. Specimen TC1 was twice as wide as the specimens of Series II. Specimens TC2 and TC3 were cast in such a way that the width of the concrete directly above and below the embedded steel member was equal to the width of the embedded steel member. Specimens TC1 and TC2 were tested under zero axial load. Specimens TC3 and TC4 were tested under pure moment.

3.3.1 Specimen TC1 (Wide Column Test)

The load deflection response and a photograph of specimen TC1 at failure are shown in Fig. 3.18. Separation of the bottom of the embedded steel member from the concrete occurred at a load of 17.7 kips(78.7 kN). Inclined vertical cracks appeared in the column face at the top corners of the embedded steel member at a load of 29.4 kips(130.8 kN) however, the diagonal cracks in the sides of the column did not form until a load of 41.2 kips(183.3 kN) was reached. At a load of 47.1 kips(209.5 kN) the concrete cover above the steel member began to spall and the ultimate load of 58.9 kips(262.0 kN) was reached at a deflection of 0.193 inches (4.90 mm). There was no yielding of the longitudinal column reinforcement. The measured width of spalling was 9.25 inches (235 mm). The maximum measured strain on the column face was 0.0040.

3.3.2 Specimen TC2 (Connection on One Side with Reduced Width)

The load deflection response and a photograph of specimen TC2 at failure are shown in Fig. 3.19. Separation of the bottom of the embedded steel member from the concrete occurred at a load of 6.5 kips(28.9 kN). At a load of 13.0 kips(57.8 kN) a horizontal crack formed in the concrete cover at the back of the column at the centerline of the steel member. The concrete cover on the front face above the steel member spalled at a load of 31.2 kips (138.8 kN). The ultimate load of 32.3 kips(143.7 kN) was reached at a deflection of 0.141 inches (3.58 mm). There was no yielding of the column longitudinal reinforcement. Even though an attempt was made to prevent significant spreading of the load by reducing the column width around the embedded member signs of spreading were observed in the column above the region of reduced width. The measured width of apparent crushing on the front face was 5.0 inches (127 mm).

The maximum recorded strains on the front and back faces of the column were 0.0038 and 0.0003 respectively.

3.3.3 Specimen TC3 (Connection with Reduced Width Subjected to Pure Moment)

The load deflection curve and a photograph of specimen TC3 at failure are shown in Fig. 3.20. Separation of the bottom of the embedded steel member from the concrete occurred at a load of 5.2 kips(23.1 kN). Signs of crushing were observed at the front and back faces of the column at a load of 16.9 kips (75.2 kN). The ultimate load of 17.5 kips(77.8 kN) was reached at a deflection of 0.230 inches (5.84 mm). There was no measured yielding of the reinforced steel of the column. As with specimen TC2 signs of spreading were observed above the region of reduced width. Signs of spalling were noticed over a width of 5.0 inches (127 mm) on the front and back faces of the column. The maximum recorded strains on the front and back faces of the column were 0.0032 and 0.0034 respectively.

3.3.4 Specimen TC4 (Connection with Hollow Structural Steel Section Subjected to Pure Moment)

The load deflection response and a photograph of specimen TC4 at failure are shown in Fig. 3.21. Separation of the embedded steel member from the concrete occurred at a load of 5.2 kips(23.1 kN). At a load of 10.4 kips(46.3 kN) diagonal cracks formed on the sides of the column. The longitudinal reinforcement in the column started yielding at a load of 16.0 kips(71.2 kN). Inclined vertical cracks appeared in the column face above the steel member at a load of 20.8 kips(92.5 kN). The concrete cover above the steel member spalled when the connection reached the ultimate load of 26.0 kips(115.6 kN) at a deflection of 0.198 inches (5.03 mm). The maximum recorded concrete strain on the face of the column was 0.0028.

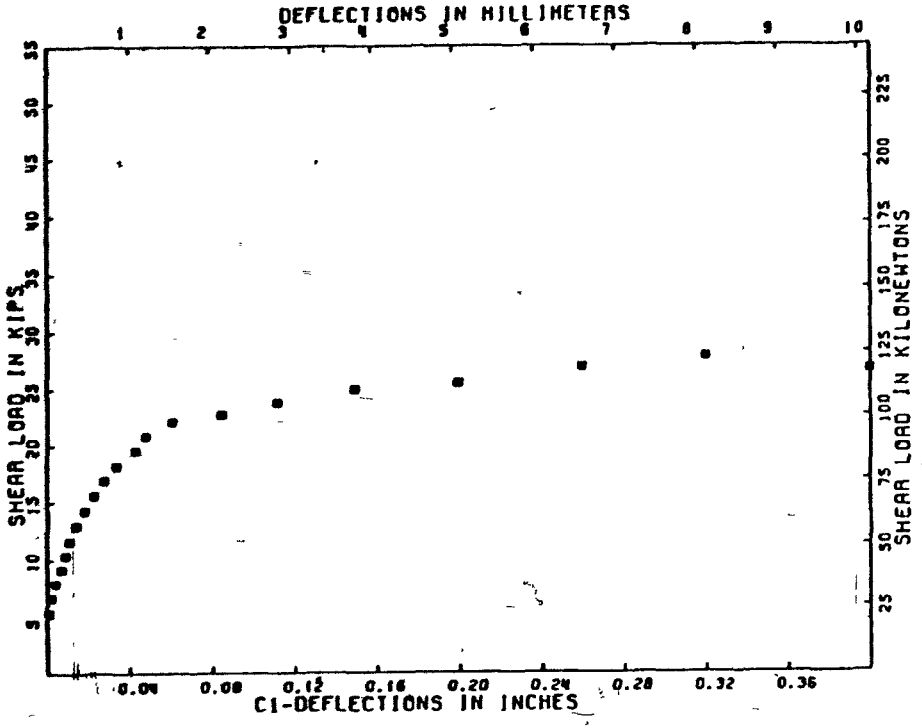

Figure 3.1 Specimen C1 - zero axial load test; the load deflection response and a photograph of the specimen after failure

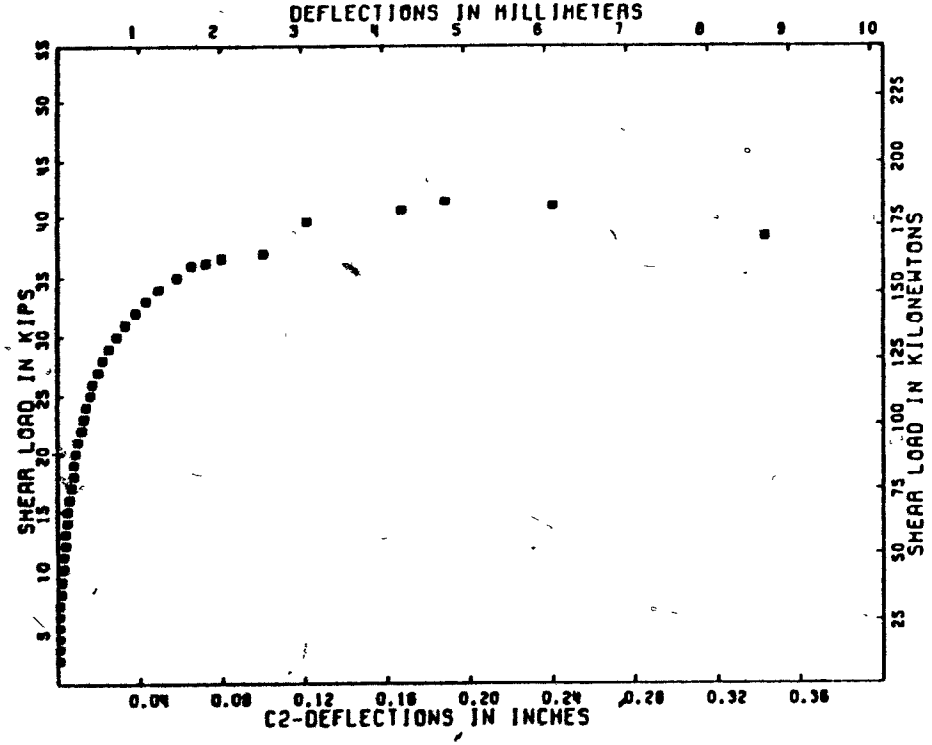

Figure 3.2 Specimen C2 - axial load of 30 kips (133 kN); the load deflection response and a photograph of the specimen after failure

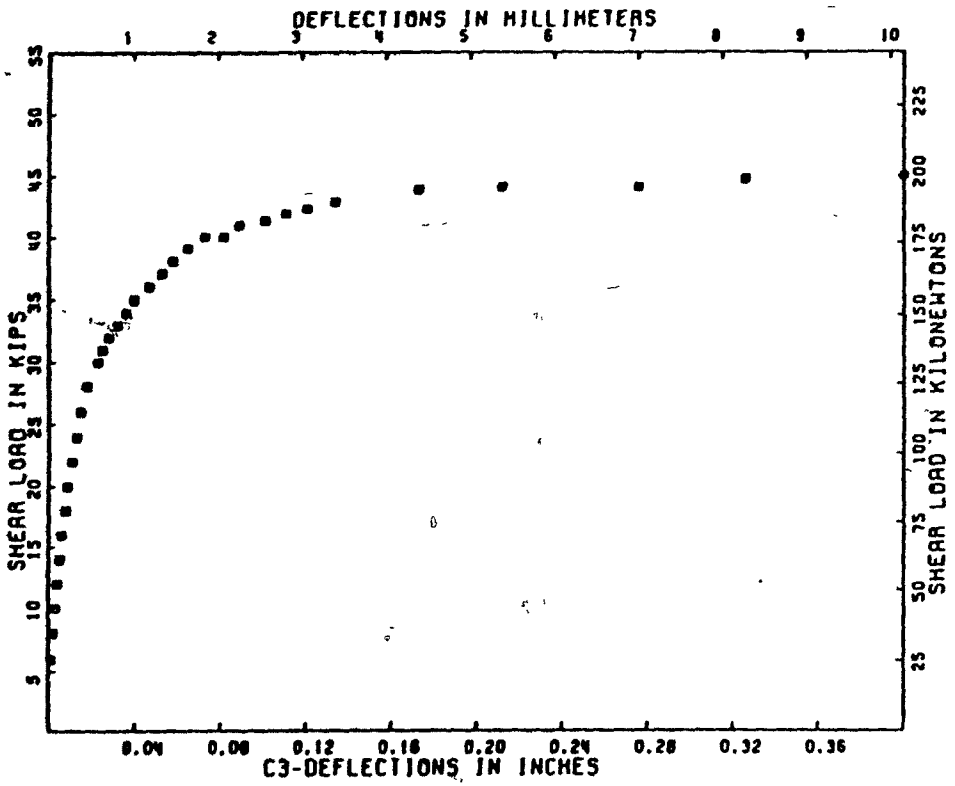

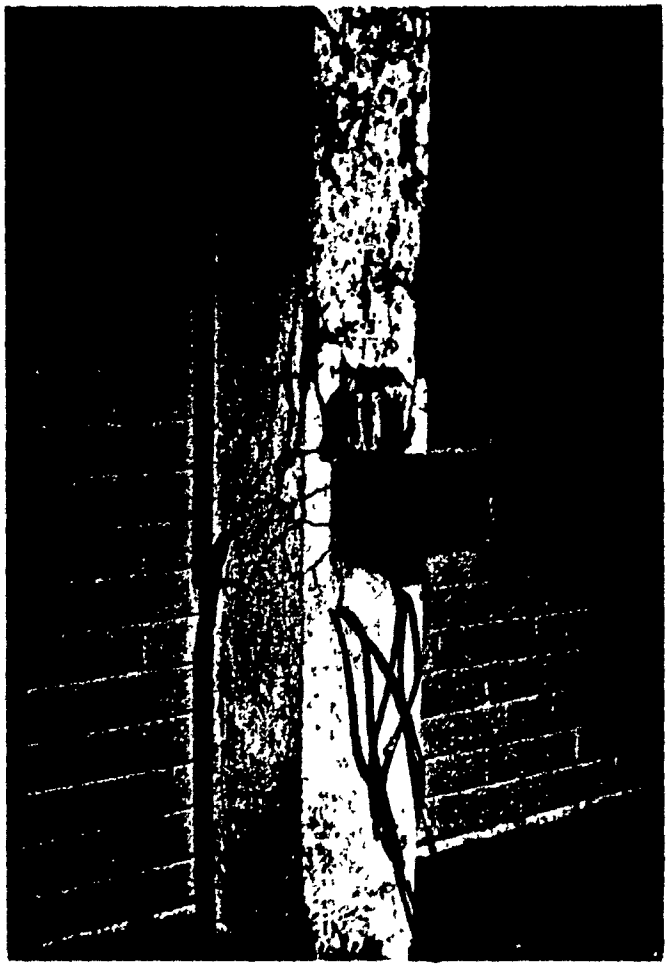

Figure 3.3 Specimen C3 - axial load of 60 kips (267 kN); the load deflection response and a photograph of the specimen after failure

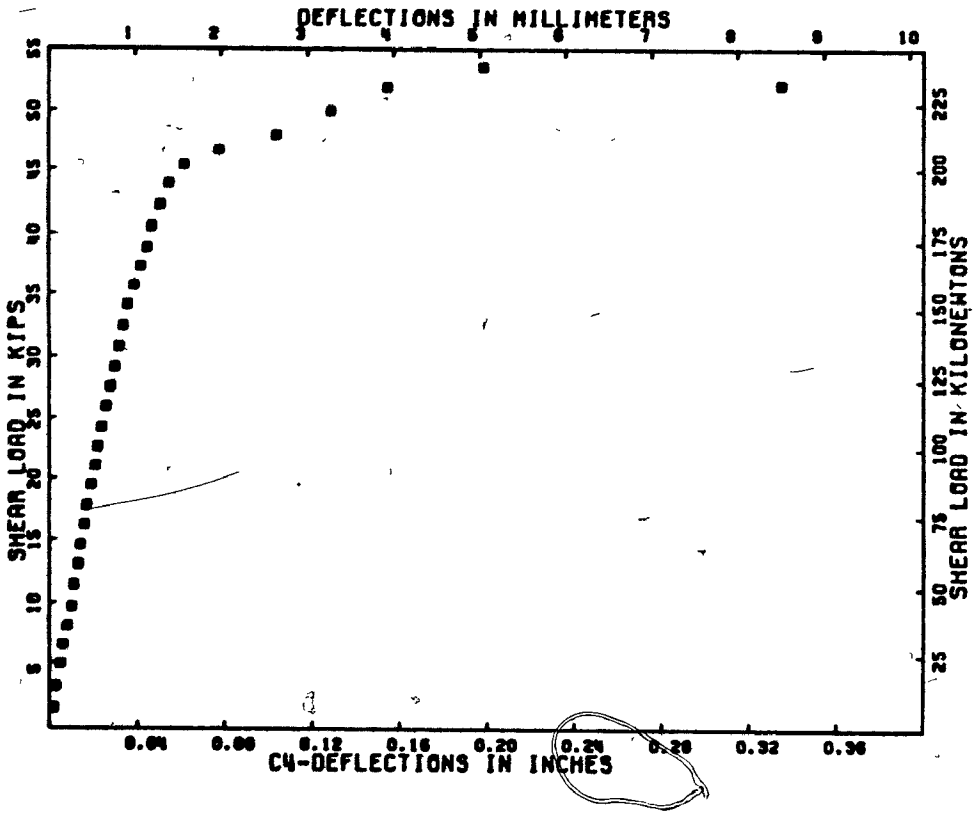

Figure 3.4 Specimen C4 - axial load of 90 kips (400 kN); the load deflection response and a photograph of the specimen after failure

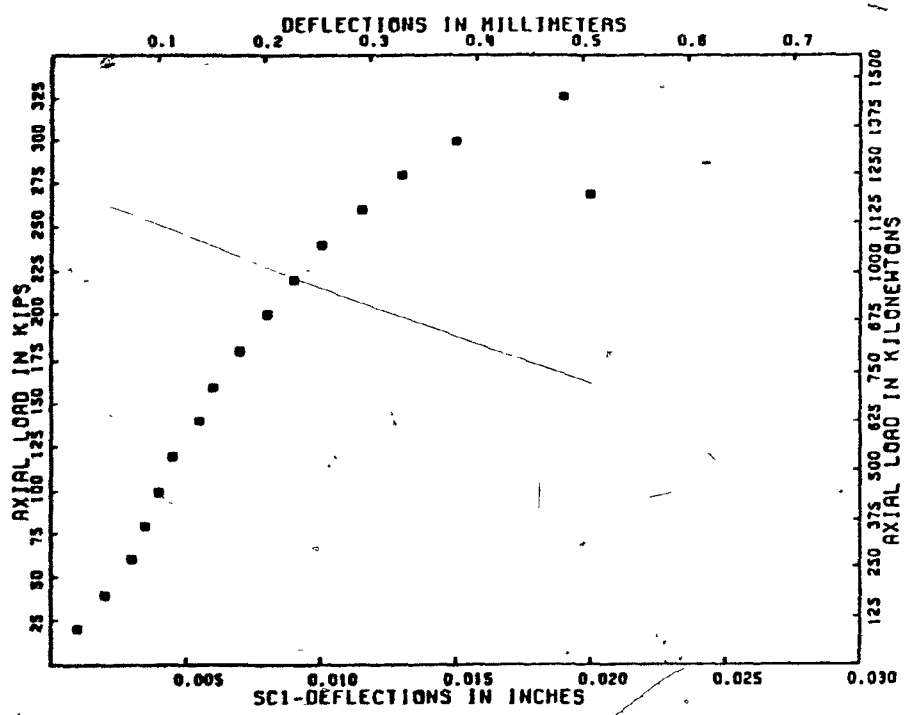

Figure 3.5 Specimen SC1 - pure axial load test; the load deflection response and a photograph of the specimen after failure

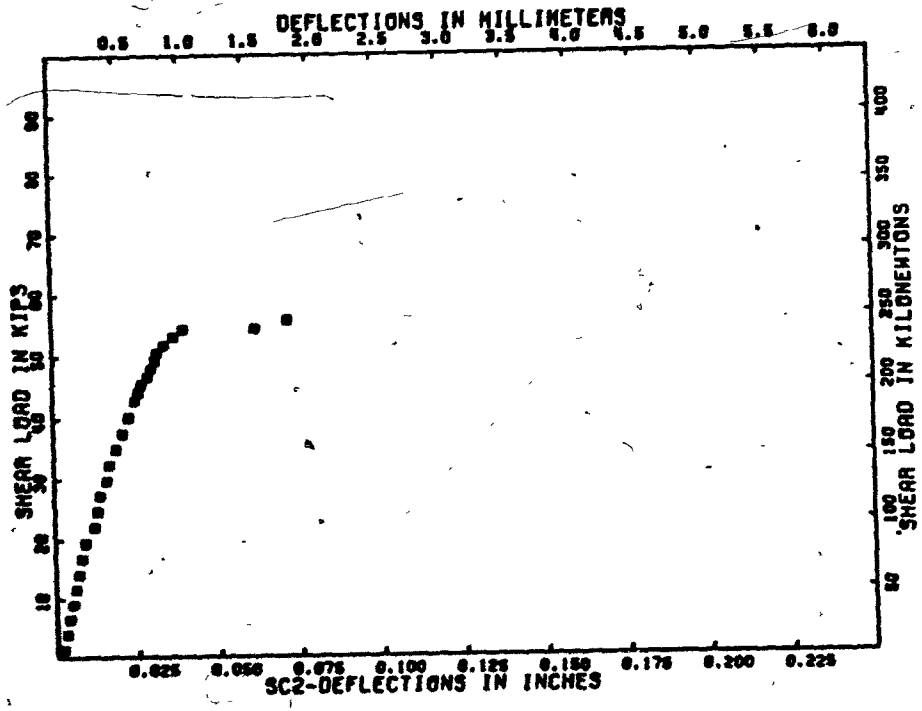

Figure 3.6 Specimen SC2 - axial load of 240 kips (1068 kN); the load deflection response and a photograph of the specimen after failure

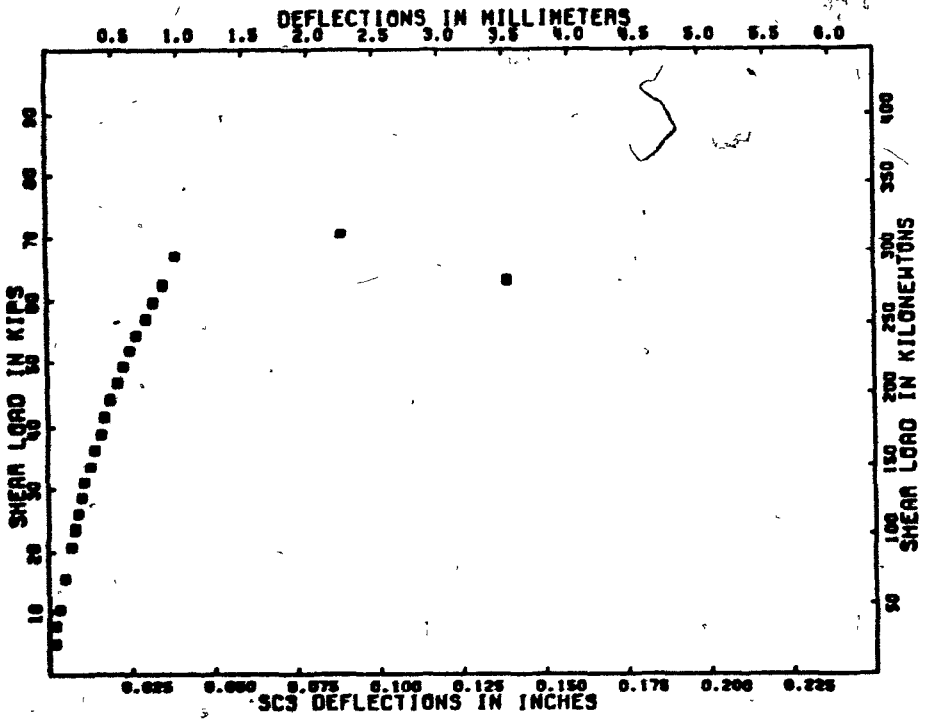

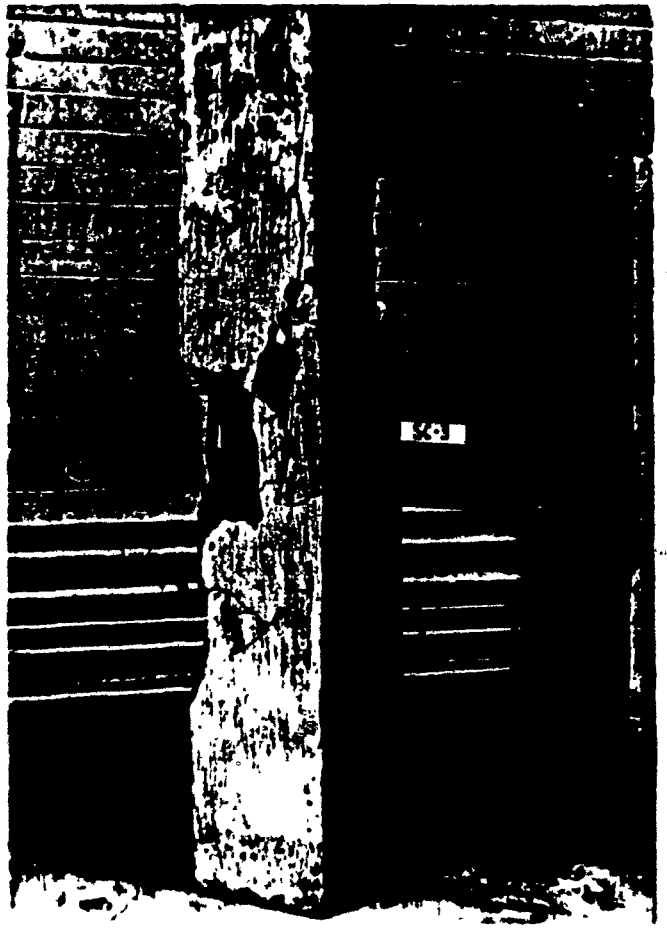

Figure 3.7 Specimen SC3 - axial load of 160 kips (712 kN); the load deflection response and a photograph of the specimen after failure

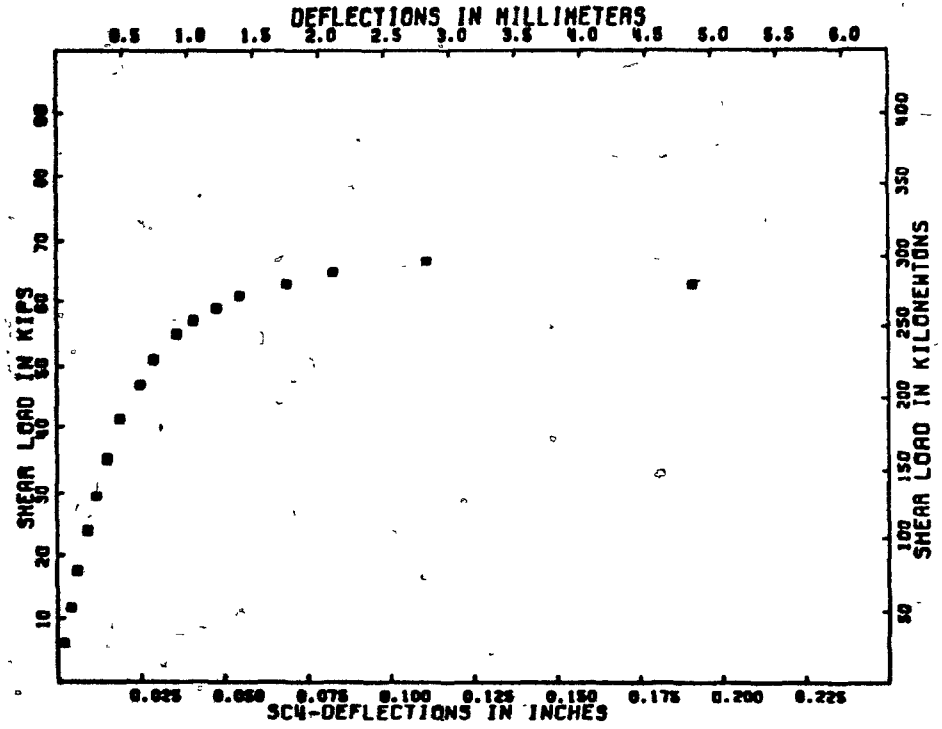

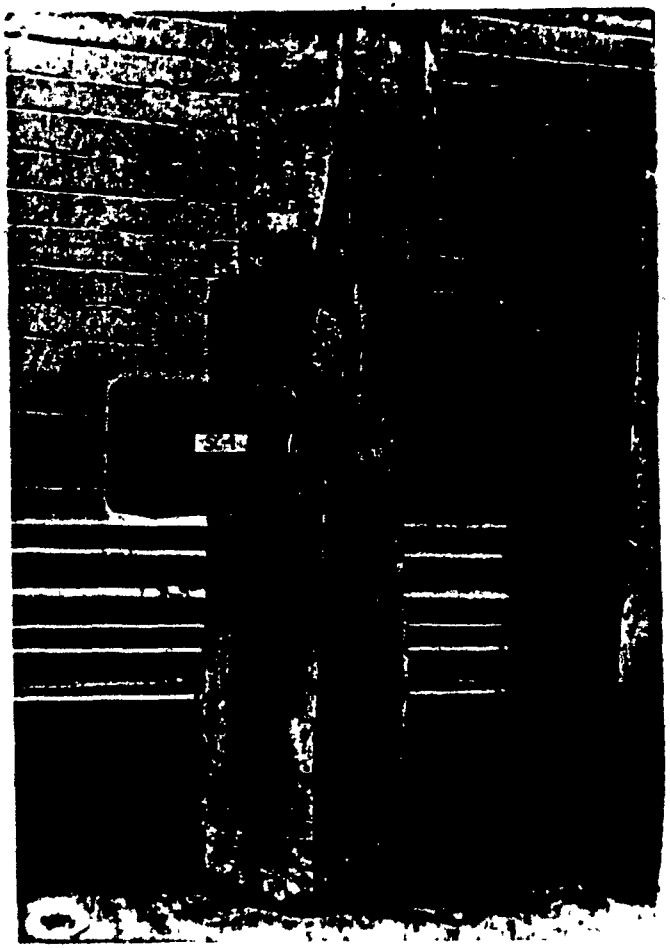

Figure 3.8 Specimen SC4 - axial load of 80 kips (356 kN); the load deflection response and a photograph of the specimen after failure

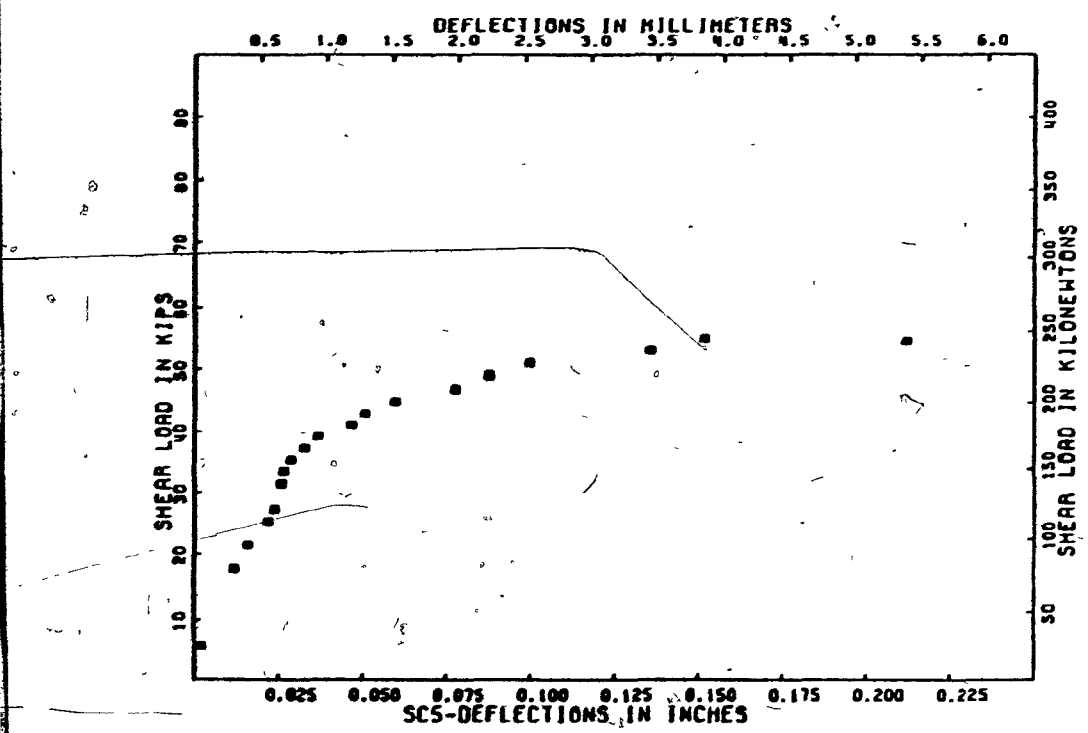

Figure 3.9 Specimen SC5 - zero axial load; the load deflection response and a photograph of the specimen after failure

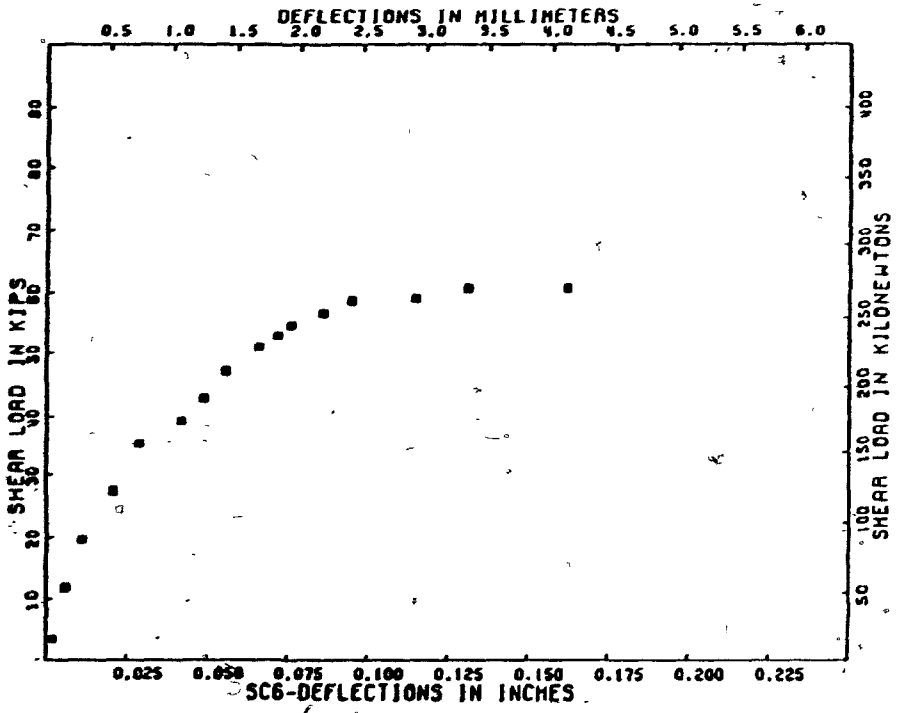

Figure 3.10 Specimen SC6 - wide flange member; the load deflection response and a photograph of the specimen after failure

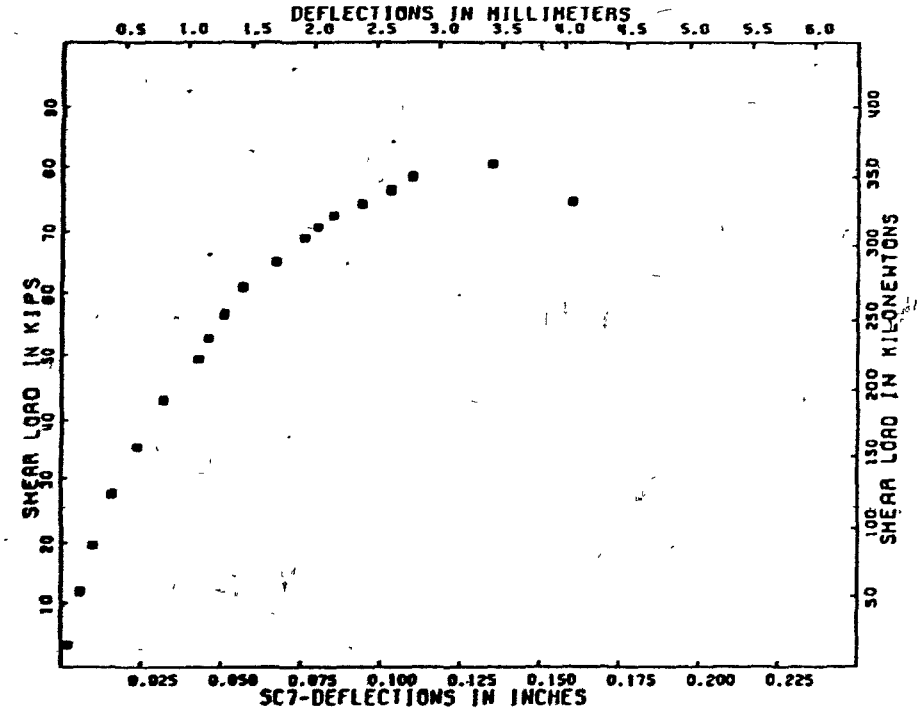

Figure 3.11 Specimen SC7 - additional reinforcement; the load deflection response and a photograph of the specimen after failure

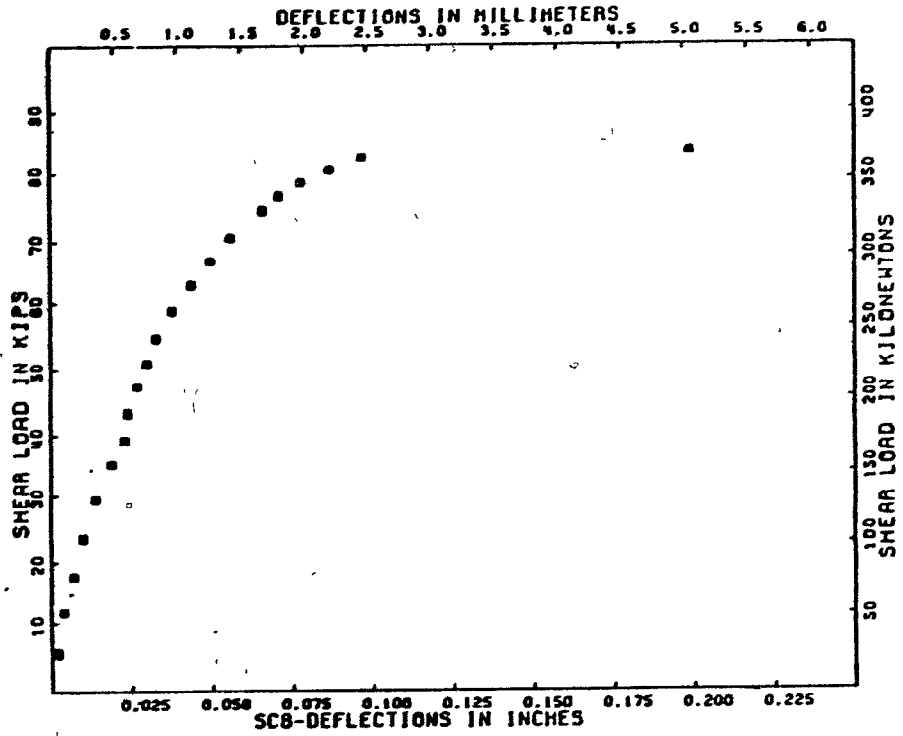

Figure 3.12 Specimen SC8 - additional reinforcement; the load deflection response and a photograph of the specimen after failure

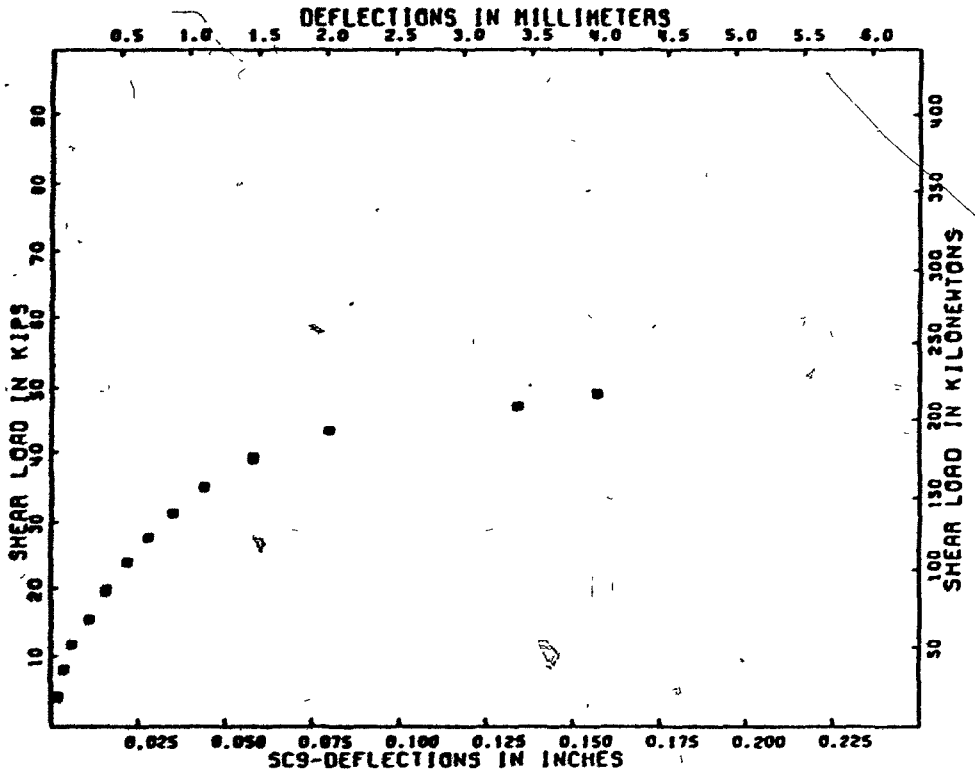

Figure 3.13 Specimen SC9 - zero concrete cover; the load deflection response and a photograph of the specimen after failure

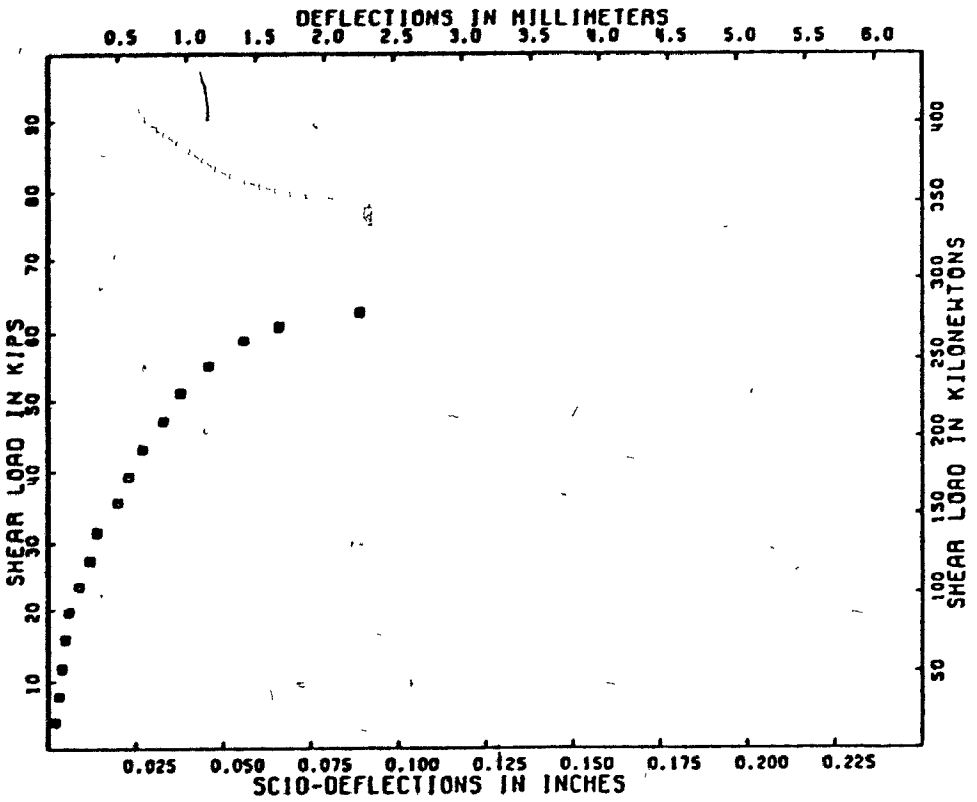

Figure 3.14 Specimen SC10 - 1 1/2 in (38 mm) concrete cover; the load deflection response and a photograph of the specimen after failure

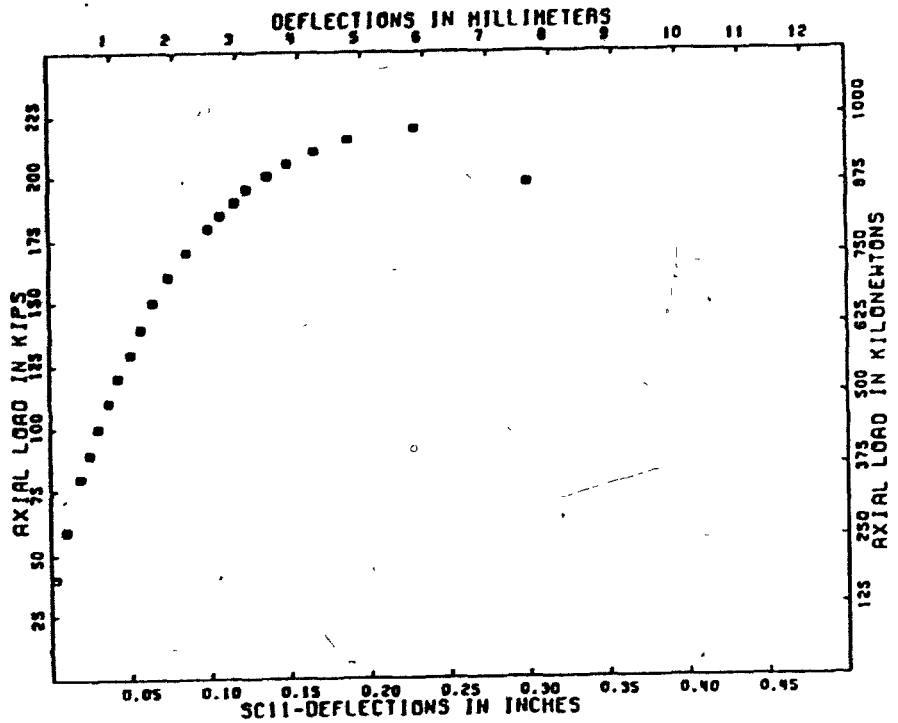

Figure 3.15 Specimen SC11 - HSS protruding from two sides; the load deflection response and a photograph of the specimen after failure

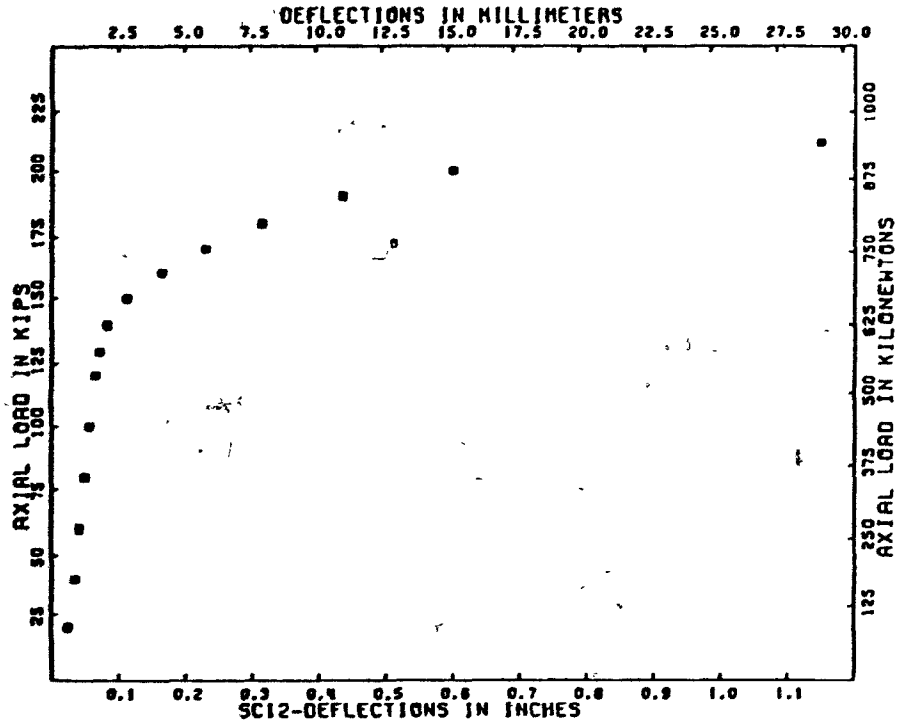

Figure 3.16 Specimen SC12 - wide flange member protruding from two sides; the load deflection response and a photograph of the specimen after failure

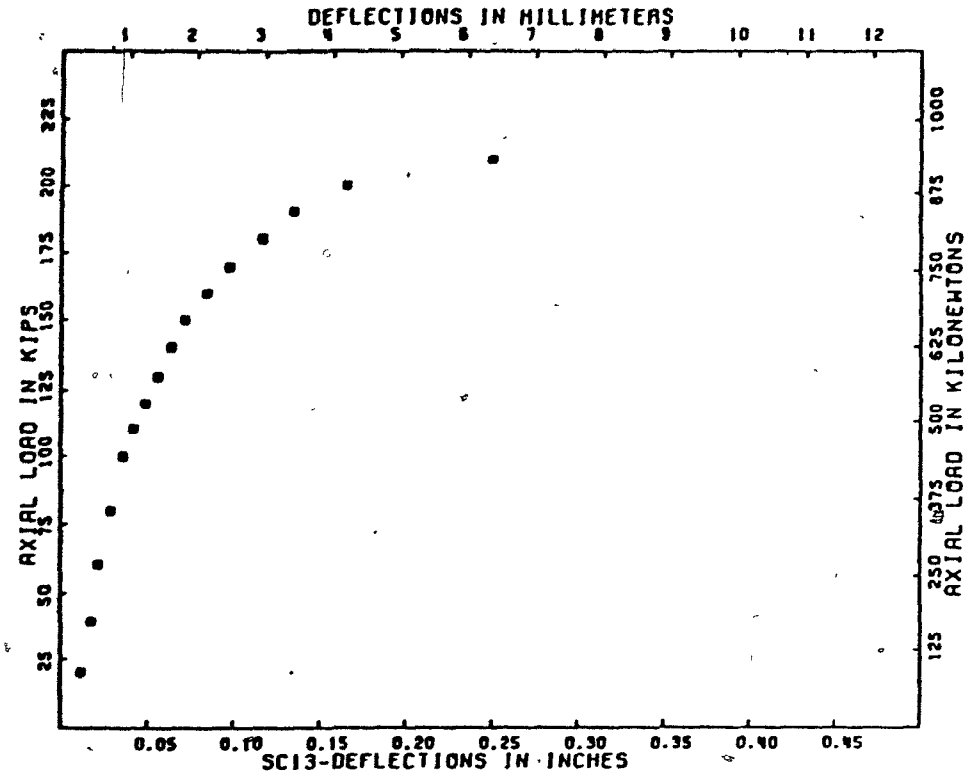

Figure 3.17 Specimen SC13 - HSS protruding from two sides; the load-deflection response and a photograph of the specimen after failure

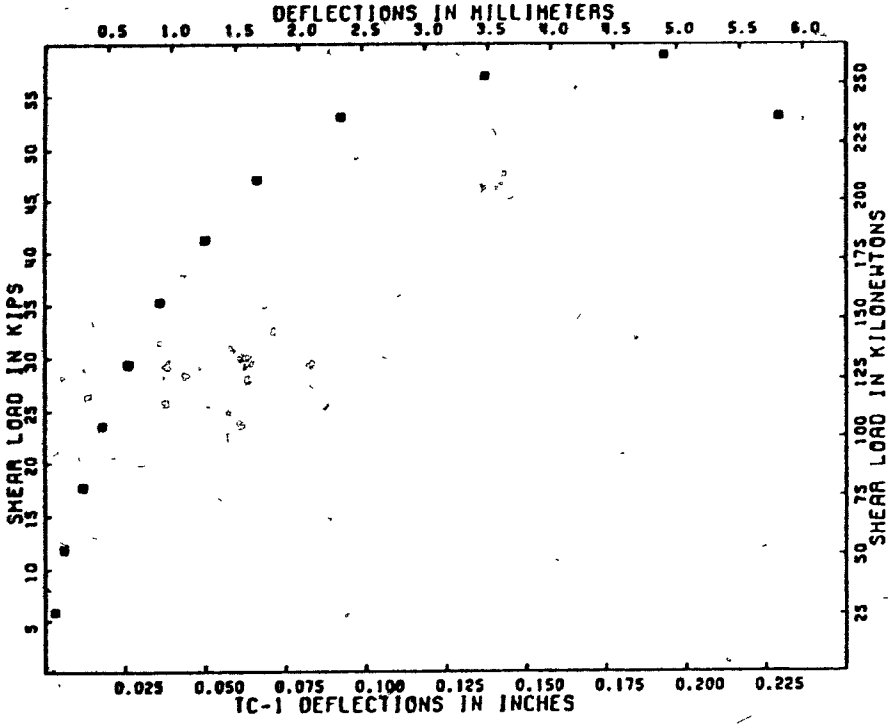

Figure 3.18 Specimen TC1 - very wide column; the load deflection response and a photograph of the specimen after failure

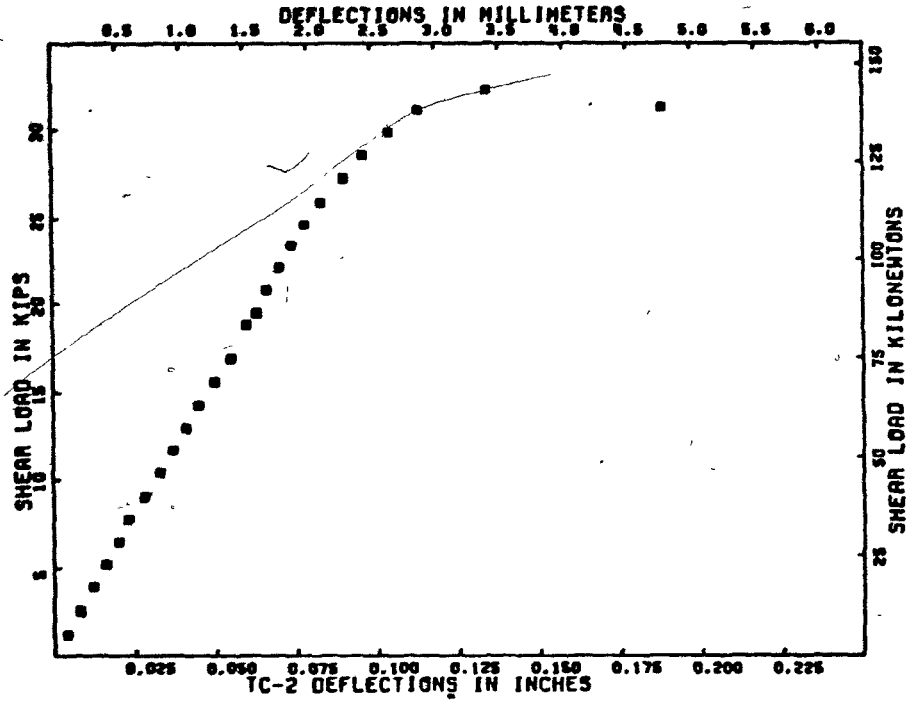

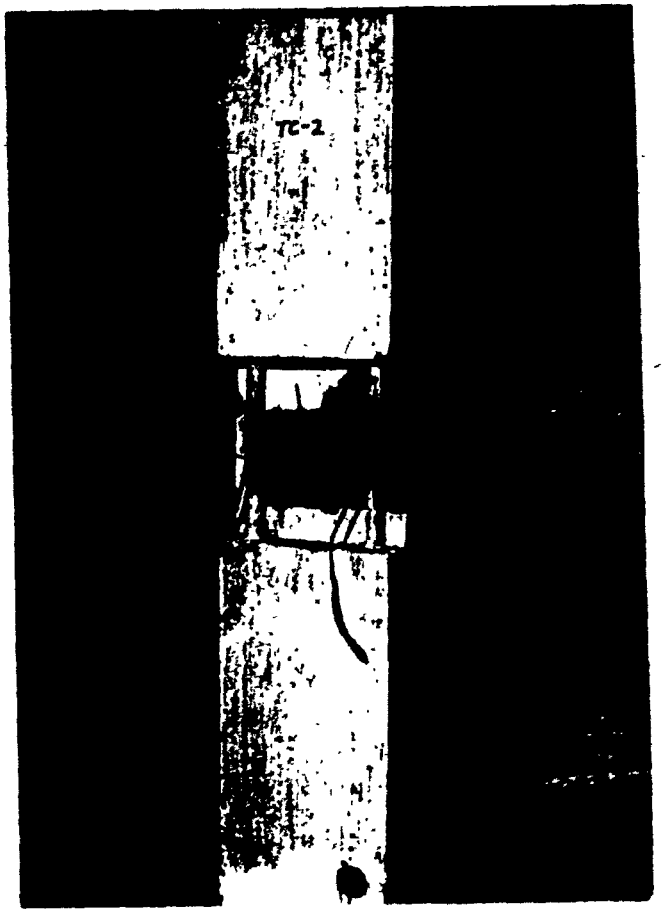

Figure 3.19 Specimen TC2 - column with reduced width; the load deflection response and a photograph of the specimen after failure

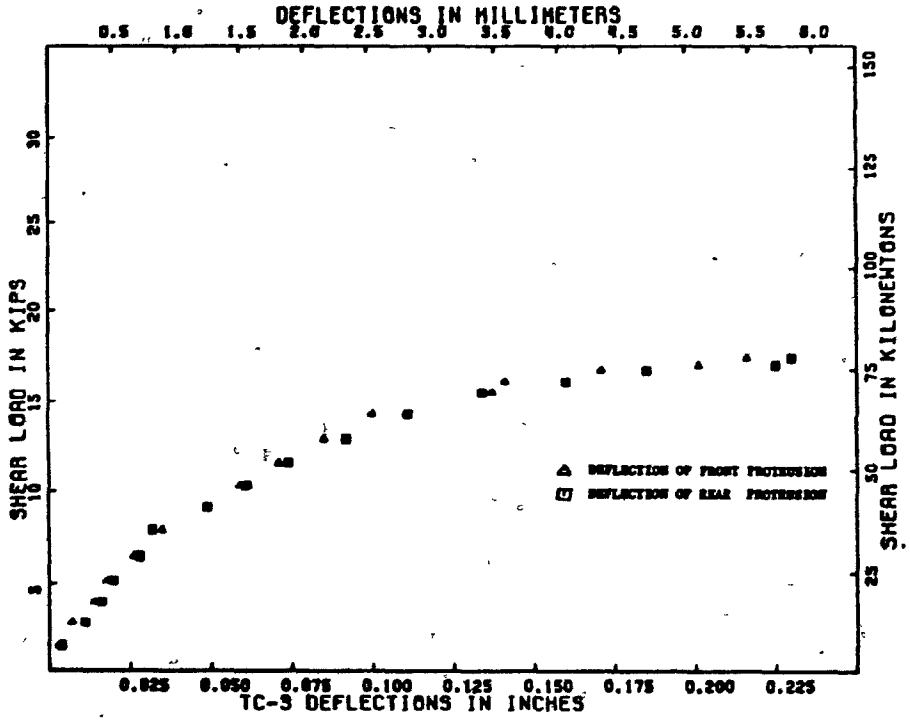

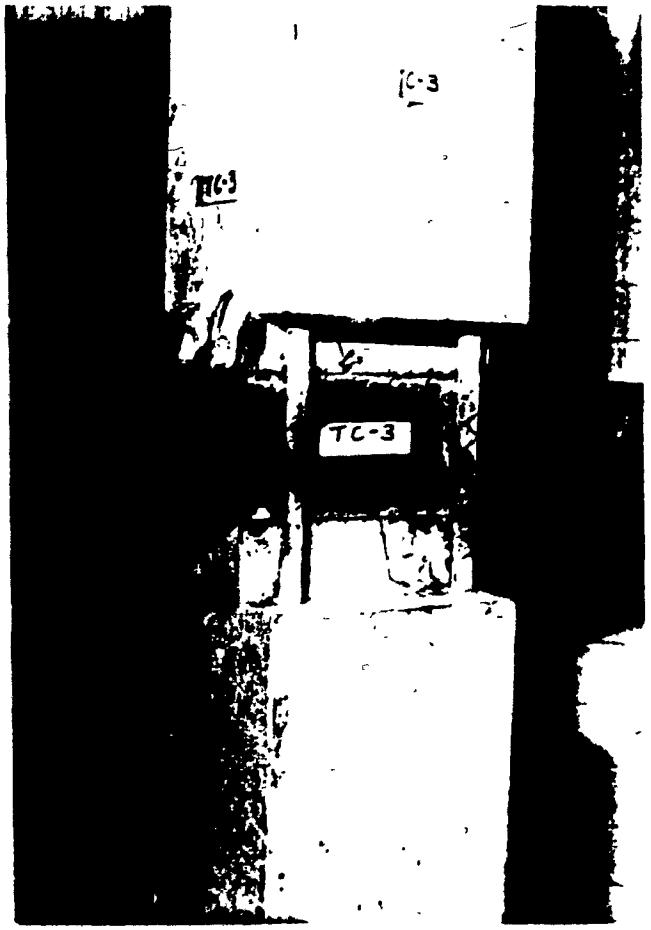

Figure 3.20 Specimen TC3 - column with reduced width subjected to pure moment; the load deflection response and a photograph of the specimen after failure

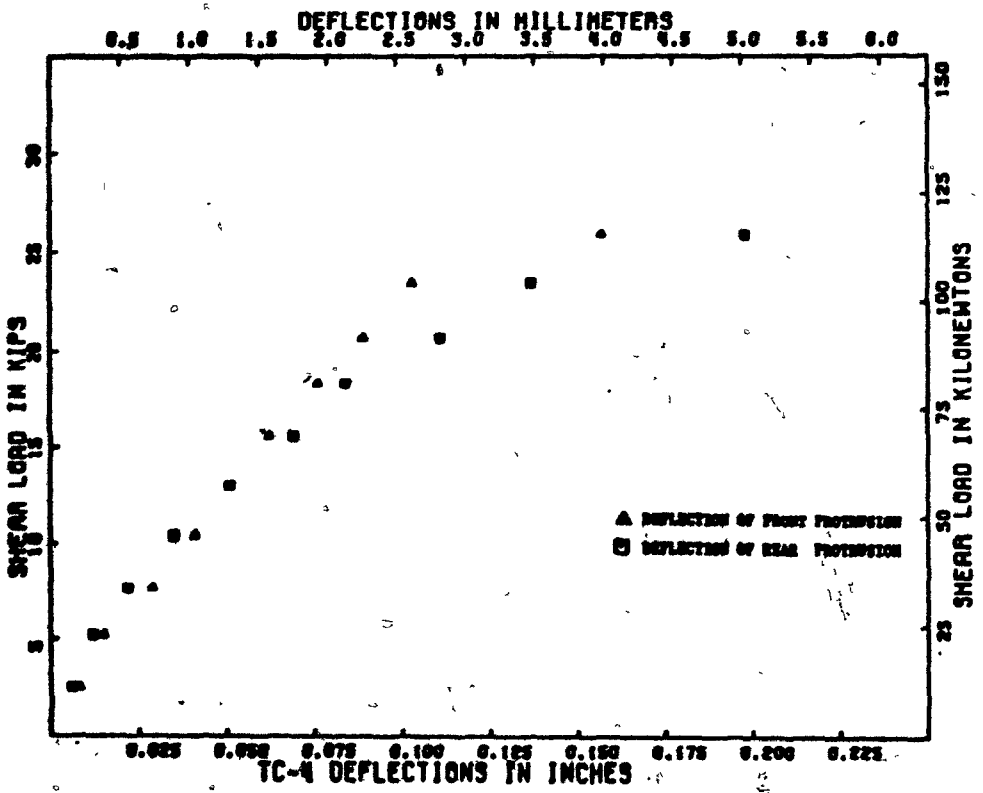

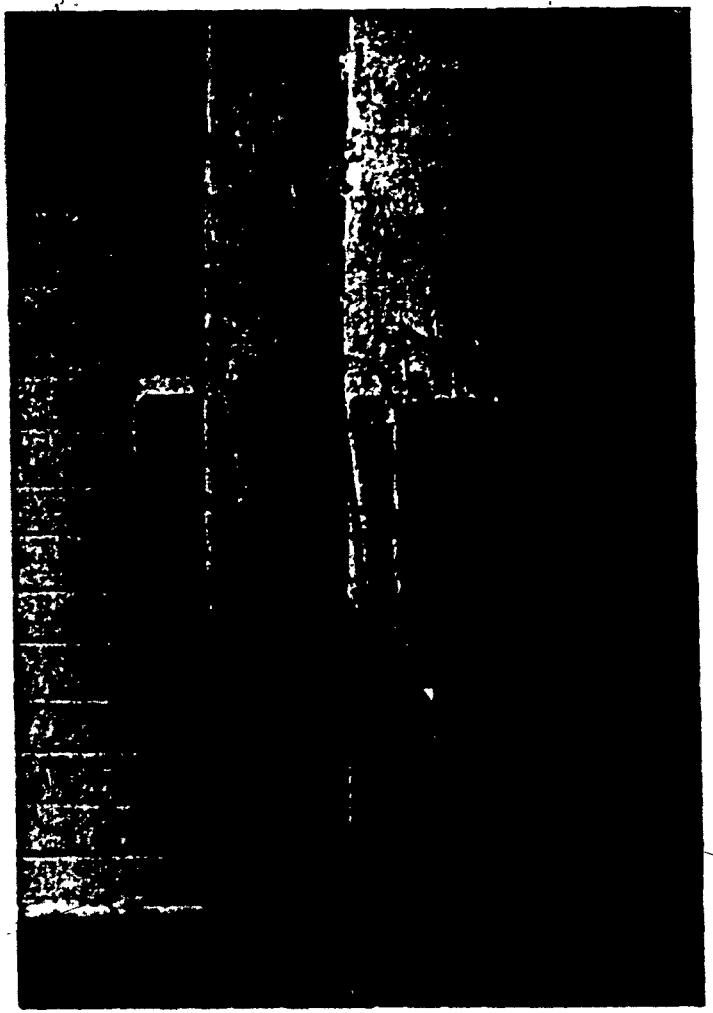

Figure 3.21 Specimen TC4 - HSS subjected to pure moment; the load deflection response and a photograph of the specimen after failure

CHAPTER IV DEVELOPMENT OF ANALYTICAL MODEL AND DISCUSSION OF TEST RESULTS

4.1 Basic Assumptions in the Analytical Model

The proposed analytical model for precast connections incorporating embedded steel members assumes that the stiffness of the steel member is sufficiently greater than that of the concrete surrounding it that it may be treated as a rigid member. Therefore, all rotations and displacements of the embedded steel member under the action of any applied loads will result in linear strain distributions in the concrete above and below the steel member as can be seen in Fig. 4.1 . The resulting curvature, ϕ, is constant above and below the embedded member as can be seen from the strain distributions of Fig. 4.1. From the assumptions of a rigid embedded member and small deformations in the connection the points of zero strain above and below the embedded steel member lie on the same vertical line. Due to the loss of contact between the steel member and the concrete over certain regions of the embedded length only compressive stresses are assumed to act on the embedded steel member.

The resulting strain distribution can be described by the following two equations:

$$\phi = \frac{\varepsilon_f}{x_g} = \frac{\varepsilon_b}{x_b} \qquad 4.1$$

and

$$x_f + x_b = \ell_e \qquad 4.2$$

where: ϕ = curvature resulting from the strain distributions

ε_f = strain on front face of column

ε_b = strain at back of steel member

x_f = distance from front face of column to neutral axis

x_b = distance from back of steel member to neutral axis

ℓ_e = embedment length of steel member

The concrete is assumed to follow a parabolic stress-strain law given by:

$$f_c = f'_c \left[2 \frac{\varepsilon}{\varepsilon_o} - \left(\frac{\varepsilon}{\varepsilon_o}\right)^2\right] \qquad 4.3$$

where ε_o is the strain corresponding to the peak concrete stress, f'_c is the compressive strength of concrete, and ε is the strain at which the stress, f_c, is being evaluated. A value of 0.002 is used for ε_o.

If an embedded member of width b is subjected to a linear distribution of depth x the resultant compressive force can be expressed as

$$C = \alpha f'_c \beta x b \qquad 4.4$$

where βx is the depth of an equivalent rectangular stress distribution and $\alpha f'_c$ is the equivalent uniform stress of that distribution. The position of the resultant of the compressive stress distribution would be at $1/2\ \beta x$ from the point of maximum compressive strain towards the neutral axis of the member. For a linear strain distribution and a parabolic stress distribution given by Eq. 4.3 values of α and β can be found such that the resultant of the equivalent rectangular stress distribution has the same magnitude and position as the parabolic stress distribution. For a given maximum concrete strain, ε, the values of α and β can be found from the following two equations:

$$\beta = \frac{4 - \varepsilon/\varepsilon_o}{6 - 2\,\varepsilon/\varepsilon_o} \qquad 4.5$$

$$\alpha\beta = \varepsilon/\varepsilon_o - 1/3\ (\varepsilon/\varepsilon_o)^2 \qquad 4.6$$

The maximum strain occurs at the front face of the connection. If a maximum strain of 0.003 is assumed together with the ACI stress block factors the resultant of the stress distribution at the front of the connection, C_f, given by

$$C_f = 0.85\, f'_c\, a\, b \qquad 4.7$$

where a, the depth of the equivalent rectangular stress block, is defined as:

$$a = \beta_1\, x_f \qquad 4.8$$

The stress block factor, β_1 is given by:

$$\beta_1 = 0.85 \quad \text{for } f'_c \text{ less than 4000 psi or 30 MPa}$$

otherwise $$\beta_1 = 0.85 - .05\,[\frac{f'_c - 4000}{1000}] \quad \text{where } f'_c \text{ is in psi}$$

or $$\beta_1 = 0.85 - 0.08\,[\frac{f'_c - 30}{10}] \quad \text{where } f'_c \text{ is in MPa}$$

but β_1 should not be taken as less than 0.65.

Since the value of the strain at the back of the steel member is less than 0.003 the ACI stress block factors do not apply. For a given value of strain at the back of the embedded member Equations 4.5 and 4.6 can be used to calculate the stress block factors α and β. The resultant, C_b, of the stress distribution at the back of the embedded member is therefore given by:

$$C_b = \alpha f'_c\, b\, \beta\, x_b \qquad 4.9$$

Summing vertical forces on the connection gives:

$$V_c = 0.85\, f'_c\, b\, \beta_1\, x_f - \alpha\beta\, f'_c\, b\, (\ell_e - x_f) \qquad 4.10$$

The distance from the point of application of the load to the center of embedment of the steel member is given by

$$e = a + \ell_e/2 \qquad 4.11$$

Taking moments about the center of embedment of the steel member gives:

$$V_c\, e = C_f[\ell_e/2 - \beta_1\, x_f/2] + C_b[\ell_e/2 - \beta(\ell_e - x_f)/2] \qquad 4.12$$

The solution of Equations 4.10 and 4.12 will give the ultimate capacity of the connection, V_c, as a function of the eccentricity, e, of the load from the center of embedment of the steel member. In order to solve Equations 4.10 and 4.12 an iteration procedure was used, the steps of which are given below:

1. choose a value of x_f
2. calculate the strain at the back of the embedded member and the corresponding values of α and β.
3. determine the magnitudes and positions of the stress resultants C_f and C_b.
4. from force equilibrium, Eq. 4.10, calculate V_c

and 5. from moment equilibrium, Eq. 4.12, calculate the corresponding value of e.

In the design of a connection the embedment length, ℓ_e, and the eccentricity of the load are chosen. Therefore, the design procedure should give the ultimate capacity of the connection as a function of e and ℓ_e. If the iteration procedure is repeated for different values of x_f a series of solutions will result for V_c versus e at ultimate. Therefore the non-dimensional shear capacity of the connection, $V_c/f'_c\, b\ell_e$, can be plotted against the ratio of e/ℓ_e giving the design curves of Fig. 4.2. V_c is the resultant of the loads acting on a connection and e is the effective

eccentricity of the resultant of the loads measured from the center of the embedment length. Once e and ℓ_e are chosen the curves of Fig. 4.2 can be used to find the ultimate capacity of the connection for a given concrete strength.

The maximum shear capacity of the connection occurs when the eccentricity, e, of the resultant of the applied loads equals zero. This case would arise when equal loads with equal eccentricities are applied to an embedded member protruding from two sides of a column. This loading case results in a uniform strain distribution of 0.003 (see Fig. 4.2) and a corresponding uniform stress distribution of 0.85 f'_c over the entire length of embedment.

It should be noted that for e/ℓ_e less than 1/2 the resultant of the applied loads would have to act at some point within the column. The resulting strain distribution for the case where e equals $\ell_e/2$ is shown in Fig. 4.2. As can be seen from Fig. 4.2 the shear capacity of the connection decreases with increasing eccentricity.

Predictions of the capacity of connections based on Fig. 4.2 and using an effective width equal to the width of the embedded steel member grossly underestimates the capacity of these connections.

These results can only be explained if the effective width of the connection is larger than the width of the embedded steel member. The larger effective width can be attributed to the high degree of confinement of the concrete in the column in the region of the connection. A discussion of the effective width to be used in design is found in Section 4.3.

4.2 Idealized Specimens

Specimens TC2 and TC3 were used to test the assumptions of the analytical model. They both incorporated 4.0 inch (102 mm) square solid steel members which were relatively rigid compared to the concrete surrounding them. The width of the concrete above and below the embedded steel member was made equal to the width of the steel member in order to have a "known" effective width as can be seen in Fig. 2.6. It was felt that the results of these specimens would test the validity of the assumptions of the analytical model without having to assume an effective width.

Since specimen TC3 was tested under pure moment an anti-symmetric concrete straindistribution with a maximum strain of 0.003 at each face of the column was assumed for the theoretical analysis. The strain distribution along the length of the embedded steel member for each load stage up to failure is shown in Fig. 4.3. The strain distribution at failure is nearly linear with maximum strains of 0.0032 on the front face and 0.0034 on the back face of the column. The strain distribution agrees well with the assumed strain distribution of the analytical model however, the failure load is 1.55 times the predicted value if an effective width of 4 inches (102 mm) is assumed. Even though this specimen had a reduced width of concrete in the region of the embedded member, signs of crushing were observed over a width of 5.75 inches (146 mm) beyond the regions of reduced width. This specimen demonstrates the ability of the load to spread even though measures had been taken to prevent the spreading.

Specimen TC2 also had a reduced width in the region of the embedded member and it was tested with the steel member protruding from one side only.

The concrete strain distribution along the length of the embedded steel member in specimen TC2 for each load stage up to failure is shown in Fig. 4.4. As can be seen from Fig. 4.4 the strain distribution across the length of the steel member was nearly linear in the final load stages. Due to the formation of a crack in the concrete at the back of the embedded steel member the strain gauge at this location was damaged.

At an early load stage a horizontal crack formed at the back of the column at the location of the embedded member and the concrete cover separated from the steel member. Consequently the back concrete cover was ineffective in carrying any load and the strains at this location were very small.

The strain distribution for specimen TC2 is therefore based on concrete strain gauges 1, 2, 3 and 4 only (see Fig. 2.12).

As with specimen TC3, specimen TC2 failed at a much higher load than that predicted by the analytical model assuming an effective width of 4 inches (102 mm). After failure crushing was observed over a width of 5.5 inches (140 mm) in the region of the column above the reduced width. Once again, this demonstrates the ability of the load to spread, resulting in a larger effective width, even though measures were taken to prevent load spreading.

The measured strain distribution at ultimate shown in Fig. 4.4 is approximately linear with a maximum strain of 0.0038 at the front face and an estimated strain of 0.0016 at the back of the embedded steel member. The analytical model assumes a linear strain distribution with 0.003 at the front face and a predicted strain of 0.0019 at the back of the steel member. The strain distribution of Fig. 4.4 indicates a neutral axis depth of 0.725 ℓ_e as compared to a depth of 0.61 ℓ_e predicted by the analytical model.

The strain distribution of Fig. 4.4 indicates that there is a basic error in the assumptions of the PCI Design Method since that method assumes the neutral axis depth is always at $\ell_e/3$.

4.3 Effective Width

4.3.1 Effects of Cover

Specimens SC9, SC5 and SC10 had clear concrete covers of zero, 1/2 in. (12.7 mm), and 1 1/2 in. (38.1 mm) respectively. The placement of the embedded steel and the point of application of the load for each specimen is shown in Fig. 2.4. The load was positioned such that the eccentricity from the center-line of the column was constant. In the analysis the eccentricity of the load is measured from the center of embedment of the steel member, therefore the three specimens had different eccentricites as well as different concrete covers. A comparison of the load-deflection responses of the three specimens and a photograph of the specimens at failure is shown in Fig. 4.5. From the photograph in Fig. 4.5 it can be seen that the effective width of the connection at the front face as bounded by the inclined vertical cracks is approximately the same for all three specimens. It is clear from this photograph that the concrete cover spalls off in the region of the connection. The results of these tests indicate that spreading does indeed occur however, it does not extend to the full width of the column because the cover is ineffective. Therefore, the analytical model assumes that the effective width cannot exceed the confined width of the column measured to the outside of the column ties.

The failure loads for specimens SC9, SC5 and SC10 were 49.1 kips(218.4 kN), 55.0 kips(244.6 kN) and 62.8 kips(279.3 kN) respectively. The analytical model predicts ultimate capacities of 38.5 kips(171 kN), 40.0 kips (178 kN) and 45.6 kips(203 kN) respectively using an effective width equal to the outside width of the column ties. The experimental capacities exceed the predictions of the analytical model by 25%, 37% and 38% for specimens SC9, SC5 and SC10 respectively.

4.3.2 Maximum Effective Width

Specimen TC1 had a width of 16 inches (406 mm) which made it twice as wide as the other specimens in Series II and Series III. It incorporated a 4 inch (102 mm) square solid steel embedded member which protruded from one side only. Since the details of this specimen favoured spreading, specimen TC1 was useful in determining the maximum effective width of the connection. The specimen reached an ultimate load of 58.9 kips(262 kN). As expected, the effective width of this specimen was less than the outside width of the column ties in the specimen. Signs of crushing were observed over a width of 8 inches (203 mm) on the front face of the column above the steel member.

If an effective width of 8 inches (203 mm) is assumed in calculating the capacity of the connection the measured capacity exceeds the prediction of the analytical model by 59%. Based on this one test it is recommended that an effective width not greater than twice the width of the embedded steel member should be used in the design of these connections.

4.3.3 Effect of Shape of Embedded Member

Specimen SC6 incorporated a wide flange steel member whose flanges were milled to give an identical width and a comparable stiffness to that of the hollow structural steel member of specimen SC5. A comparison of the load-deflection response and a photograph of the two specimens at failure is shown in Fig. 4.6. As can be seen in Fig. 4.6, the response of the two specimens is identical up to a load of 40 kips(178 kN) and both specimens exhibited approximately the same ductility at ultimate.

The failure loads for specimens SC5 and SC6 were 55.0 kips(245 kN) and 60.9 kips(271 kN) respectively.

It can be seen from the photograph of Fig. 4.6 that inclined vertical cracks are formed from both the top and the bottom flanges of the wide flange section. This indicates that both flanges are effective in distributing the load. The hollow structural steel member on the other hand has only one loading surface to distribute the load. Therefore, a wide flange section results in a more favourable distribution of stresses in the connection.

Although the connection incorporating a wide flange member exhibited an 11% larger capacity than the specimen with the hollow structural steel member, the analytical model conservatively reflects this additional capacity.

4.3.4 Effects of Stiffness of Embedded Member

The results of specimen C1 demonstrate the importance of using an embedded steel member which is stiff enough to ensure relatively uniform bearing conditions. In specimen C1, since the hollow structural steel member had thin walls and since it was not filled with concrete the bearing of the concrete against the top wall of the steel member caused severe local bending. This resulted in stress concentrations in the concrete above the webs of the hollow steel member, which reduced the effective width of the connection and led to a premature failure. Therefore if the walls of a hollow structural steel member are not stiff enough it should be filled with concrete to ensure a more uniform bearing stress which will enable the effective width to attain its maximum value.

4.4 Effects of Additional Welded Reinforcement

Specimens SC7 and SC8 were tested with additional reinforcing bars welded to the embedded steel member. A total of eight pieces of #3 bar, 12 in. (305 mm) long, were welded to the embedded steel member. Four bars were welded to the top surface of the steel member and four bars were welded to its bottom surface as shown in Fig. 2.3. The bars were provided with sufficient length to enable them to develop their ultimate capacity in both tension and compression.

The strain in the bars is assumed to be equal to the strain in the concrete surrounding them. Therefore from the strain distribution of Fig. 4.1 the total force in the bars at the front of the embedded member, C_{fs}, is given by:

$$C_{fs} = A_s f_s \qquad 4.14$$

where A_s is the total area of reinforcing steel welded to the front of the connection above and below the embedded steel member and f_s is the stress in the reinforcing bars.

Similarly the total force in the bars at the back of the connection, C_b, is given by:

$$C_{bs} = A_s' f_s' \qquad 4.15$$

where A_s' is the total area of reinforcing steel welded to the back of the embedded member and f_s' is the stress in the reinforcing bars.

The stresses in the bars at the front and at the back of the connection, f_s and f_s' respectively, are given by:

$$f_s = 0.003\, E_s\, [1 - d_f/x_f] \leq f_y \qquad 4.16$$

and

$$f_s' = 0.003\, E_s\, [(\ell_e - d_b)/x_f - 1] \leq f_y \qquad 4.17$$

where: E_s = modulus of elasticity of steel

d_f = distance of welded reinforcement at front of embedded member from the front face of the column

d_b = distance of welded reinforcement at the back of the connection from the end of the embedded steel member.

From equilibrium of vertical forces, the ultimate capacity of a connection with additional welded reinforcement, V_u, is given by:

$$V_u = C_f + C_{fs} - C_b - C_{bs} \qquad 4.18$$

which upon substitution of Eq. 4.7, Eq. 4.9, Eq. 4.14 and Eq. 4.15 gives:

$$V_u = 0.85\, f_c'\, b\, \beta_1 x_f + A_s f_s - \alpha\beta\, f_c'\, b\, (\ell_e - x_f) - A_s'\, f_s' \qquad 4.19$$

Equation 4.19 defines the ultimate capacity of a connection containing additional welded reinforcement. The moment on the connection corresponding to the ultimate capacity as defined by Eq. 4.19 is given by:

$$V_u\, e = C_f\, (\ell_e/2 - \beta_1 x_f/2) + A_s f_s\, (\ell_e/2 - d_f) + C_b[\ell_e/2 - \beta(\ell_e - x_f)/2] + A_s' f_s'\, [\ell_e/2 - d_b] \qquad 4.20$$

In order to determine the capacity of a connection containing additional welded reinforcement an iteration procedure can be used by assuming different values of x_f until Equation 4.19 and Equation 4.20 are both satisfied.

Specimens SC7 and SC8 had capacities which were 25.5 kip (113 kN) and 28.5 kip (127 kN) greater than the capacity of specimen SC5. This increased capacity is due to the presence of additional welded reinforcement in specimens SC7 and SC8. The predicted increases in capacity according to the PCI Design Method and the analytical model were 13.4 kip (59.6 kN) and 13.6 kip (60.5 kN) respettively. The two methods predict almost the same

additional capacity for this particular case because the strain in the steel as calculated by the analytical model was close to the yield strain as is always assumed by the PCI Design Method.

The total capacity of specimen SC8 was 83.5 kips(371 kN). The PCI Design Method predicts a capacity of 31.4 kips(140 kN). The analytical model predicts an ultimate capacity of 53.6 kips(238 kN).

4.5 Effects of Axial Load

Four identical specimens SC2, SC3, SC4 and SC5, were tested with axial loads of 240 kips (1068 kN), 160 kips(712 kN), 80 kips (356 kN) and zero axial load respectively. A comparison of the load-deflection responses of the four specimens and a photograph of the specimens after failure are shown in Fig. 4.7.

From the photograph of Fig. 4.7 it can be seen that the region of spalling on the front face of the connection above the embedded steel member increases and the diagonal cracks on the sides become steeper as the axial load is increased. The specimens with higher axial load also exhibited spalling on the back face of the column. As can be seen from the load deflection responses of the four specimens, the deflection at ultimate, which is a measure of the ductility, decreases with an increase in axial load.

In order to show the effect of axial load on the capacity of the connection the axial load-shear interaction diagram was plotted in Fig. 4.8 in terms of the non dimensional variables P/P_o, where P_o is the pure axial capacity of the column, and $V/f'_c\ b\ \ell_e$. In addition to the specimens described above an identical specimen, SC1 was tested under pure axial load. As can be seen in Fig. 4.8 the shear capacity of the connection increases with increasing

axial load until a maximum shear capacity is reached when the column is subjected to approximately 50 percent of its axial capacity. For values of axial load greater than 50 per cent of the axial capacity of the column the shear capacity decreases with increasing axial load. The shear capacities of the connection for axial loads less than 75 per cent of the axial capacity of the column were greater than the capacity of the connection at zero load.

The analytical model can therefore be used to conservatively predict the capacity of connections where the axial load in the column does not exceed 75 percent of its axial capacity.

4.6 Comparison of Predictions with Test Results

Table 4.1 compares the predictions of the analytical model and the PCI Design Method with the test results. The effective width used in the predictions of the analytical model is also given in this table. It is noted that all specimens had an effective width equal to the outer dimension of the column ties except for specimen TC1. Since TC1 was an extremely wide specimen the effective width used was equal to twice the width of the embedded steel member. As specified in the PCI Design Method, only the width of the embedded steel member was considered to be effective.

The analytical model is conservative for all properly detailed connections. Specimen C1 incorporated thin walled hollow structural steel member which was not filled with concrete. This specimen therefore failed prematurely without developing its full effective width due to local bending of the walls. Specimen TC3 had a reduced width of concrete in the region of the connection and thus was unable to develop its full effective width.

	b		V_{exp}		V_{PCI}		V_{theory}				
	in	mm	kips	kN	kips	kN	kips	kN	$\frac{V_{exp}}{V_{PCI}}$	$\frac{V_{exp}}{V_{theory}}$	$\frac{V_{theory}}{V_{PCI}}$
SERIES I											
C1	5.5	140	27.8	124	17.3	77	30.5	136	1.61	0.91	1.77
C2	6.0	152	41.4	184	14.0	62	27.3	121	2.96	1.52	1.95
C3	6.0	152	45.0	200	18.7	83	35.7	159	2.41	1.26	1.91
C4	6.0	152	53.5	238	20.9	93	39.4	175	2.56	1.36	1.88
SERIES II											
SC2	7.0	178	55.8	248	19.9	89	45.1	201	2.80	1.23	2.28
SC3	7.0	178	70.7	314	18.0	80	40.0	178	3.93	1.76	2.22
SC4	7.0	178	66.8	297	18.0	80	40.0	178	3.71	1.67	2.22
SC5	7.0	178	55.0	245	18.0	80	40.0	178	3.06	1.37	2.22
SC6	7.0	178	60.9	271	18.0	80	40.0	178	3.38	1.52	2.22
SC7	7.0	178	80.5	358	31.4	140	53.6	238	2.57	1.50	1.71
SC8	7.0	178	83.5	371	31.4	140	53.6	238	2.66	1.56	1.71
SC9	7.0	178	49.1	218	17.3	77	38.5	171	2.84	1.27	2.23
SC10	7.0	178	62.8	279	20.3	90	45.6	203	3.09	1.38	2.25
SC11	7.0	178	220.0	979	81.6	363	214.2	953	2.70	1.02	2.65
SC12	7.0	178	212.0	943	81.6	363	214.2	953	2.60	0.99	2.63
SC13	7.0	178	210.0	934	81.6	363	214.2	953	2.57	0.98	2.62
SERIES III											
TC1	8.0	203	58.9	262	14.3	64	37.0	165	4.12	1.59	2.59
TC2	7.0	178	32.3	144	14.3	64	32.4	144	2.26	1.00	2.26
TC3	7.0	178	17.5	78	-	-	19.8	88	-	0.88	-
TC4	7.0	178	26.0	116	-	-	19.8	88	-	1.31	-

TABLE 4.1 COMPARISON OF ANALYTICAL MODEL AND PCI DESIGN METHOD WITH EXPERIMENTAL RESULTS

Specimens SC3 and SC4 reflect the conservative predictions of the analytical model for specimens with axial load less than 75 percent of the pure axial load capacity of the column. The capacities of the specimens with zero eccentricity, SC11, SC12 and SC13, are predicted within two percent accuracy by the analytical model.

The predictions of the PCI Design Method are overly conservative for all the properly detailed specimens. The ratio of the experimental capacity of a connection to the capacity predicted by the PCI Design Method varies from 2.41 to 4.12 for these specimens. Even for the specimens tested with zero eccentricity (SC11, SC12, and SC13) the PCI Design Method is overly conservative. Fig. 4.9 gives the variation in the non-dimensionalized shear capacity of a connection as a function of the e/ℓ_e ratio as derived in section 4.1.

These design curves are compared with the experimental results of specimens SC5, SC6, SC9, SC10, SC11, SC12 and SC13 each specimen having a measured concrete strength of 4500 psi (31 MPa). This figure illustrates that the analytical model conservatively predicts the reduction in the capacity of connections incorporating embedded structural steel members with increasing eccentricity.

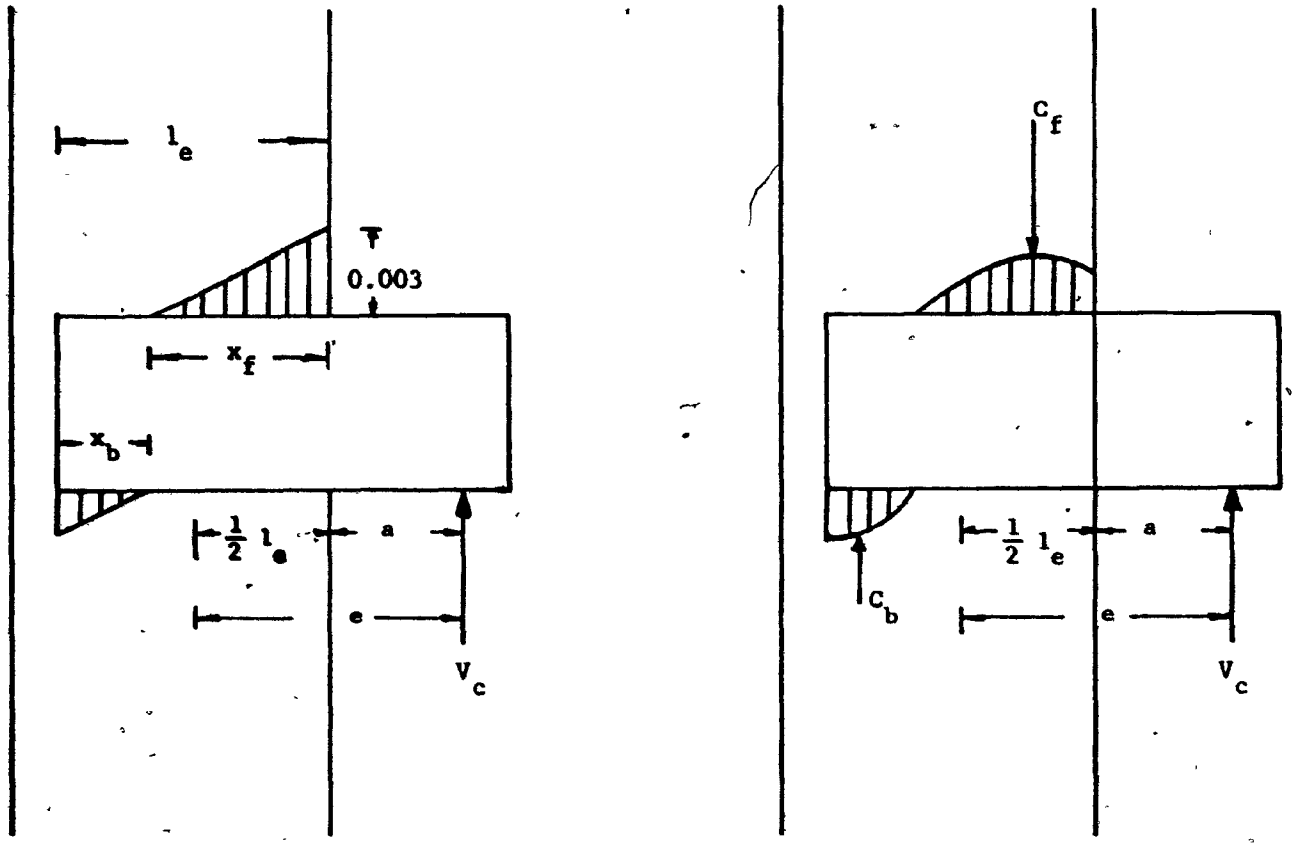

Figure 4.1 Stress and strain distributions of the analytical model

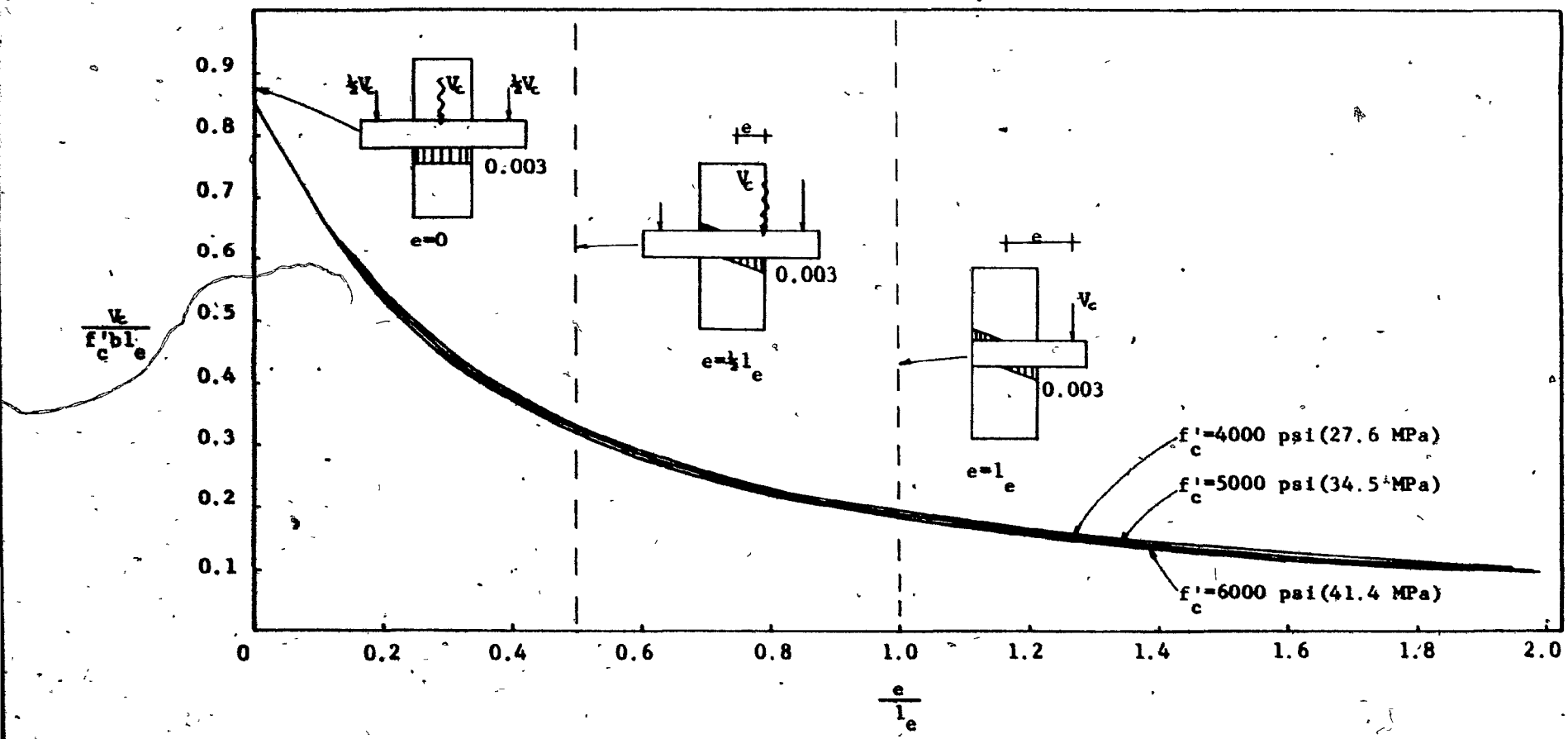

Figure 4.2 Proposed Design Curves

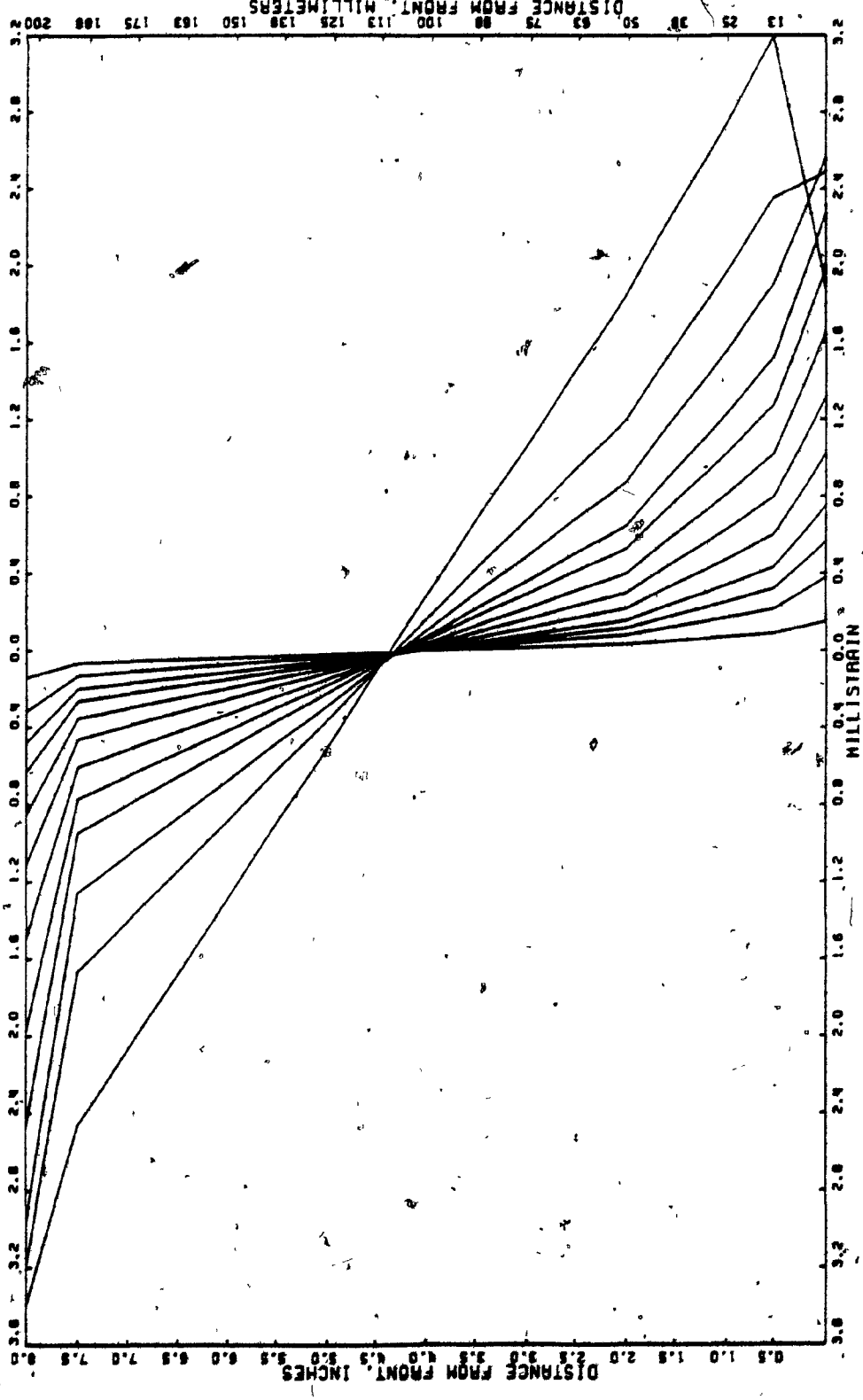

Figure 4.3 Strain distribution in specimen TC3

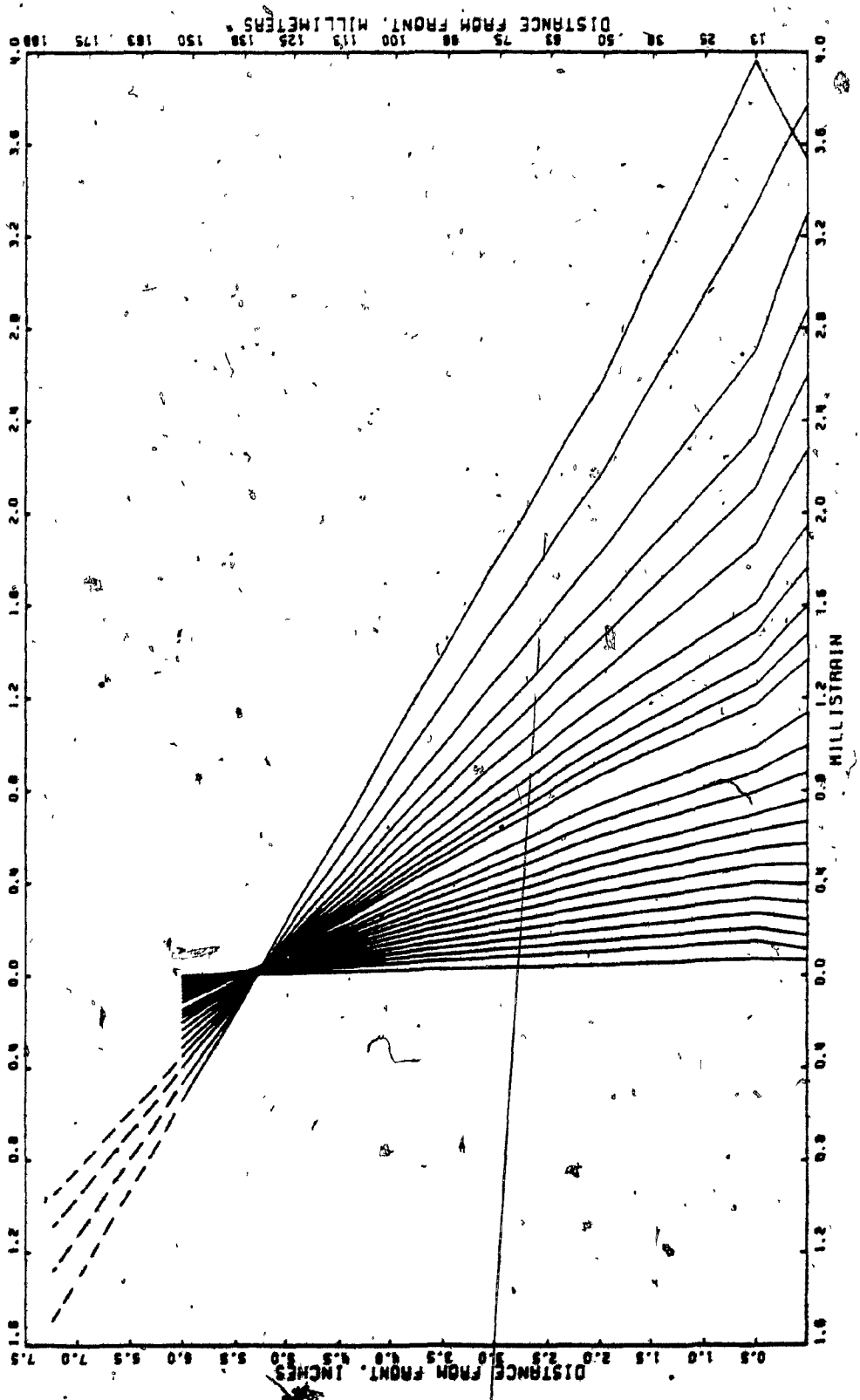

Figure 4.4 Strain distribution in specimen TC2

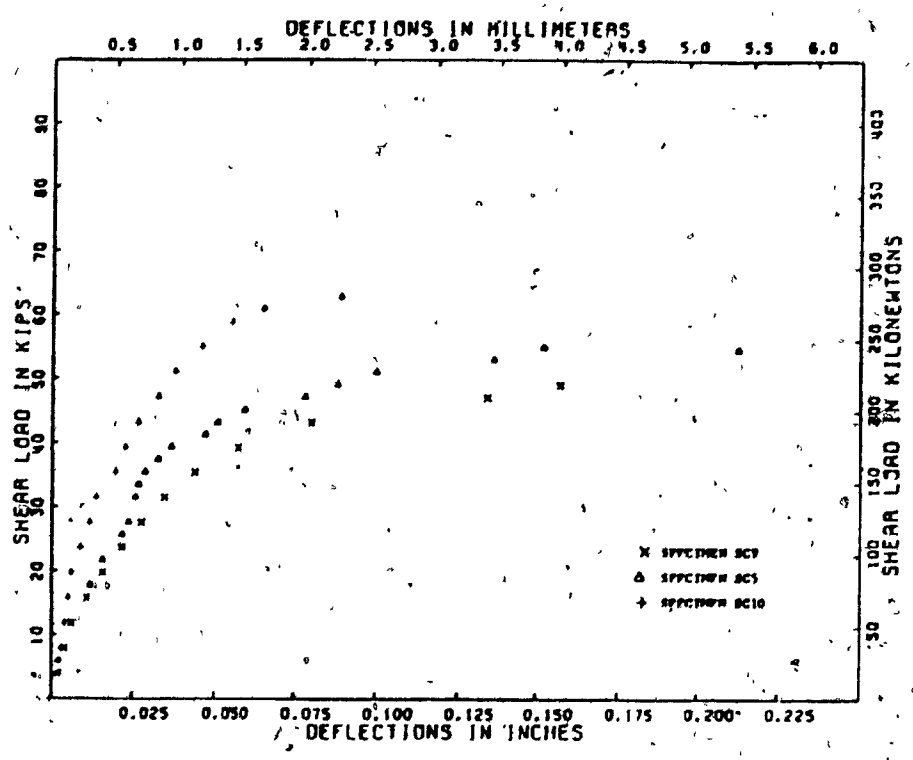

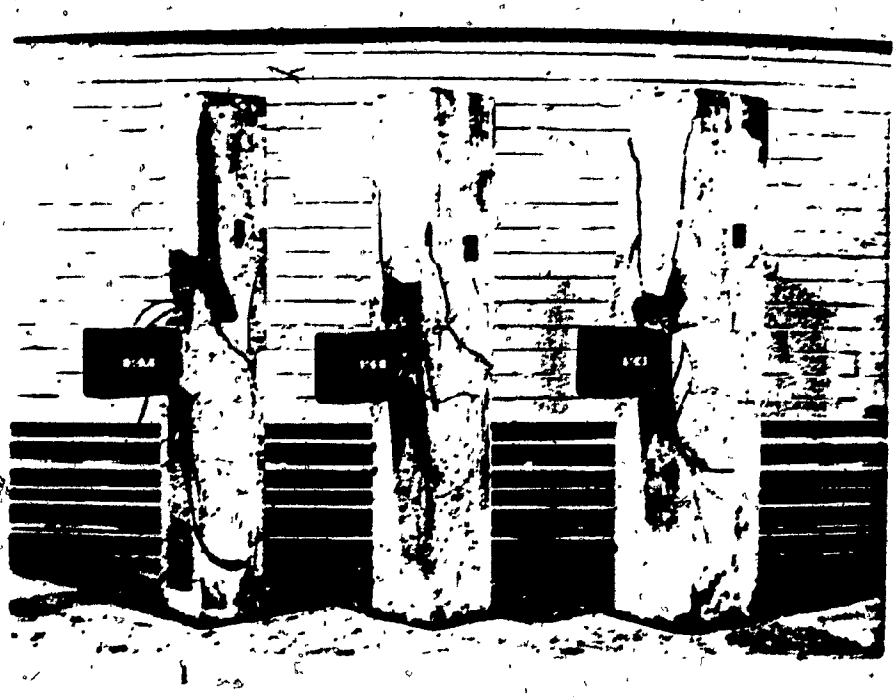

Figure 4.5 A comparison of the load deflection response and a photograph of specimens SC9, SC5 and SC10 at failure

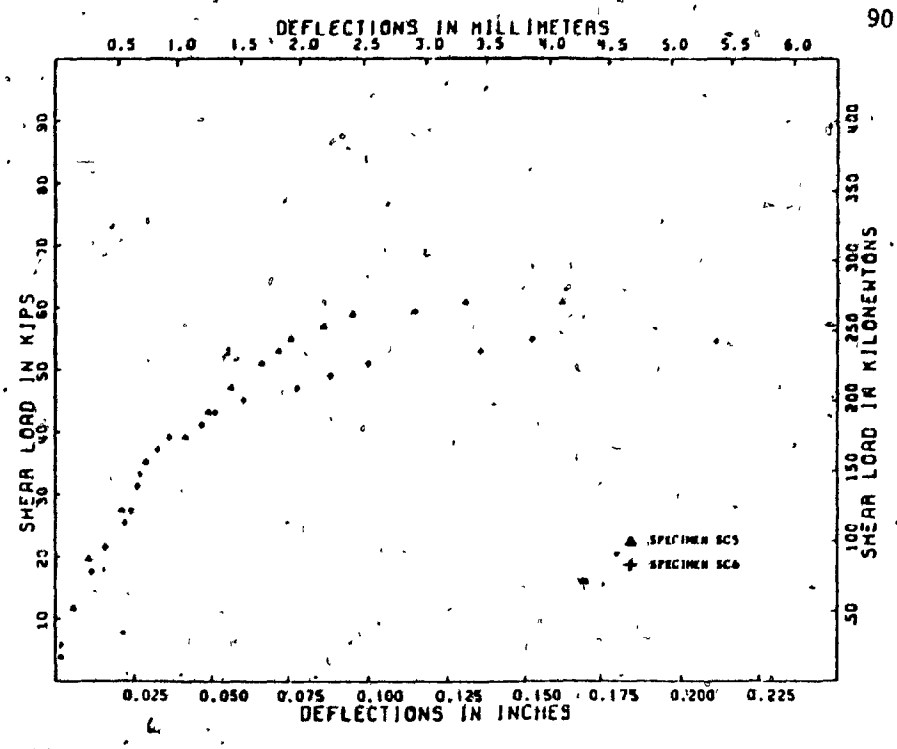

Figure 4.6 A comparison of the load deflection responses and a photograph of specimens SC5 and SC6 at failure

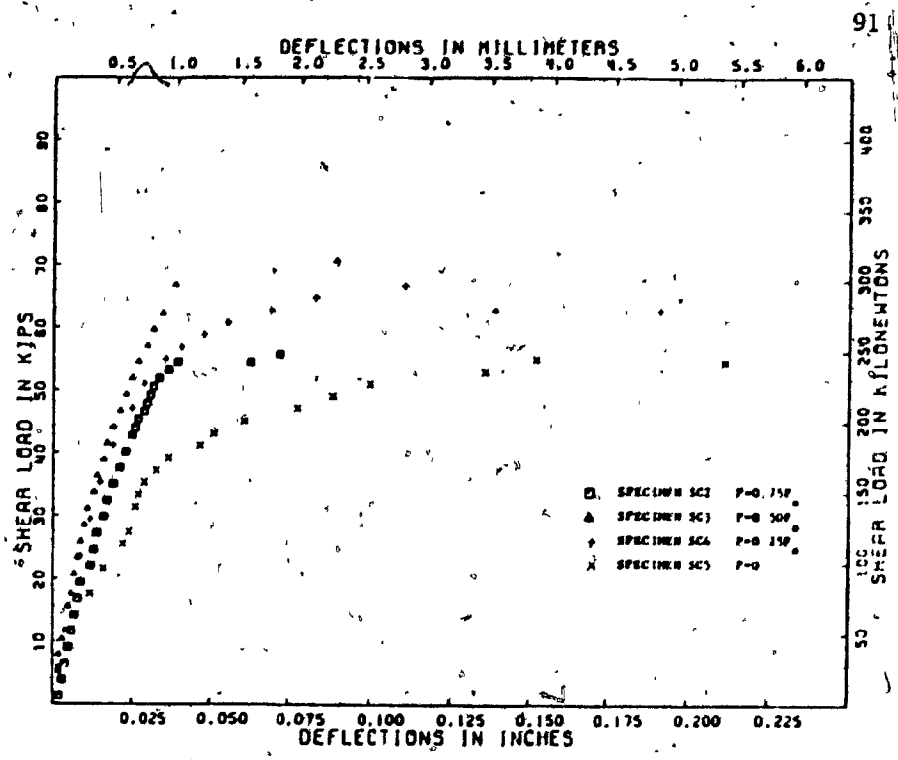

Figure 4.7 A comparison of the load deflection responses and a photograph of specimens SC2, SC3, SC4 and SC5 at failure

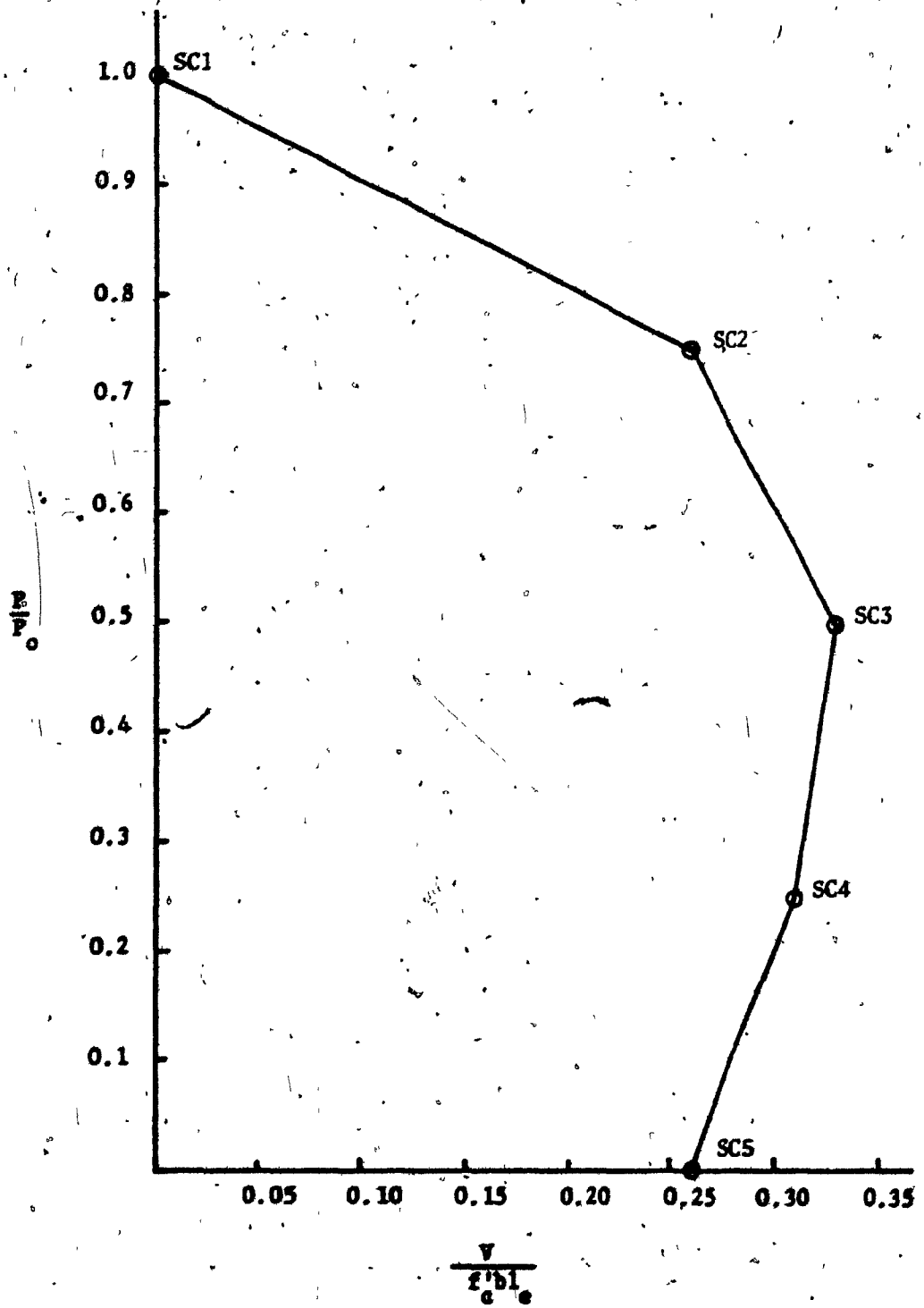

Figure 4.8 Axial load shear interaction diagram

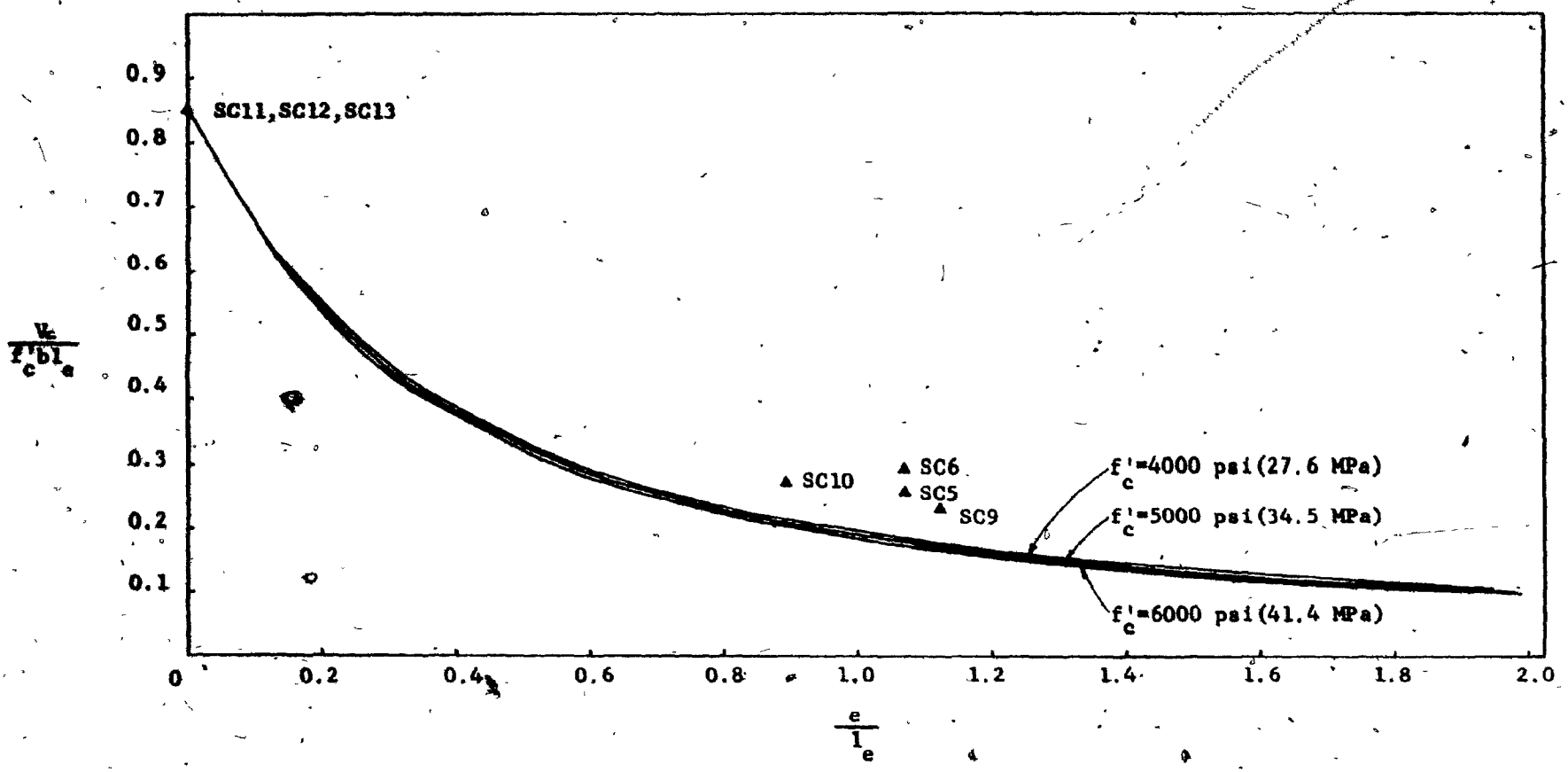

Figure 4.9 Comparison of the design curves of the analytical model with the test results

CHAPTER 5 CONCLUSIONS

The analytical model developed in this thesis together with recommendations for the design of these connections are described below.

5.1 Basic Assumptions of the Analytical Model

A linear strain distribution with a maximum strain of 0.003 is assumed. It is also assumed that the neutral axis depth is the same above and below the embedded structural steel member. The neutral axis depth is determined such that equilibrium of forces and moments on the steel is achieved (see Equations 4.10 and 4.12). In calculating the stress resultant of the triangular strain distribution having a maximum strain of 0.003 the American Concrete Institute stress block factors are used. Where the maximum strain is less than 0.003 a parabolic stress distribution (see Equation 4.3) is assumed and the stress block factors are calculated based on the value of this maximum strain.

It is assumed that a connection protruding from two sides of a column with zero effective eccentricity (e.g. equal loads and equal eccentricities on both sides) has a uniform strain distribution at ultimate of 0.003. A connection protruding from one side only results in:

a] a maximum strain of 0.003 on the front face of the connection

b] a neutral axis depth exceeding one half of the embedment length of the steel member

and c] a resulting strain in the concrete at the back of the embedded steel member which is less than 0.003 depending on the eccentricity of the applied load on the connection.

The results of specimens TC2 and TC3 with measured strain distributions confirmed the validity of these assumptions.

5.2 Effective Width of the Connection at Ultimate

All of the specimens tested indicated that the effective width of the connection at ultimate is larger than the width of the embedded structural steel member. A study of the specimens indicated that at ultimate the concrete cover spalls off in the vicinity of the connection and therefore is ineffective. Thus the maximum effective width that may be used in calculating the capacity of a connection is the width of the confined concrete core measure to the outside of the column ties.

If the width of the column is very large compared to the width of the embedded structural steel member then it may not be possible for spreading of the load to develop over the entire width of the confined core. This was demonstrated by specimen TC1 having a confined core width of 15 inches (381 mm) and an embedded member width of 4 inches (102 mm). A study of the specimen at ultimate together with the need to have a conservative prediction for this well confined specimen resulted in an 8 inch (203 mm) effective width used in the predictions.

It is recommended that the effective width used in design be taken as equal to the smaller of the following:

a] the width of the confined concrete core measured to the outside of the column ties

or b] twice the width of the embedded structural steel member.

The latter requirement is conservative since it is based on only one test and therefore further research is required.

5.3 Effect of Shape of Embedded Steel Member

The results of specimens SC5 and SC6 indicate that a connection incorporating a wide flange member is able to develop a larger capacity. This is due to the effect of the additional loading surface provided by the bottom flange of the wide flange member. This effect, however, is not accounted for in the design recommendations.

5.4 Effect of Additional Reinforcement

Additional welded reinforcement considerably increases the capacity of these connections as demonstrated by the results of specimens SC7 and SC8. The analytical model is capable of including the effects of the additional welded reinforcement as outlined in Section 4.4. The analytical model accounts for the effect of the presence of the additional welded reinforcement on the strain distribution and bases the stresses in the reinforcement on the strains derived from compatibility.

5.5 The Effect of Axial Load

It was found that increasing the axial load decreases the ductility of the connection. The capacity of the connection was found to increase with increasing axial load to a maximum value when the column is subjected to 50 percent of its axial load capacity. For values of axial load greater than this value the capacity of the connection was observed to decrease with increasing axial load. For the range of axial loads less than 75 percent of the axial capacity of the column the connection strength exceeded the capacity of the connection at zero axial load.

Based on the results of five specimens it is tentatively recommended that the capacity of the connection be determined by Equation 4.10 and Equation 4.12 for axial loads less than 75 percent of the axial capacity of the column.

5.6 Guidance for Detailing

Specimen C1 demonstrated that if the embedded structural steel member is sensitive to local bending then the full effective width of the connection may not be developed. This can be avoided by choosing a stiffer member or in the case of a hollow structural steel member by filling the embedded member with concrete.

Since the effective width is dependent on the confinement of the concrete it is necessary to ensure that the region around the connection be adequately confined with column ties. Since spalling of the concrete cover takes place at ultimate the free ends of the column ties should be anchored in the confined core of the column.

5.7 Design Aid

To facilitate the design of these connections design curves are presented in Fig. 4.9 for connections with concrete strengths of 4000 psi (27.6 MPa), 5000 psi (34.5 MPa) and 6000 psi (41.4 MPa). The design curves predict the decrease in connection strength with increasing eccentricity of the load. The shear capacity is presented in non-dimensional form as $V_c/f'_c b \ell_e$ and the effective eccentricity of the load is expressed as the ratio of the eccentricity divided by the embedment length of the steel member. These design curves were prepared by the methods outlined in Section 4.1.

The results of the tests shown in Fig. 4.9 indicate that the analytical model conservatively predicts the trend in the results.

5.8 Comparisons of Predictions

The PCI Design Method and the analytical model developed in this thesis are compared with the test results in Table 4.1. The PCI Design Method uses an effective width equal to the width of the embedded member and a strain distribution that is independent of the eccentricity of the applied load. In addition this method assumes that the additional welded reinforcement always yields.

The PCI Design Method is overly conservative with measured strengths ranging from 2.41 to 4.12 times the predicted capacity of the connection for properly detailed specimens. The analytical model accurately predicts the capacity of the specimens with zero effective eccentricity within 2 percent. The properly detailed specimens having zero axial load had measured strengths ranging from 1.27 to 1.59 times the capacity predicted by the analytical model.

It is concluded that the analytical model presented in this thesis provides a more rational design approach for precast concrete connections incorporating embedded structural steel members.

NOTATION

a	eccentricity of the load from the concrete surface, shear span
a	depth of equivalent rectangular stress block as defined by the ACI[4]
A'_s	area of additional welded reinforcement at the rear of the embedded member
A_s	area of additional welded reinforcement at the front of the connection
b	width of the embedded steel member
b	effective width in compression of the connection
C	compressive force
C_b	resultant compressive force at back of embedded member
C_{bs}	force in additional reinforcement at back of embedded member
C_f	resultant compressive force at front of connection
C_{fs}	force in additional reinforcement at front of connection
E_s	modulus of elasticity of steel
f'_c	compressive strength of concrete
f_c	stress in concrete
f'_{sb}	stress in additional reinforcement at back of embedded member
f_s	stress in additional reinforcement at front of connection
f_y	yield stress of steel
ℓ_e	embedment length
s	distance from extreme compression fibre to neutral axis
x_b	distance from back of embedded member to neutral axis
x_f	distance from front of connection to neutral axis
P	axial load
P_o	pure axial capacity of column

V	shear load
V_c	nominal shear capacity of connection
V_n	nominal shear capacity of each side of a connection protruding from two sides with symmetrical loading
V_r	additional nominal shear capacity provided by welded reinforcement
V_u	nominal shear capacity of a connection with additional welded reinforcement.
α	ratio of average stress of equivalent uniform stress distribution to peak concrete stress
β	ratio of depth of equivalent uniform stress distribution from extreme compression fibre to depth of neutral axis from extreme compression fibre.
β_1	ACI stress block factor
ε	strain
ε_b	maximum strain in concrete at back of embedded member
ε_f	maximum strain in concrete at front face of connection
ε_o	strain in concrete at peak compressive stress
ϕ	curvature resulting from strain distribution
Δ	displacement

REFERENCES

1. PCI Design Handbook
   Prestressed Concrete Institute, Chicago, Illinois 1971

2. Raths, Charles H., "Embedded Structural Steel Connections",
   PCI Journal, May-June, 1974

3. PCI Design Handbook: Second Edition
   Prestressed Concrete Institute, Chicago, Illinois 1978

4. ACI Committee 318, "Building Code Requirements for Reinforced
   Concrete (ACI 318-77)"
   American Concrete Institute, Detroit, Michigan, 1977

APPENDIX A

TABLES OF TEST RESULTS

SPECIMEN C1

LOAD		MICROSTRAINS ON FRONT FACE OF COLUMN							
kips	kN	1	2	3	4	5	6	7	8
0.0	0.0	4.	28.	-11.	-9.	-12.	13.	2.	-3.
0.9	4.0	-5.	17.	-29.	-50.	-27.	-5.	-6.	-12.
1.9	8.5	-29.	-25.	-39.	-89.	-41.	-22.	-21.	-20.
3.2	14.2	-126.	-99.	-58.	-165.	-79.	-69.	-54.	-37.
5.2	23.1	-161.	-247.	-93.	-328.	-97.	-116.	-99.	-59.
6.5	28.9	-140.	-397.	-125.	-504.	-97.	-157.	-141.	-83.
7.8	34.7	30.	-588.	-162.	-750.	-161.	-211.	-195.	-113.
9.1	40.5	187.	-805.	-199.	-1046.	-258.	-281.	-265.	-185.
10.4	46.3	315.	-1060.	-240.	-1444.	-326.	-360.	-335.	-204.
11.7	52.0	410.	-1306.	-268.	-1869.	-324.	-419.	-399.	-251.
13.0	57.8	451.	-1570.	-296.	0.	-291.	-469.	-484.	-308.
14.3	63.6	435.	-1862.	-343.	0.	-257.	-468.	-584.	-372.
15.6	69.4	388.	-1961.	-396.	0.	-226.	-416.	-670.	-435.
16.9	75.2	305.	-1945.	-512.	0.	-194.	-490.	-769.	-519.
18.2	81.0	217.	-1864.	-594.	-2110.	-162.	-488.	-857.	-588.
19.5	86.7	63.	-1475.	-714.	-1906.	-115.	-471.	-996.	-678.
20.8	92.5	-97.	-1255.	-828.	-1222.	-77.	-455.	-1144.	-766.
22.1	98.3	-167.	-1207.	-874.	-884.	-51.	-459.	-1306.	-824.
23.4	104.1	-219.	-1119.	-962.	-580.	-33.	-473.	-1476.	-886.
24.7	109.9	-215.	-887.	-1144.	-620.	-53.	-415.	-1730.	-968.
26.0	115.6	-301.	-785.	-1450.	-482.	-141.	-187.	-1964.	-1008.
26.3	117.0	-61.	-759.	-1852.	20.	-171.	-143.	-2016.	-1036.
26.9	119.7	21.	-711.	-1842.	430.	-173.	-123.	-2034.	-1058.
27.8	123.7	31.	733.	-1648.	528.	-171.	-111.	-1952.	-1074.

SPECIMEN C1

LOAD		STEEL MICROSTRAINS				CONCRETE MICROSTRAINS ON SIDE OF COLUMN			
kips	kN	1	2	3	4	1	2	3	4
0.0	0.0	65.	-15.	-7.	-2.	35.	-3.	6.	-1.
0.9	4.0	112.	-6.	-5.	5.	40.	-15.	9.	4.
1.9	8.5	102.	3.	-1.	8.	31.	-31.	7.	5.
3.2	14.2	52.	10.	-14.	-8.	-14.	-81.	-10.	-12.
5.2	23.1	57.	17.	-11.	-15.	-33.	-125.	-14.	-13.
6.5	28.9	74.	79.	-11.	-16.	-46.	-164.	-18.	-16.
7.8	34.7	129.	195.	-8.	-5.	-59.	-208.	-24.	-22.
9.1	40.5	211.	345.	-8.	3.	-86.	-270.	-36.	-34.
11.7	52.0	495.	635.	7.	36.	-110.	-343.	-52.	-48.
10.4	46.3	371.	510.	-2.	18.	-138.	-407.	-69.	-64.
13.0	57.8	600.	761.	20.	66.	-200.	-490.	-98.	-79.
14.3	63.6	711.	894.	35.	101.	-285.	-511.	-130.	-101.
15.6	69.4	815.	1037.	54.	140.	-349.	-447.	-159.	-130.
16.9	75.2	904.	1193.	74.	184.	-411.	-417.	-183.	-165.
18.2	81.0	990.	1351.	96.	230.	-475.	-422.	-195.	-199.
19.5	86.7	1070.	1550.	140.	308.	-565.	-452.	-190.	-251.
20.8	92.5	1130.	1790.	190.	396.	-661.	-476.	-113.	-307.
22.1	98.3	1206.	1990.	248.	494.	-757.	-478.	-50.	-363.
23.4	104.1	1248.	2204.	328.	618.	-849.	-432.	32.	-379.
24.7	109.9	1264.	2350.	428.	760.	-953.	-350.	120.	-381.
26.0	115.6	1144.	2350.	566.	924.	-1113.	-200.	146.	-229.
26.3	117.0	1008.	2298.	702.	1044.	-1125.	-182.	176.	-181.
26.9	119.7	834.	2230.	864.	1556.	-965.	-158.	306.	-127.
27.8	123.7	770.	2196.	970.	1256.	-875.	-146.	462.	-59.

SPECIMEN C2

LOAD		STEEL MICROSTRAINS				CONCRETE MICROSTRAINS				
kips	kN	1	2	3	4	1	2	3	4	5
0.0	0.0	-158.	-168.	-114.	-113.	4.	-47.	-139.	-101.	-115.
1.0	4.4	-166.	-188.	-157.	-77.	0.	-61.	-181.	-124.	-145.
2.0	8.9	-170.	-201.	-132.	-75.	38.	-75.	-214.	-144.	-173.
3.0	13.3	-164.	-207.	-133.	-83.	83.	-82.	-238.	-156.	-191.
4.0	17.8	-162.	-217.	-139.	-92.	127.	-94.	-266.	-172.	-216.
5.0	22.2	-160.	-227.	-153.	-100.	131.	-108.	-295.	-190.	-244.
6.0	26.7	-161.	-240.	-155.	-114.	130.	-124.	-326.	-211.	-276.
7.0	31.1	-151.	-244.	-156.	-118.	131.	-135.	-350.	-224.	-302.
8.0	35.6	-142.	-251.	-162.	-129.	163.	-149.	-387.	-246.	-342.
9.0	40.0	-141.	-261.	-169.	-139.	265.	-172.	-424.	-268.	-384.
10.0	44.5	-131.	-264.	-175.	-143.	260.	-187.	-455.	-285.	-419.
11.0	48.9	-118.	-265.	-178.	-147.	256.	-205.	-493.	-306.	-462.
12.0	53.4	-121.	-275.	-187.	-158.	278.	-225.	-534.	-330.	-507.
13.0	57.8	-110.	-274.	-189.	-162.	285.	-250.	-580.	-351.	-554.
14.0	62.3	-109.	-282.	-197.	-173.	200.	-277.	-632.	-383.	-612.
15.0	66.7	-103.	-285.	-203.	-181.	166.	-306.	-686.	-414.	-669.
16.0	71.2	-98.	-290.	-206.	-191.	211.	-339.	-750.	-450.	-732.
17.0	75.6	-81.	-287.	-209.	-195.	274.	-374.	-812.	-487.	-790.
18.0	80.1	-81.	-292.	-220.	-206.	239.	-413.	-879.	-526.	-861.
19.0	84.5	-67.	-288.	-222.	-210.	223.	-445.	-934.	-563.	-913.
20.0	89.0	-54.	-287.	-229.	-218.	320.	-489.	-1005.	-609.	-984.
21.0	93.4	-37.	-273.	-233.	-218.	606.	-540.	-1088.	-661.	-1067.
22.0	97.9	-27.	-262.	-242.	-224.	721.	-632.	-1225.	-757.	-1213.
23.0	102.3	-9.	-248.	-250.	-225.	1656.	-697.	-1328.	-828.	-1328.
24.0	106.8	27.	-211.	-254.	-222.	3037.	-779.	-1452.	-914.	-1483.
25.0	111.2	0.	-221.	-267.	-230.	0.	-810.	-1494.	-947.	-1560.
26.0	115.6	35.	-198.	-275.	-235.	4889.	-893.	-1624.	-1040.	-1708.
27.0	120.1	79.	-158.	-278.	-231.	6132.	-991.	-1759.	-1143.	-1878.
28.0	124.5	112.	-108.	-288.	-227.	6200.	-1117.	-1936.	-1279.	-2158.
29.0	129.0	140.	-65.	-284.	-198.	0.	-1270.	-2164.	-1449.	-2408.
30.0	133.4	183.	-10.	-263.	-160.	5800.	-1430.	-2368.	-1627.	-2648.
31.0	137.9	245.	63.	-217.	-121.	0.	-1657.	-2604.	-1892.	-2928.
32.0	142.3	300.	144.	-169.	-91.	4800.	-1973.	-2878.	-2290.	-3224.
33.0	146.8	330.	181.	-155.	-78.	0.	-2110.	-2962.	-2418.	-3302.
34.0	151.2	363.	234.	-125.	-60.	3200.	-2244.	-3028.	-2564.	-3364.
35.0	155.7	425.	340.	-80.	-9.	1790.	-2586.	-3130.	-2948.	-3492.
36.0	160.1	476.	475.	-38.	43.	328.	-2890.	-3256.	-3312.	-3570.
36.6	162.8	520.	714.	21.	146.	-606.	-3688.	-2783.	-4628.	-3323.
37.0	164.6	556.	827.	63.	212.	-1042.	-3898.	-2323.	-5073.	-3253.
39.6	176.1	595.	1088.	185.	386.	0.	-3283.	-611.	-5768.	-2018.
40.6	180.6	629.	1335.	340.	597.	0.	-2208.	496.	-4193.	-383.
41.4	184.1	744.	1882.	809.	1105.	0.	-1427.	879.	0.	3257.

SPECIMEN C3

LOAD		STEEL MICROSTRAINS				CONCRETE MICROSTRAINS				
kips	kN	1	2	3	4	1	2	3	4	5
0.0	0.0	-332.	-318.	-339.	-333.	-131.	-161.	-318.	-160.	-198.
2.0	8.9	-358.	-351.	-342.	-358.	-184.	-206.	-423.	-205.	-235.
4.0	17.8	-364.	-361.	-335.	-362.	-219.	-234.	-488.	-233.	-264.
6.0	26.7	-299.	-402.	-403.	-362.	-291.	-301.	-603.	-298.	-328.
8.0	35.6	-416.	-421.	-364.	-421.	-351.	-355.	-691.	-352.	-376.
10.0	44.5	-429.	-435.	-369.	-440.	-418.	-418.	-773.	-405.	-428.
12.0	53.4	-437.	-449.	-374.	-459.	-475.	-471.	-841.	-459.	-472.
14.0	62.3	-447.	-461.	-379.	-478.	-546.	-540.	-906.	-519.	-531.
16.0	71.2	-453.	-470.	-385.	-495.	-616.	-610.	-965.	-584.	-587.
18.0	80.1	-456.	-477.	-390.	-515.	-703.	-704.	-1040.	-664.	-659.
20.0	89.0	-462.	-483.	-398.	-535.	-790.	-796.	-1107.	-743.	-730.
22.0	97.9	-466.	-486.	-407.	-556.	-887.	-905.	-1171.	-936.	-810.
24.0	106.8	-464.	-483.	-424.	-580.	-1026.	-1058.	-1255.	-964.	-921.
26.0	115.6	-451.	-477.	-429.	-598.	-1156.	-1205.	-1323.	-1090.	-1021.
28.0	124.5	-428.	-558.	-439.	-621.	-1380.	-1412.	-1422.	-1250.	-1157.
30.0	133.4	-366.	-402.	-461.	-656.	-1509.	-1686.	-1577.	-1470.	-1331.
31.0	137.9	-334.	-365.	-469.	-671.	-1598.	-1794.	-1636.	-1554.	-1402.
32.0	142.3	-272.	-290.	-475.	-684.	-1672.	-1968.	-1732.	-1696.	-1511.
33.0	146.8	-250.	-256.	-482.	-698.	-1759.	-2142.	-1821.	-1815.	-1602.
34.0	151.2	-229.	-217.	-489.	-710.	-1861.	-2294.	-1942.	-1956.	-1703.
35.0	155.7	-199.	-173.	-492.	-721.	-1942.	-2416.	-2052.	-2080.	-1783.
36.0	160.1	-176.	-87.	-498.	-733.	-2118.	-2738.	-2268.	-2360.	-1969.
37.0	164.6	-151.	-20.	-499.	-740.	-2198.	-2896.	-2368.	-2506.	-2076.
38.0	169.0	-132.	32.	-501.	-746.	-2250.	-2996.	-2396.	-2610.	-2178.
39.0	173.5	-104.	107.	-505.	-751.	-2262.	-2926.	-2402.	-2668.	-2286.
40.0	177.9	-84.	172.	-515.	-757.	-2242.	-2578.	-2458.	-2586.	-2340.
41.0	182.4	-40.	334.	-508.	-751.	-2178.	-1547.	-2546.	-2106.	-2110.
42.0	186.8	-34.	538.	-498.	-613.	-1733.	-948.	-2232.	-1863.	-1846.
43.0	191.3	48.	767.	-420.	-444.	-1552.	-880.	-1973.	-1680.	-1648.
44.0	195.7	79.	943.	-304.	-258.	-1093.	-848.	-1553.	-1300.	-1456.
44.2	196.6	92.	1098.	-167.	-89.					
44.8	199.3	138.	1458.	322.	468.					

SPECIMEN C4

LOAD		STEEL MICROSTRAINS				CONCRETE MICROSTRAINS				
kips	kN	1	2	3	4	1	2	3	4	5
0.0	0.0	-643.	-566.	-614.	-404.	-382.	-299.	-470.	-370.	-504.
2.0	8.9	-640.	-583.	-642.	-416.	-458.	-339.	-555.	-417.	-569.
4.0	17.8	-660.	-613.	-714.	-467.	-521.	-403.	-608.	-489.	-601.
6.0	26.7	-623.	-597.	-675.	-441.	-523.	-397.	-659.	-478.	-645.
8.0	35.6	-650.	-647.	-713.	-464.	-586.	-432.	-724.	-534.	-712.
8.0	35.6	-676.	-636.	-671.	-393.	-722.	-759.	-943.	-810.	-1026.
10.0	44.5	-655.	-673.	-593.	-444.	-768.	-787.	-1005.	-850.	-1089.
12.0	53.4	-690.	-693.	-634.	-446.	-828.	-851.	-1098.	-889.	-1143.
14.0	62.3	-670.	-682.	-642.	-497.	-880.	-891.	-1184.	-944.	-1200.
16.0	71.2	-641.	-649.	-604.	-481.	-917.	-936.	-1255.	-988.	-1242.
18.0	80.1	-665.	-705.	-683.	-560.	-993.	-1011.	-1346.	-1076.	-1304.
20.0	89.0	-645.	-705.	-634.	-557.	-1043.	-1064.	-1447.	-1107.	-1384.
22.0	97.9	-665.	-685.	-691.	-586.	-1124.	-1163.	-1572.	-1190.	-1493.
24.0	106.8	-645.	-670.	-703.	-592.	-1174.	-1218.	-1667.	-1270.	-1581.
26.0	115.6	-612.	-679.	-682.	-596.	-1208.	-1293.	-1738.	-1300.	-1644.
28.0	124.5	-638.	-678.	-665.	-615.	-1258.	-1374.	-1800.	-1341.	-1714.
30.0	133.4	-617.	-707.	-722.	-688.	-1316.	-1460.	-1916.	-1434.	-1842.
32.0	142.3	-657.	-647.	-730.	-700.	-1392.	-1618.	-2034.	-1502.	-1994.
34.0	151.2	-623.	-649.	-690.	-734.	-1516.	-1720.	-2184.	-1642.	-2086.
36.0	160.1	-601.	-623.	-738.	-790.	-1548.	-1780.	-2270.	-1736.	-2210.

SPECIMEN SC1

LOAD		STEEL MICROSTRAINS				CONCRETE MICROSTRAINS		
kips	kN	1	2	3	4	1	2	3
20.0	89.0	-65.	-61.	-64.	-54.	-56.	-41.	-66.
40.0	177.9	-135.	-125.	-135.	-123.	-117.	-95.	-138.
60.0	266.9	-220.	-200.	-182.	-170.	-217.	-183.	-249.
80.0	355.8	-356.	-329.	-324.	-309.	-350.	-306.	-375.
100.0	444.8	-384.	-343.	-339.	-319.	-364.	-320.	-386.
120.0	533.8	-448.	-416.	-417.	-396.	-440.	-392.	-459.
140.0	622.7	-530.	-492.	-498.	-481.	-515.	-467.	-532.
160.0	711.7	-621.	-579.	-594.	-581.	-604.	-553.	-612.
180.0	800.6	-717.	-666.	-690.	-680.	-689.	-640.	-695.
200.0	889.6	-836.	-776.	-811.	-803.	-794.	-742.	-798.
220.0	978.6	-950.	-882.	-932.	-931.	-897.	-839.	-881.
240.0	1067.5	-1091.	-1015.	-1080.	-1085.	-1016.	-964.	-996.
260.0	1156.5	-1238.	-1150.	-1231.	-1247.	-1134.	-1090.	-1117.
280.0	1245.4	-1437.	-1327.	-1424.	-1464.	-1276.	-1253.	-1270.
300.0	1334.4	-1719.	-1580.	-1692.	-1777.	-1459.	-1466.	-1492.
326.0	1450.0	-2000.	-1874.	-1938.	-2080.	-1638.	-1642.	-1684.
269.0	1196.5	-273.	-302.	-273.	-349.	-188.	-328.	-95.

SPECIMEN SC2

LOAD		STEEL MICROSTRAINS			CONCRETE MICROSTRAINS		
kips	kN	1	2	3	1	2	3
0.0	0.0	-998.	-905.	-1021.	-1190.	-1033.	-809.
2.6	11.5	-1196.	-1036.	-1190.	-1403.	-1312.	-960.
5.2	23.1	-1220.	-1050.	-1190.	-1464.	-1383.	-1000.
7.8	34.6	-1257.	-1058.	-1194.	-1537.	-1475.	-1050.
10.4	46.2	-1300.	-1064.	-1194.	-1622.	-1590.	-1108.
13.0	57.7	-1348.	-1070.	-1195.	-1711.	-1720.	-1173.
15.6	69.3	-1375.	-1074.	-1191.	-1775.	-1811.	-1220.
18.2	80.8	-1412.	-1076.	-1182.	-1866.	-1963.	-1292.
20.8	92.4	-1480.	-1086.	-1186.	-1996.	-2196.	-1394.
23.4	103.9	-1524.	-1094.	-1188.	-2086.	-2352.	-1460.
26.0	115.5	-1558.	-1098.	-1184.	-2164.	-2486.	-1514.
28.6	127.0	-1590.	-1102.	-1178.	-2246.	-2634.	-1572.
31.2	138.6	-1644.	-1116.	-1180.	-2344.	-2842.	-1650.
33.7	150.1	-1688.	-1126.	-1178.	-2412.	-3046.	-1718.
36.3	161.7	-1722.	-1134.	-1174.	-2458.	-3210.	-1776.
38.9	173.2	-1772.	-1150.	-1174.	-2508.	-3474.	-1854.
41.5	184.8	-1820.	-1166.	-1170.	-2546.	-3752.	-1926.
44.1	196.3	-1870.	-1188.	-1174.	-2592.	-3994.	-1992.
46.7	207.8	-1892.	-1202.	-1172.	-2608.	0.	-2042.
49.3	219.4	-1912.	-1222.	-1178.	-2616.	0.	-2108.
51.9	230.9	-1926.	-1240.	-1182.	-2606.	0.	-2170.
54.5	242.5	-1842.	-1322.	-1502.	-1716.	0.	-1548.
55.8	248.3	-1790.	-1328.	-1538.	-1614.	-3660.	-1382.

SPECIMEN SC3

LOAD		STEEL MICROSTRAINS				CONCRETE MICROSTRAINS		
kips	kN	1	2	3	4	1	2	3
0.0	0.0	-572.	-234.	0.	-62.	-783.	-816.	-831.
5.2	23.1	-591.	-197.	0.	-60.	-891.	-936.	-941.
7.9	34.9	-1134.	-432.	0.	-729.	-1440.	-3606.	-1806.
10.4	46.2	-618.	-203.	0.	-75.	-984.	-1029.	-1028.
15.6	69.3	-643.	-209.	0.	-86.	-1080.	-1131.	-1126.
15.7	69.9	-1126.	-424.	0.	-739.	-1520.	-3710.	-1872.
20.8	92.4	-673.	-222.	0.	-104.	-1192.	-1257.	-1237.
23.6	104.8	-1150.	-436.	0.	-777.	-1632.	-3848.	-1968.
28.0	115.5	-704.	-234.	0.	-121.	-1307.	-1403.	-1356.
31.2	138.6	-736.	-249.	0.	-142.	-1427.	-1577.	-1481.
33.7	150.1	-753.	-256.	0.	-154.	-1496.	-1691.	-1551.
36.3	161.7	-774.	-262.	0.	-166.	-1560.	-1804.	-1619.
38.9	173.2	-794.	-267.	0.	-179.	-1621.	-1919.	-1688.
41.5	184.8	-810.	-272.	0.	-190.	-1680.	0.	-1759.
44.1	196.3	-846.	-280.	0.	-214.	-1762.	-2236.	-1860.
46.7	207.8	-848.	-288.	0.	-223.	-1818.	-2382.	-1928.
49.3	219.4	-898.	-292.	0.	-245.	-1972.	-2596.	-2014.
51.9	230.9	-932.	-300.	0.	-261.	-1952.	-2826.	-2090.
54.5	242.5	-974.	-302.	0.	-283.	-2006.	-3164.	-2170.
57.1	254.0	-1008.	-310.	0.	-305.	-2068.	-3500.	-2240.
59.7	265.6	-1040.	-312.	0.	-323.	-2112.	-3882.	-2294.
62.3	277.1	-1078.	-318.	0.	-345.	-2152.	0.	-2348.
66.8	297.0	-1167.	-359.	0.	-1127.	-2111.	-3330.	-2283.
70.7	314.5	-1407.	-349.	0.	-1407.	-461.	-480.	-1893.
62.8	279.5	-1637.	-354.	0.	-2122.	-641.	725.	-2388.

SPECIMEN SC4

LOAD		STEEL MICROSTRAINS				CONCRETE MICROSTRAINS		
kips	kN	1	2	3	4	1	2	3
0.0	0.0	-349.	-257.	0.	-265.	-417.	-353.	-553.
5.9	26.2	-380.	-263.	0.	-283.	-535.	-432.	-693.
11.8	52.4	-410.	-261.	0.	-304.	-667.	-526.	-863.
17.7	78.6	-440.	-258.	0.	-325.	-801.	-627.	-1045.
23.6	104.8	-462.	-245.	0.	-352.	-975.	-747.	-1252.
29.5	131.0	-489.	-228.	0.	-375.	-1143.	-912.	-1505.
35.4	157.2	-510.	-204.	0.	-404.	-1369.	-1157.	-1791.
41.2	183.5	-521.	-178.	0.	-427.	-1692.	-1536.	-2243.
47.1	209.7	-481.	-142.	0.	-421.	-1888.	-1740.	-2535.
51.1	227.1	-413.	-48.	0.	-395.	-1908.	-1948.	-2867.
55.0	244.6	-349.	0.	0.	-379.	-1716.	-1934.	-3037.
57.0	253.3	-221.	76.	0.	-335.	-1430.	-1890.	-2987.
58.9	262.1	-7.	162.	0.	-253.	-1008.	-1792.	-2701.
60.9	270.8	360.	309.	0.	-82.	-944.	-1913.	-1829.
62.8	279.5	659.	458.	0.	127.	-924.	-2054.	-1513.
64.8	288.3	1341.	799.	0.	750.	-771.	-1707.	-1208.
66.8	297.0	2817.	1188.	0.	2081.	-522.	-1582.	-1081.

SPECIMEN SC5.

LOAD		STEEL MICROSTRAINS				CONCRETE MICROSTRAINS		
kips	kN	1	2	3	4	1	2	3
5.9	26.2	-16.	-153.	20.	-61.	-173.	-99.	-90.
11.8	52.4	-28.	149.	50.	-138.	-408.	-258.	-216.
17.7	78.6	176.	753.	43.	-554.	-982.	-709.	-600.
19.6	87.4	632.	876.	84.	-384.	-1185.	-884.	-756.
21.6	96.1	838.	962.	130.	-327.	-1386.	-1076.	-885.
23.6	104.8	992.	1069.	188.	-277.	-1630.	-1323.	-1060.
25.5	113.6	1107.	1160.	220.	-241.	-1787.	-1498.	-1188.
27.5	122.3	1154.	1206.	253.	-223.	-1936.	-1664.	-1302.
29.5	131.0	1131.	1190.	281.	-236.	-2058.	-1815.	-1388.
31.4	139.8	1177.	1226.	267.	-238.	-2108.	-1883.	-1424.
33.4	148.5	1187.	1230.	273.	-234.	-2200.	-1993.	-1518.
35.4	157.2	1293.	1342.	349.	-104.	-2514.	-2379.	-1818.
37.3	166.0	1271.	1328.	369.	-130.	-2498.	-2459.	-1832.
39.3	174.7	1481.	1572.	493.	218.	-2564.	-2879.	-1986.
41.2	183.5	1539.	1574.	585.	262.	-2362.	-3203.	-2034.
43.2	192.2	1595.	1638.	709.	380.	-2006.	-2663.	-1806.
45.2	200.9	1729.	1751.	866.	1415.	-1609.	-1308.	-1254.
47.1	209.7	1938.	1967.	1190.	1952.	-999.	-862.	-604.
49.1	218.4	2039.	2068.	1383.	2246.	-602.	-745.	-576.
51.1	227.1	2117.	2186.	1497.	2604.	-298.	-561.	-574.
51.1	227.1	2179.	2352.	1725.	3156.	-366.	-749.	-596.
53.0	235.9	2285.	2436.	1837.	3684.	-398.	-717.	-608.
55.0	244.6	2968.	2467.	1976.	4362.	-391.	-704.	-603.

SPECIMEN SC6

LOAD		STEEL MICROSTRAINS				CONCRETE MICROSTRAINS		
kips	kN	1	2	3	4	1	2	3
3.9	17.5	-17.	33.	-9.	-28.	53.	-79.	-44.
7.9	34.9	-30.	69.	11.	-21.	-91.	-166.	-89.
11.8	52.4	-46.	152.	14.	-34.	-129.	-278.	-138.
15.7	69.9	-59.	339.	25.	-22.	-193.	-392.	-189.
19.6	87.4	-68.	486.	93.	6.	-273.	-552.	-250.
23.6	104.8	-60.	626.	126.	41.	-348.	-738.	-314.
27.5	122.3	-10.	772.	216.	105.	-456.	-1017.	-435.
35.4	157.2	567.	1099.	401.	193.	-828.	-1920.	-1104.
39.3	174.7	867.	1284.	513.	275.	-1092.	-2534.	-1528.
43.2	192.2	1203.	1456.	629.	355.	-1422.	-3304.	-1984.
47.1	209.7	1277.	1438.	633.	329.	-1576.	307.	-2190.
51.1	227.1	1409.	1484.	623.	297.	-1770.	307.	-2476.
53.0	235.9	1581.	1594.	711.	356.	-1944.	-4931.	-2782.
55.0	244.6	1681.	1689.	746.	371.	-1984.	-5381.	-3042.
57.0	253.3	1966.	2054.	906.	461.	-2034.	-6521.	-3802.
58.9	262.1	2161.	2309.	1016.	516.	-1924.	-6801.	-4867.
59.3	263.8	2431.	2654.	1156.	696.	-1184.	-6171.	-822.
60.9	270.8	2681.	2734.	1221.	986.	-914.	-5601.	-232.

SPECIMEN SC7

LOAD		STEEL MICROSTRAINS				CONCRETE MICROSTRAINS	
kips	kN	1	2	3	4	1	2
0.0	0.0	106.	-135.	96.	206.	105.	109.
7.9	34.9	104.	-74.	126.	171.	-82.	41.
15.7	69.9	132.	86.	156.	145.	-269.	-59.
23.6	104.8	186.	215.	184.	135.	-493.	-183.
31.4	139.8	285.	353.	187.	140.	-727.	-329.
39.3	174.7	712.	442.	229.	206.	-1132.	-559.
47.1	209.7	985.	542.	272.	268.	-1812.	-920.
51.1	227.1	1064.	563.	291.	259.	0.	-1146.
53.0	235.9	1108.	583.	296.	258.	0.	-1230.
55.0	244.6	1184.	614.	320.	268.	0.	-1428.
57.0	253.3	1257.	637.	310.	254.	0.	-1541.
58.9	262.1	1343.	668.	329.	287.	0.	-1665.
60.9	270.8	1414.	694.	339.	302.	0.	-1784.
62.8	279.5	1469.	715.	329.	314.	-2219.	-2004.
64.8	288.3	1573.	761.	355.	344.	-1731.	-2508.
66.8	297.0	1641.	793.	379.	368.	-1611.	-3024.
68.7	305.8	1767.	855.	415.	408.	-1563.	-3330.
70.7	314.5	1869.	885.	433.	390.	-1539.	-3544.
72.7	323.2	2019.	949.	441.	372.	-1607.	-3416.
74.6	332.0	2201.	1055.	523.	400.	-1633.	-3398.
76.6	340.7	2319.	1099.	571.	406.	-1589.	-3504.
78.6	349.4	2481.	1181.	629.	416.	-1429.	-3538.
80.5	358.2	1333.	1565.	643.	638.	-1835.	-3184.

SPECIMEN SC8

LOAD		STEEL MICROSTRAINS			CONCRETE MICROSTRAINS		
kips	kN	1	2	3	1	2	3
5.9	26.2	-17.	19.	2.	-121.	-77.	-55.
11.8	52.4	-26.	91.	18.	-246.	-180.	-162.
17.7	78.6	-18.	245.	53.	-391.	-324.	-299.
23.6	104.8	-8.	429.	81.	-559.	-470.	-455.
29.5	131.0	36.	574.	55.	-741.	-647.	-618.
35.4	157.2	172.	767.	97.	-1088.	-964.	-879.
39.3	174.7	191.	800.	121.	-1280.	-1134.	-1021.
43.2	192.2	185.	783.	118.	-1429.	-1255.	-1108.
47.1	209.7	213.	799.	117.	-1594.	-1390.	-1213.
51.1	227.1	340.	816.	110.	-1826.	-1561.	-1355.
55.0	244.6	435.	845.	122.	0.	-1759.	-1522.
58.9	262.1	552.	894.	138.	-2552.	-1958.	-1732.
62.8	279.5	584.	930.	160.	-2986.	-2212.	-1960.
66.8	297.0	654.	984.	166.	-3176.	-1354.	-1958.
70.7	314.5	730.	1046.	184.	-2566.	-882.	-1794.
74.6	332.0	870.	1138.	190.	-1712.	-684.	-1112.
76.6	340.7	1000.	1210.	226.	-1462.	-594.	-532.
78.6	349.4	1068.	1239.	252.	-1304.	-552.	-140.
80.5	358.2	1794.	1476.	472.	-538.	-560.	138.
82.5	366.9	2098.	1542.	630.	-514.	-628.	128.
83.5	371.3	2616.	1656.	864.	-464.	-654.	44.

SPECIMEN SC9

LOAD		STEEL MICROSTRAINS				CONCRETE MICROSTRAINS		
kips	kN	1	2	3	4	1	2	3
0.0	0.0	-11.	0.	-2.	-23.	-3.	-7.	-15.
3.9	17.5	-11.	0.	24.	-16.	-152.	-162.	-125.
7.9	34.9	-4.	0.	57.	-22.	-294.	-343.	-258.
11.8	52.4	292.	0.	96.	48.	-524.	-635.	-469.
15.7	69.9	649.	0.	173.	144.	-812.	-996.	-711.
19.6	87.4	608.	0.	250.	254.	-1201.	-1465.	-965.
23.6	104.8	778.	0.	304.	457.	-1724.	-2150.	-1278.
27.5	122.3	952.	0.	326.	383.	-2212.	-2878.	-1606.
31.4	139.8	1104.	0.	472.	811.	-2714.	-3834.	-1982.
35.4	157.2	1329.	0.	643.	1332.	-3223.	-5325.	-2590.
39.3	174.7	1684.	0.	858.	1832.	-3478.	-6385.	-3175.
43.2	192.2	2060.	0.	1286.	2905.	-3170.	-2330.	-2114.
47.1	209.7	0.	0.	1698.	8217.	-2058.	-1046.	-615.
49.1	218.4	0.	0.	1784.	0.	-2152.	-968.	-498.

SPECIMEN SC10

LOAD		STEEL MICROSTRAINS				CONCRETE MICROSTRAINS		
kips	kN	1	2	3	4	1	2	3
0.0	0.0	-14.	-17.	0.	-16.	-12.	-14.	-12.
3.9	17.5	2.	10.	0.	0.	-52.	-30.	-61.
7.9	34.9	3.	13.	0.	-8.	-106.	-70.	-123.
11.8	52.4	4.	18.	0.	-16.	-163.	-118.	-196.
15.7	69.9	11.	27.	0.	-25.	-237.	-181.	-295.
19.6	87.4	26.	112.	0.	-40.	-321.	-248.	-395.
23.6	104.8	175.	624.	0.	49.	-558.	-445.	-671.
27.5	122.3	289.	786.	0.	94.	-713.	-589.	-885.
31.4	139.8	402.	899.	0.	129.	-875.	-745.	-1130.
35.4	157.2	1055.	1081.	0.	179.	-1261.	-1142.	-1709.
39.3	174.7	1164.	1153.	0.	198.	-1512.	-1435.	-2078.
43.2	192.2	1294.	1257.	0.	226.	-1690.	-1681.	-2372.
47.1	209.7	1488.	1409.	0.	282.	-1780.	-2027.	-2668.
51.1	227.1	1530.	1427.	0.	312.	-1608.	-2501.	-1744.
55.0	244.6	1682.	1511.	0.	364.	-888.	-1573.	-980.
58.9	262.1	1877.	1578.	0.	432.	-611.	-1032.	-533.
60.9	270.8	2096.	1679.	0.	512.	-448.	-875.	-592.
62.8	279.5	2336.	1867.	0.	620.	-356.	-831.	-700.

SPECIMEN SC11

LOAD		STEEL MICROSTRAINS				CONCRETE MICROSTRAINS		
kips	kN	1	2	3	4	1	2	3
20.0	89.0	-34.	-31.	34.	-101.	-24.	-16.	-76.
40.0	177.9	-42.	-75.	62.	-169.	-112.	-51.	-177.
60.0	266.9	-27.	-114.	76.	-186.	-300.	182.	-310.
80.0	355.8	-21.	-176.	95.	-117.	-508.	69.	-436.
90.0	400.3	-27.	-162.	96.	-72.	-624.	-26.	-509.
100.0	444.8	9.	-116.	114.	67.	-737.	-115.	-562.
110.0	489.3	28.	-46.	111.	181.	-853.	-146.	-602.
120.0	533.8	54.	10.	109.	265.	-977.	-171.	-644.
130.0	578.2	89.	70.	105.	359.	-1209.	-449.	-671.
140.0	622.7	110.	84.	108.	409.	-1370.	101.	-679.
150.0	667.2	135.	99.	124.	463.	-1537.	171.	-684.
160.0	711.7	185.	129.	179.	534.	-1713.	16.	-674.
170.0	756.2	245.	148.	305.	584.	-1764.	-274.	-659.
175.0	778.4	307.	157.	467.	627.	-1799.	-113.	-639.
180.0	800.6	333.	166.	547.	652.	-1814.	235.	-639.
185.0	822.9	369.	178.	640.	685.	-1825.	456.	-633.
190.0	845.1	413.	190.	739.	720.	-1832.	1146.	-604.
195.0	867.4	471.	208.	853.	764.	-1805.	1913.	-553.
200.0	889.6	523.	212.	968.	796.	-1793.	1994.	-522.
205.0	911.8	596.	219.	1129.	840.	-1753.	1758.	-434.
210.0	934.1	665.	226.	1274.	872.	-1721.	1602.	-509.
215.0	956.3	783.	242.	1478.	888.	-1619.	4288.	-494.
220.0	978.6	923.	267.	1723.	838.	-1409.	4803.	-484.

SPECIMEN SC12

LOAD		STEEL MICROSTRAINS				CONCRETE MICROSTRAINS		
kips	kN	1	2	3	4	1	2	3
20.0	89.0	84.	35.	67.	81.	44.	-16.	14.
40.0	177.9	91.	2.	90.	50.	24.	-204.	-38.
60.0	266.9	96.	-24.	90.	11.	5.	-384.	-91.
80.0	355.8	103.	-50.	92.	-25.	-20.	-564.	-147.
100.0	444.8	108.	-75.	93.	-768.	-46.	-39.	-202.
120.0	533.8	113.	-97.	95.	-122.	-64.	-903.	-246.
130.0	578.2	117.	-105.	96.	-152.	-67.	-959.	-261.
140.0	622.7	124.	-105.	97.	-193.	-62.	-996.	-264.
150.0	667.2	128.	-111.	104.	-223.	-67.	-1054.	-299.
160.0	711.7	139.	-132.	110.	-231.	-83.	-882.	-385.
170.0	756.2	155.	-167.	109.	-227.	-87.	-734.	-836.
180.0	800.6	188.	-210.	109.	-223.	-59.	-544.	-1084.
190.0	845.1	261.	-256.	114.	-211.	-13.	-386.	-1263.
200.0	889.6	356.	-264.	135.	-202.	42.	199.	-938.
212.0	943.0	446.	-103.	226.	-231.	227.	-202.	-46.

SPECIMEN SC13

LOAD		STEEL MICROSTRAINS				CONCRETE MICROSTRAINS		
kips.	kN	1	2	3	4	1	2	3
20.0	89.0	100.	35.	113.	2.	29.	103.	-12.
40.0	177.9	87.	-9.	113.	-65.	-68.	85.	-165.
60.0	266.9	64.	-51.	112.	-111.	-239.	50.	-338.
80.0	355.8	55.	-117.	120.	-124.	-439.	16.	-545.
100.0	444.8	57.	-181.	127.	-61.	-645.	-27.	-745.
110.0	489.3	68.	-196.	127.	27.	-776.	-48.	-845.
120.0	533.8	100.	-178.	150.	159.	-866.	-87.	-974.
130.0	578.2	137.	-103.	196.	265.	-897.	-135.	-1134.
140.0	622.7	176.	37.	252.	353.	-888.	-225.	-1375.
150.0	667.2	231.	244.	359.	443.	-704.	-311.	-1589.
160.0	711.7	351.	692.	532.	549.	-504.	-543.	-1816.
170.0	756.2	466.	1390.	654.	635.	-183.	-776.	-1849.
180.0	800.6	538.	0.	757.	721.	20.	-956.	-1707.
190.0	845.1	626.	0.	734.	199.	279.	-1276.	-1238.
200.0	889.6	627.	0.	1069.	726.	499.	-1366.	-1003.
210.0	934.1	764.	0.	1545.	1046.	207.	-665.	-1206.

SPECIMEN TC1

LOAD		STEEL MICROSTRAINS				CONCRETE MICROSTRAINS
kips	kN	1	2	3	4	1
0.0	0.0	0.	0.	0.	0.	0.
5.9	26.2	2.	51.	-4.	-16.	-24.
11.8	52.4	19.	-3.	-7.	-14.	-111.
17.7	78.6	73.	89.	-10.	-17.	-237.
23.6	104.8	111.	150.	-5.	-2.	-332.
29.5	131.0	174.	344.	19.	46.	-430.
35.3	157.2	291.	360.	128.	120.	-522.
41.2	183.4	395.	391.	291.	199.	-680.
47.1	209.6	468.	407.	454.	295.	-1024.
47.9	213.1	511.	388.	665.	527.	-698.
25.1	111.8	442.	325.	593.	453.	-428.
17.7	78.6	413.	297.	556.	425.	-402.
9.8	43.7	342.	229.	509.	371.	-391.
0.0	0.0	189.	100.	405.	248.	-373.
0.0	0.0	182.	115.	330.	235.	-367.
11.8	52.4	287.	212.	374.	272.	-391.
17.7	78.6	351.	269.	417.	302.	-391.
35.3	157.2	501.	698.	480.	380.	-444.
41.2	183.4	538.	359.	522.	415.	-499.
47.1	209.6	574.	390.	581.	446.	-518.
53.0	235.8	606.	419.	651.	568.	-419.
56.9	253.3	595.	498.	892.	911.	-384.
58.9	262.0	571.	588.	926.	1015.	-328.
53.0	235.8	302.	760.	911.	1012.	-334.
29.5	131.0	223.	703.	789.	834.	-278.
11.8	52.4	121.	564.	668.	674.	-281.
0.0	0.0	82.	282.	476.	413.	

SPECIMEN TC2

LOAD		STEEL MICROSTRAINS		CONCRETE MICROSTRAINS					
kips	kN	1	2	1	2	3	4	5	6
0.0	0.0	0.	0.						
1.3	5.8	-63.	-8.	-67.	-71.	-45.	-2.	-1.	-25.
2.6	11.5	115.	-31.	-116.	-149.	-104.	-2.	-14.	-31.
3.9	17.3	160.	-44.	-175.	-206.	-150.	-5.	-29.	-42.
5.2	23.1	203.	-56.	-244.	-270.	-200.	-12.	-47.	-56.
6.5	28.9	253.	-72.	-317.	-335.	-252.	-21.	-71.	-76.
7.8	34.6	305.	-82.	-397.	-404.	-306.	-29.	-92.	-96.
9.1	40.4	359.	-89.	-485.	-477.	-362.	-38.	-112.	-115.
10.4	46.2	408.	-96.	-574.	-549.	-417.	-49.	-132.	-132.
11.7	52.0	454.	-101.	-667.	-626.	-476.	-59.	-151.	-149.
13.0	57.7	499.	-106.	-759.	-698.	-531.	-68.	-169.	-164.
14.3	63.5	544.	-108.	-881.	-795.	-605.	-84.	-192.	-181.
15.6	69.3	591.	-110.	-997.	-882.	-668.	-98.	-218.	-191.
16.9	75.1	638.	-107.	-1141.	-990.	-744.	-115.	-255.	-194.
18.8	83.7	695.	-114.	-1370.	-1171.	-869.	-150.	-293.	-212.
19.5	86.6	720.	-115.	-1478.	-1260.	-929.	-166.	-307.	-218.
20.8	92.4	759.	-117.	-1604.	-1357.	-993.	-182.	-329.	-232.
22.1	98.1	800.	-118.	-1767.	-1489.	-1076.	-205.	-352.	-246.
23.4	103.9	836.	-118.	-1952.	-1612.	-1181.	-238.	-371.	-255.
24.7	109.7	878.	-113.	-2282.	-1869.	-1310.	-273.	-400.	-262.
26.0	115.5	916.	-105.	-2606.	-2112.	-1460.	-313.	-424.	-270.
27.3	121.2	958.	-97.	-2890.	-2344.	-1610.	-351.	-454.	-274.
28.6	127.0	994.	-79.	-3302.	-2707.	-1832.	-399.	-486.	-266.
29.9	132.8	1020.	-54.	-3776.	-3336.	-2170.	-471.	-535.	-235.
31.2	138.6	1070.	-14.	-3541.	-3964.	-2565.	-546.	-605.	-200.
32.3	143.8	1110.	81.	-1733.	-3792.	-3145.	-681.	-780.	-40.
31.3	139.1	1145.	311.	-346.	-1692.	-1335.	-1951.	1775.	50.
0.0	0.0	15.	10.	-156.	-1541.	-1225.	-516.	557.	29.

SPECIMEN. TC3

LOAD		STEEL MICROSTRAINS		CONCRETE MICROSTRAINS					
kips	kN	1	2	1	2	3	4	5	6
0.0	0.0	0.	0.						
1.3	5.8	81.	96.	-152.	-88.	-33.	0.	-64.	-140.
2.6	11.5	164.	200.	-384.	-214.	-80.	0.	-128.	-316.
3.9	17.3	209.	270.	-570.	-321.	-117.	0.	-197.	-478.
5.2	23.1	262.	346.	-758.	-432.	-156.	0.	-261.	-630.
6.5	28.9	321.	445.	-1030.	-602.	-220.	0.	-350.	-852.
7.8	34.6	367.	533.	-1326.	-797.	-300.	0.	-458.	-1111.
9.1	40.4	428.	629.	-1669.	-1020.	-401.	0.	-602.	-1494.
10.4	46.2	488.	718.	-1993.	-1275.	-530.	0.	-766.	-1981.
11.7	52.0	556.	814.	-2284.	-1523.	-650.	0.	-942.	-2474.
13.0	57.7	640.	918.	-2576.	-1903.	-878.	0.	-1252.	-3171.
14.3	63.5	734.	1026.	-2491.	-2353.	-1204.	0.	-1660.	-3193.
15.6	69.3	832.	1130.	-1874.	-3206.	-1850.	0.	-2458.	-3396.
16.2	72.2	927.	1210.	-974.	-1976.	-2055.	0.	-1153.	-1848.
16.9	75.1	1087.	1330.	-834.	-931.	-1925.	0.	-993.	-1296.
17.1	76.2	1212.	1400.	-837.	-556.	-1775.	0.	-968.	-1138.
17.5	77.9	1272.	1450.	-729.	1524.	-680.	0.	-958.	-843.
14.9	66.4	1262.	1360.	-719.	1309.	-520.	0.	-958.	-833.
0.0	0.0	37.	-45.	-684.	269.	-220.	0.	-908.	-896.

SPECIMEN TC4

LOAD		STEEL MICROSTRAINS				CONCRETE MICROSTRAINS		
kips	kN	1	2	3	4	1	2	3
0.0	0.0	0.	0.	0.	0.	0.	0.	0.
2.6	11.5	-19.	48.	110.	-29.	-64.	-16.	-64.
5.5	24.3	-28.	128.	243.	-49.	-171.	-51.	-172.
7.8	34.6	313.	263.	336.	153.	-404.	-96.	-439.
10.4	46.2	514.	362.	424.	454.	-647.	-185.	-813.
13.0	57.7	691.	474.	523.	673.	-913.	-322.	-1249.
15.6	69.3	1591.	596.	623.	873.	-1190.	-554.	-1697.
18.2	80.8	2074.	712.	729.	1077.	-1506.	-884.	-2105.
20.8	92.4	2696.	824.	826.	1289.	-1898.	-1250.	-2469.
23.4	103.9	0.	1004.	1053.	1605.	-2032.	-1778.	-2777.
26.0	115.5	3731.	1060.	3469.	1955.	-2016.	-651.	-1916.
24.7	109.7	0.	1225.	3799.	1595.	699.	-276.	-1096.
0.0	0.0	2196.	635.	1844.	1465.			